10-1971

Investigation of the water table in a tidal beach : final report

W. Harrison
Virginia Institute of Marine Science

John D. Boon
Virginia Institute of Marine Science

L. E. Fausak
Virginia Institute of Marine Science

C. S. Fang
Virginia Institute of Marine Science

S. N. Wang
Virginia Institute of Marine Science

FINAL REPORT

INVESTIGATION OF THE WATER TABLE IN A TIDAL BEACH

Harrison, Boon, Fang, Fausak, and Wang

ONR CONTRACT NO. N00014-70-C-0004
TASK NO. NR 388-097
GEOGRAPHY BRANCH, OFFICE OF NAVAL RESEARCH

SPECIAL SCIENTIFIC REPORT NO. 60

VIRGINIA INSTITUTE of MARINE SCIENCE
GLOUCESTER POINT, VIRGINIA 23062

OCTOBER 1971

FINAL REPORT

"INVESTIGATION OF THE WATER TABLE IN A TIDAL BEACH"

W. HARRISON
Principal Investigator

I. Instrumentation for Measurement of Water Table Fluctuations
by John D. Boon, III, and W. Harrison

II. The Beach Water Table as a Response Variable of the System
by L. E. Fausak

III. Changes in Foreshore Sand Volume: Role of Fluctuations in Water Table and Ocean Still Water Level
by W. Harrison

IV. One-dimensional Finite Element Analysis of the Groundwater Flow
by W. Harrison, C. S. Fang, and S. N. Wang

V. Two-dimensional Finite Element Analysis of the Groundwater Flow
by C. S. Fang, S. N. Wang, and W. Harrison

SPECIAL SCIENTIFIC REPORT NO. 60

Virginia Institute of Marine Science
Gloucester Point, Virginia 23062

Dr. William J. Hargis, Jr.
Director

ONR Contract No. N00014-70-C-0004
Task No. NR 388-097
Geography Branch, Office of Naval Research

October 1, 1971

TABLE OF CONTENTS

TABLE OF CONTENTS (Cont'd)

TABLE OF CONTENTS (Cont'd)

TABLE OF CONTENTS (Cont'd)

TABLE OF CONTENTS (Cont'd)

TABLE OF CONTENTS (Cont'd)

TABLE OF CONTENTS (Cont'd)

INSTRUMENTATION FOR MEASUREMENT OF BEACH WATER-TABLE FLUCTUATIONS

John D. Boon, III, and W. Harrison

ABSTRACT

A suitable system for acquisition of water-level data from the water table of a sandy ocean beach consists of 1) a 10.16-cm (4-in.) I.D. slotted PVC well pipe with non-slotted upper section, housing a float and float wire, 2) a 3.8-cm (1.5-in.) O.D. galvanized steel pipe, housing a counterweight and counterweight line, and 3) a float-gage system consisting of a differential pulley connected to a 10-turn, 5 K-ohm precision potentiometer, both mounted on a covered wooden platform at the top of the pipes some 1 m above the beach surface. A low-voltage power source connects to the potentiometer which gives an output in the 0-100 mv range, corresponding to the elevation of the water table [one turn = 30.48 cm (1.00 ft.) or 10 mv]. The response of such a float-pulley system is considered accurate to ±3.0 mm, and it exhibits a high degree of precision. Details of fabrication and installation of the monitoring system are given together with selected portions of an analog plot of output from 11 to 13 wells that operated continuously for 31 days.

INTRODUCTION

The water table in a sandy beach at Virginia Beach, Virginia, was expected to rise and fall from place to place in response to a variety of factors, including local oceanic tides, storm-wave flooding, rainfall, and fluctuations in atmospheric pressure. Thus, it was necessary that a water-level monitoring system be capable of covering a range of more than 2 m, to handle storm-flooding and storm-surge conditions in addition to measuring tidal fluctuations (in the maximum range of 104 cm). A compact, quick-response system was needed, one incorporating a well pipe that could pass fluid freely without undue "lag" effects or dampening of small-scale fluctuations. Because no equipment was available commercially that could satisfy all of the special requirements, it was necessary to develop the system described herein. The system is comprised of the following major components: an electromechanical device consisting of a differential pulley and a precision potentiometer,

a slotted PVC pipe, a counterweighted float, and steel counterweight pipe. The final system configuration was based on suggestions by Mr. George Smoot of the U. S. Geological Survey, Water Resources Division.

SYSTEM COMPONENTS

PVC Well Pipe For Float

A 3-m section of slotted, 10.16-cm (4-in.) I.D., PVC well pipe, joined to a 1.0-m section of solid PVC pipe, formed the well for the float. The pipe slot size was #18, which restricted sand-size material from entering the walls of the pipe, yet permitted water to enter and exit freely. The solid PVC section was intended for the above-ground support of the gage mechanism where it also served to prevent wind and wave runup from entering the well. The PVC pipe was obtained from Gator Sales, Inc., Box 15020, Baton Rouge, La., 70815.

Steel Well Pipe For Counterweight

A 4-m section of 3.8-cm (1.5-in.) galvanized steel pipe was jetted into the beach so that its side touched the side of the PVC well pipe. In this configuration the steel pipe could house a counterweight for the float-pulley system astride the top of the PVC pipe. The tops of both pipes were squared off level with one another.

Differential Pulley and Precision Potentiometer

A plexiglas (acrylic, type G) pulley, consisting of two drums of differing diameters, was machined. The larger drum accommodated a 0.397-mm (1/64-in.) stainless steel stranded wire within a helical, v-shaped groove (Fig. 1). The smaller drum, which had a smooth surface, accommodated a light monofilament line. This light line was wound in a direction opposite to the stainless steel wire of the large drum. The pulley had a stainless-steel shaft mounted on ball-bearing supports attached to an aluminum frame. The pulley shaft was coupled to a 10-turn 5 K-ohm precision potentiometer, which itself had a ball-bearing shaft. The potentiometer was a Spectrol Model 800 with a linear tolerance of ±0.025%, manufactured by Spectrol Electronics Division of the Carrier Corporation, San Gabriel, California. The grooved

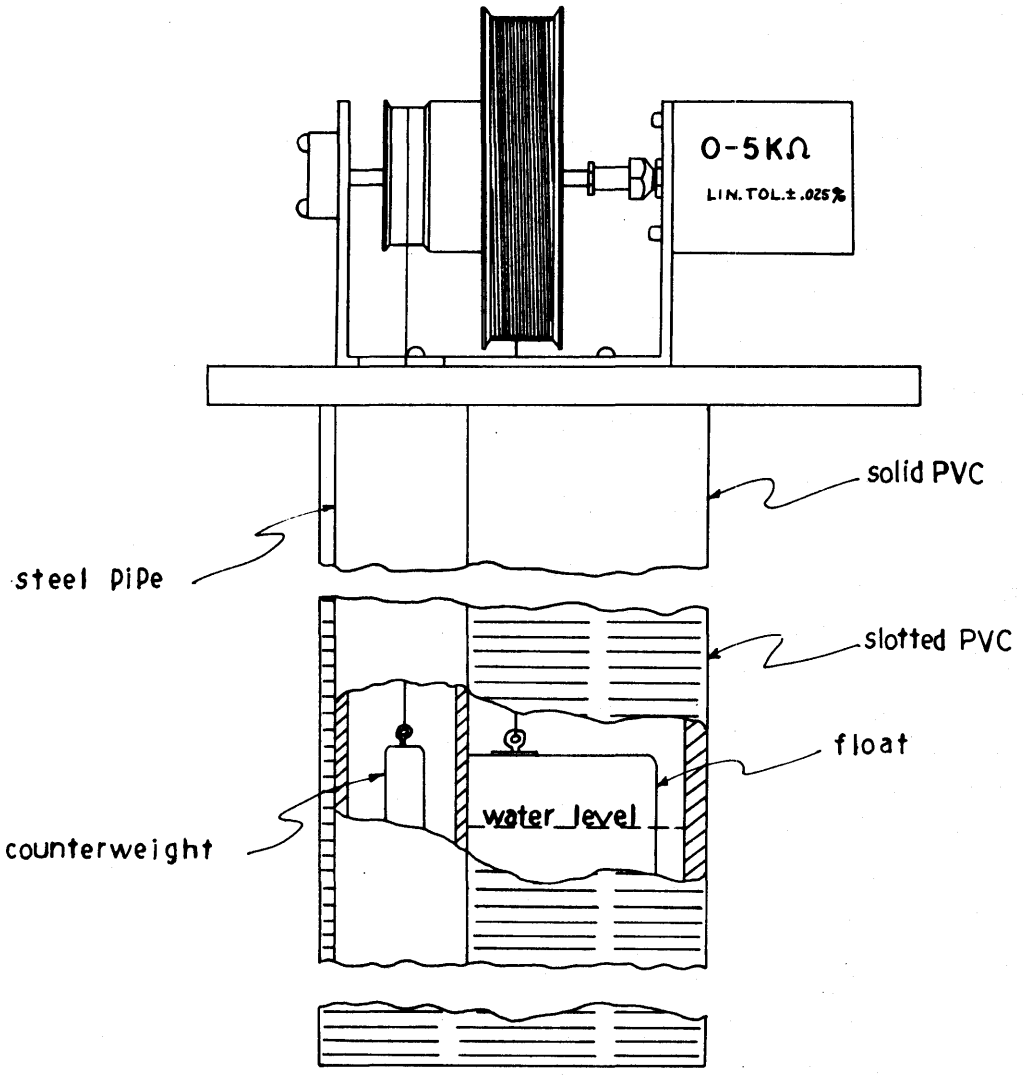

FIG. 1. Schematic of float-pulley system.

drum of the differential pulley was precision machined (Fig. 2) to accept 30.48 cm (1.00 ft.) of stainless-steel wire per revolution. A low-voltage input to the potentiometer than gave an output in the 0-100 mv range. This output corresponded to the level of the water table, at an approximate rate of 30.48 cm per 10 mv. This rate was adjustable via other electronic components in the remote data-acquisition center.

The frame containing the pulley and potentiometer was screwed into a wooden platform; this platform was in turn fixed by brackets to the top of the PVC pipe. Holes were cut in the platform to permit passage of the float wire and counterweight lines. A hard plastic cover was placed over the platform and fixed by screws. All edges and joints were caulked to effect a tight weather seal around the components.

Float and Counterweight

The gage float was made from a 8.255-cm-diameter float of plastic foam of the type used to support fishing nets. The center hole of the float was plugged, an eyelet was screwed in, and the insertions were sealed with epoxy. A swivel-link connection was made to the float wire at the point of its attachment to the eyelet. A small trim weight was added beneath the float to provide tension and to position the water line on the side of the float. The counterweight consisted of approximately 198 gm (7 oz.) of lead, cast in a thin cylindrical form. It was connected to the monofilament line and placed in the counterweight well.

FIELD INSTALLATION

Thirteen well units were placed in the beach in the positions shown on Figure 3. At each installation point the slotted, 3-m-long PVC pipe was first jetted into the beach. This was accomplished by inserting a length of slightly smaller diameter, solid PVC pipe within the slotted PVC pipe. A steel pipe was then inserted within the solid PVC pipe and water was pumped down the steel pipe. The solid PVC pipe acted as a return-flow "casing" for advancing all three pipes into the sand. Water was pumped down the steel pipe at a rate sufficient to flush sand grains up and over the top of the solid PVC pipe. A baffle ring prevented sand from running back down between the two PVC pipes. The pipes were advanced slowly, the tip of

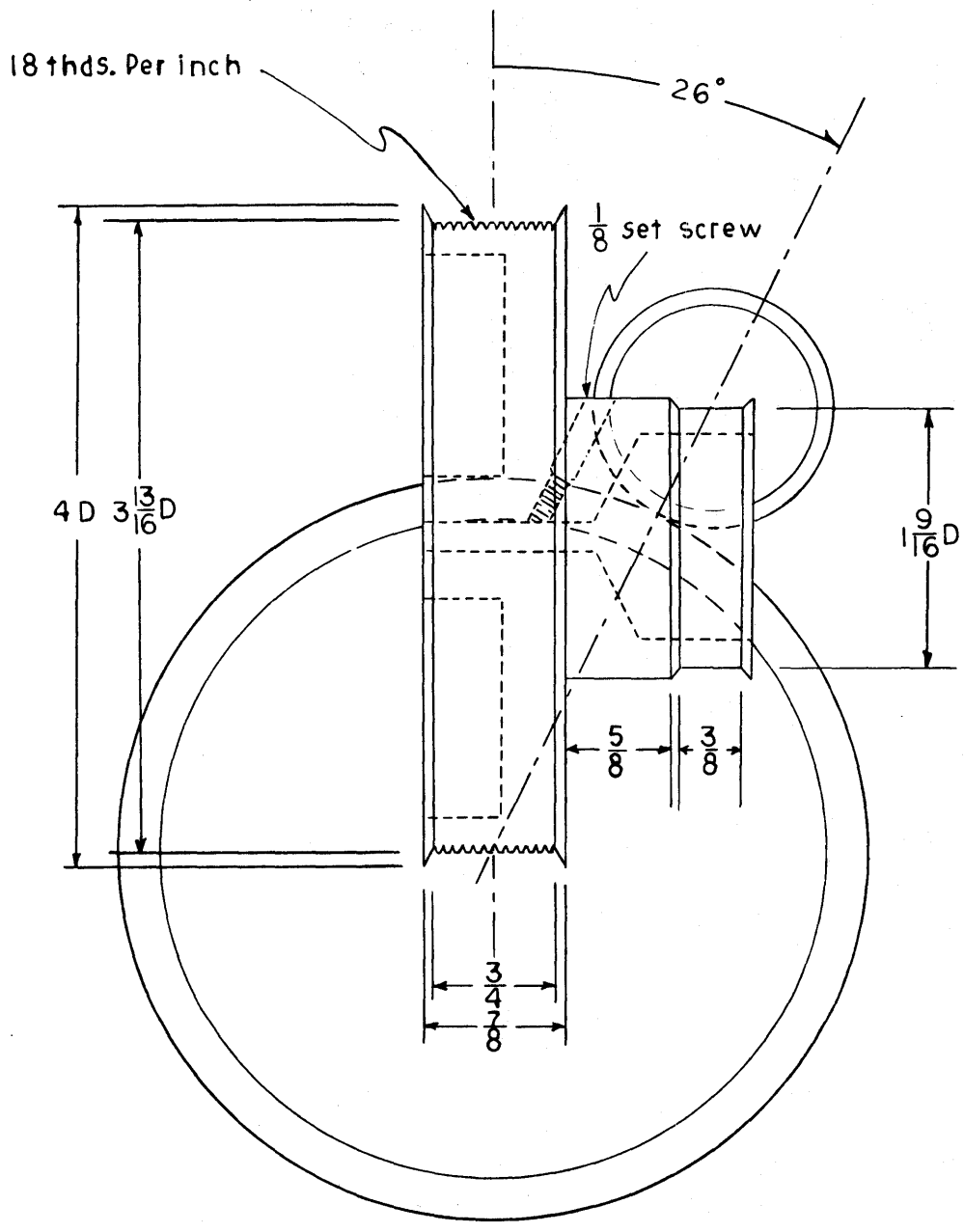

FIG. 2. Top view of pulley showing position relative to PVC, steel pipes. (Dimensions are in inches).

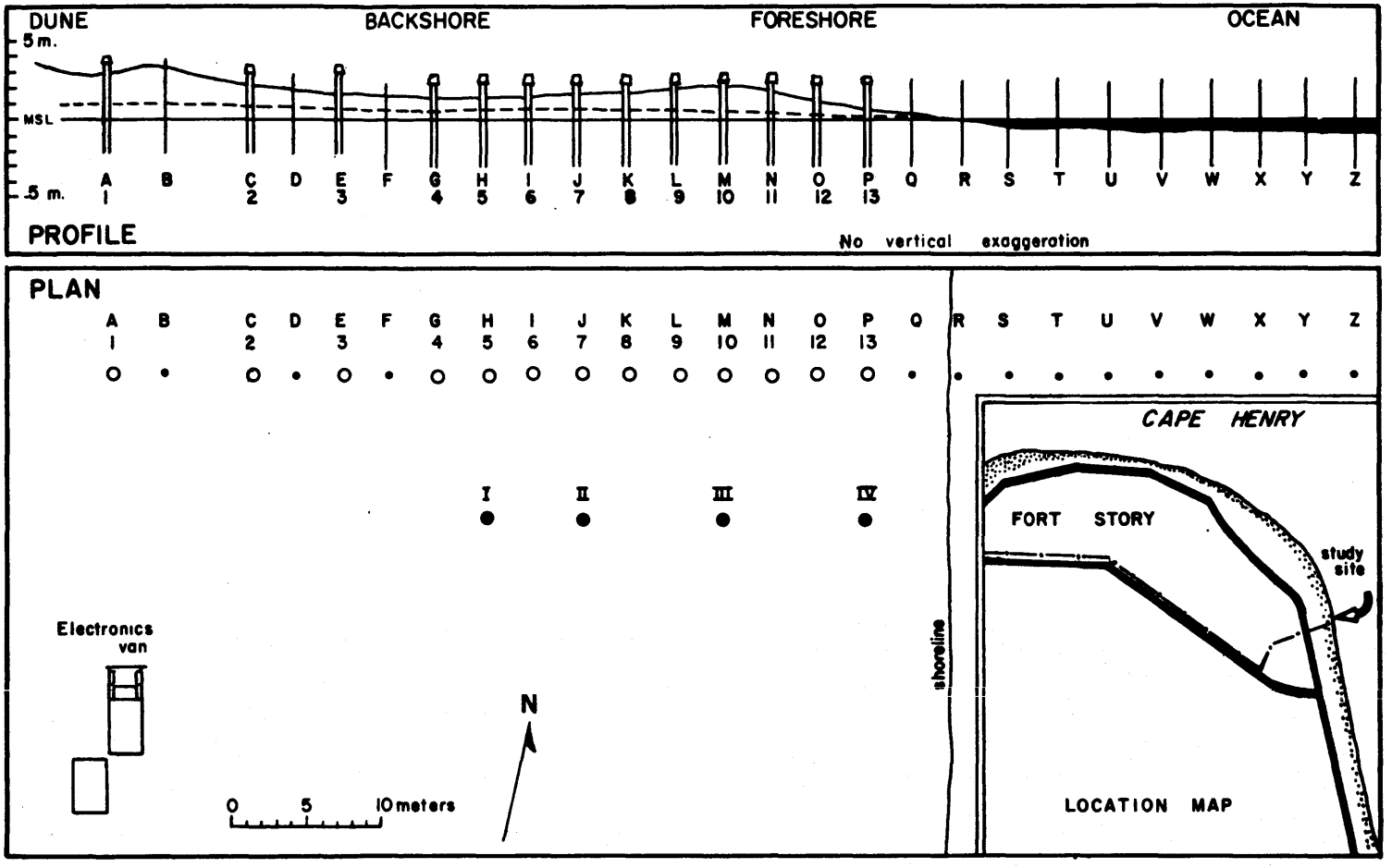

FIG. 3. Plan and profile views of the Fort Story water-table study site, showing typical beach and water-table profiles, water-table monitoring wells (1-13), profiling stations (A-Z), and groundwater sampling probes (I-IV).

the steel pipe leading the PVC pipes by a few cm. Success in such an operation requires a portable high-volume water pump. A gasoline-engine-powered Jabsco pump was used. Some sticking of the slotted PVC pipe was experienced during the pipe-jetting process.

Water for jetting was obtained directly from the ocean for the seawardmost wells; a tank truck had to be used for a supply of water for jetting the more landward wells (Fig. 3, nos. 1-10).

After emplacement and prior to packing sand around the top, the slotted PVC section was trimmed so as to be about one foot below the sand surface. A solid PVC section was then added and the entire upper portion of the well was aligned vertically with a carpenter's level. The steel pipe for the counter-weight was then jetted into the beach, its side touching the PVC pipe. The two pipes were snugged together tightly with stainless-steel wire and the pulley-potentiometer system was then added. It was found that sand rose up only a few cm in the bottoms of the pipes after termination of jetting. Thus, capping of the bottom ends was unnecessary.

Electrical cables were strung out to each well unit on cross braces fixed just below the instrument platform of each well. A single waterproof multi-conductor cable entered the base of each instrument platform. The wires connected the potentiometers to a low-level, digital data acquisition system (DATUM, Inc., Model 120-115). Power for the potentiometer input circuit was obtained from a power supply in the DATUM system that operated off line voltage. Output signals were amplified and digitized by the DATUM unit and then recorded on a computer-compatible magnetic tape recorder (DIGIDATA No. 1339-800).

Water levels were determined every 10 or 15 minutes. Four several-hour-long gaps in data acquisition were experienced, owing to failures in one of the circuit boards of the DATUM system. A storm on August 21-23 damaged wells 12 and 13 (Fig. 3). With these two exceptions, the entire system functioned continuously for 31 days.

RESULTS

The results of this investigation have been published by Harrison and Fausak (1970, Appendix III) in the form of a computer listing of digital values for water level at the 13 wells. L. E. Fausak programmed the digital data for a Calcomp plotter. The portions of the Calcomp printout that appear in Figures 4-8 were selected to give the reader an idea of the reliability of the instrumentation.

Figure 4 shows some obviously spurious data, that were obtained at about 10,000 minutes (elapsed time), for wells 2 and 4. The anomalies should be discarded and the gaps bridged by interpolation. The significance of other sharp oscillations in the output signals, however, may be much more difficult to interpret (for example, Fig. 5, 14,750 minutes).

Fluctuations in water level due to surf action are evident in wells 11, 12, and 13 during non-storm conditions (Fig. 4, 2800 to 3100 minutes) around the time of high tide. Such fluctuations are common at many more of the wells during the storm flooding that began at roughly 15400 minutes (Fig. 6). The spurious signals from wells 12 and 13, the wells that were damaged by the storm, are evident in Figures 7 and 8 (uppermost two traces).

CONCLUSION AND RECOMMENDATIONS

With the exception of certain failures in the electronics of the DATUM system, the instrumentation met the needs of this study. Installation and removal of water wells requires manpower and machinery that go beyond the needs of casual beach studies. The electronic and water-well equipment alone cost about $18,000 in 1969. The cost of support equipment cannot be estimated because surplus materials and vehicles were used.

For most studies of water-table fluctuations, far less than 13 water wells are needed to adequately sample over a distance such as that (83 m) which was investigated in this study. Future students of beach water-table fluctuations or groundwater flow can use the data of this study as a guide when designing their measurement systems. In general, it should be possible to use less wells and, perhaps, simpler and less-expensive recording equipment.

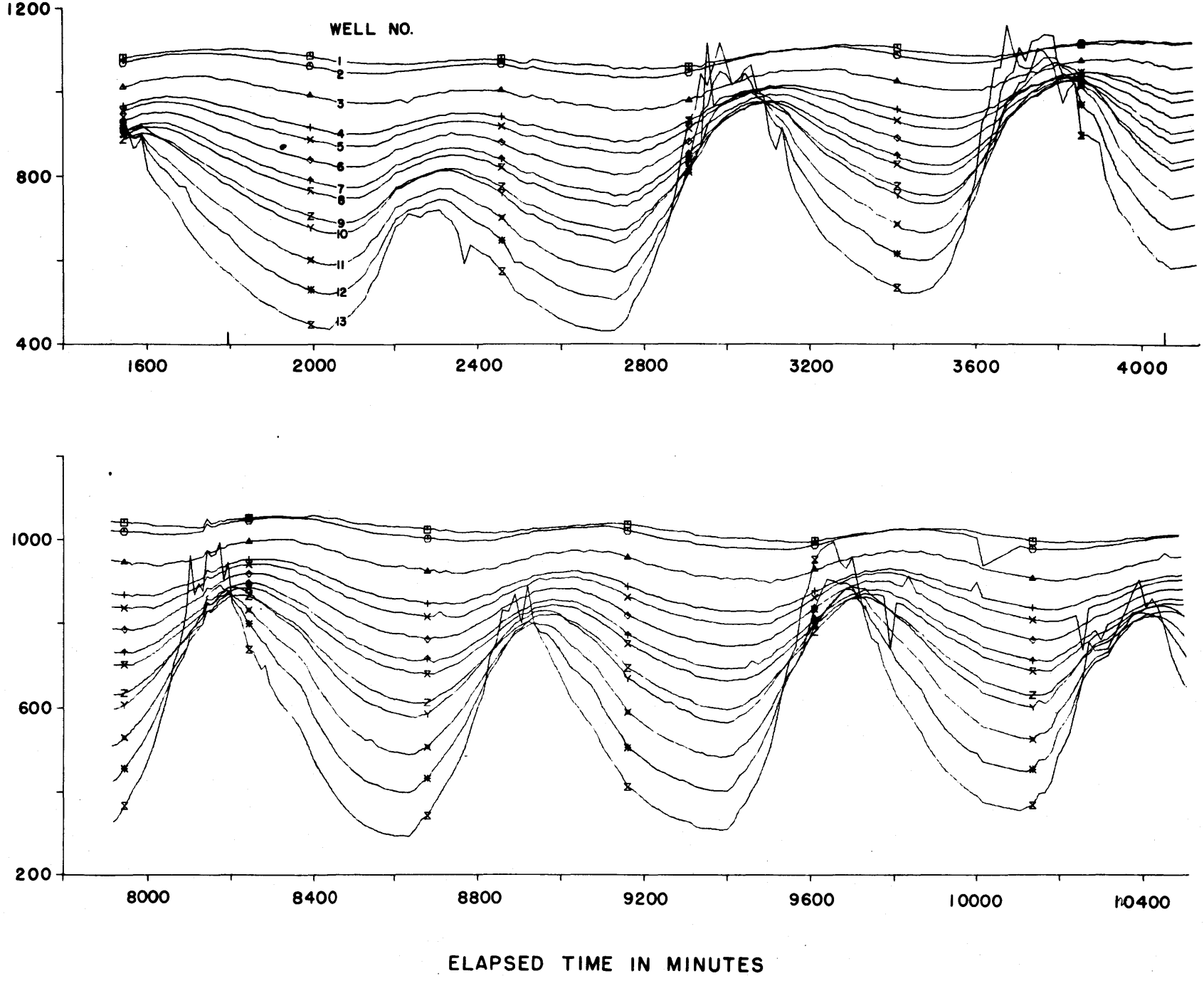

FIG. 4. Water table elevation at the 13 wells of Figure 3, as a function of time. (Pre-storm conditions).

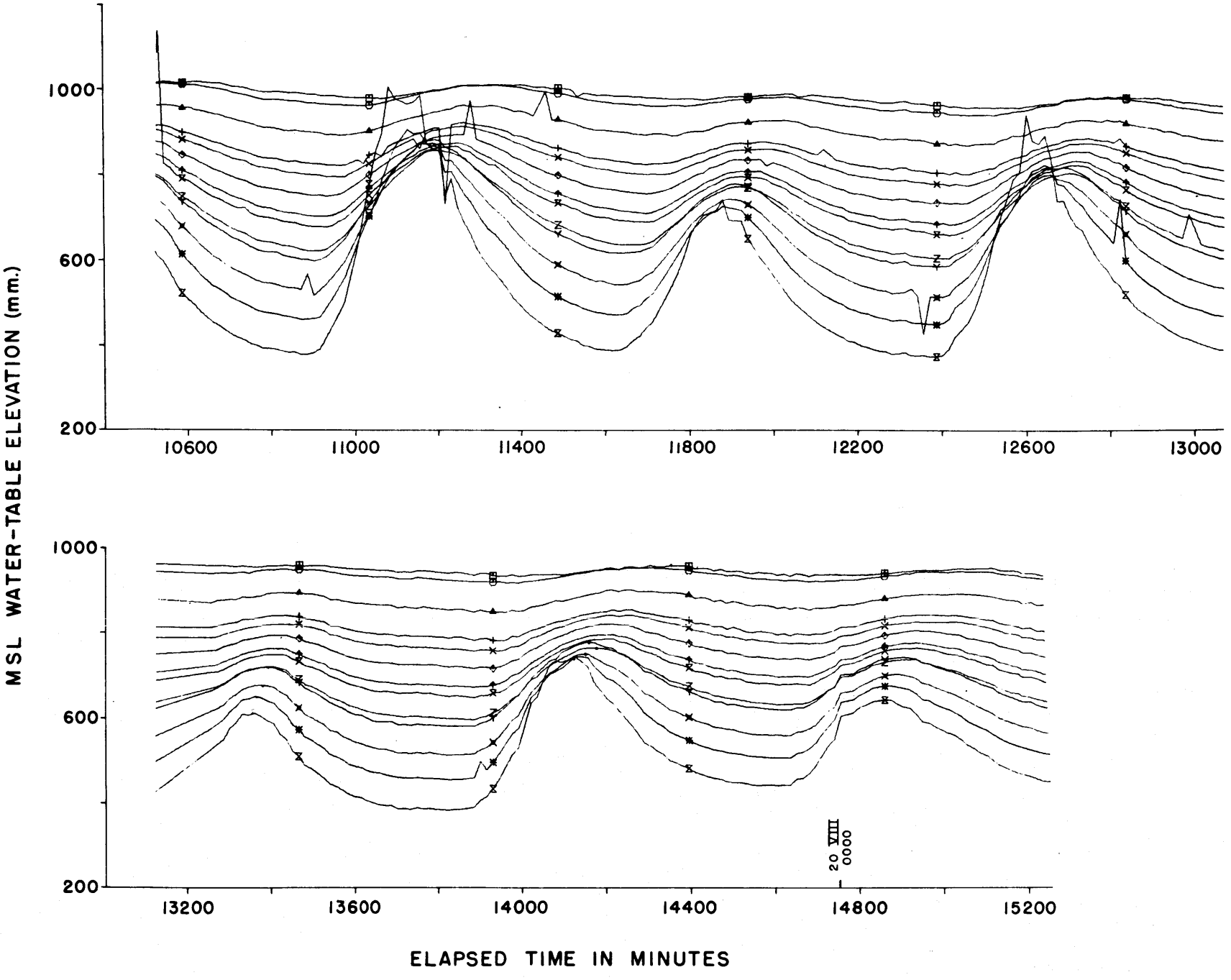

FIG. 5. Water table elevations as a function of time. (Pre-storm conditions).

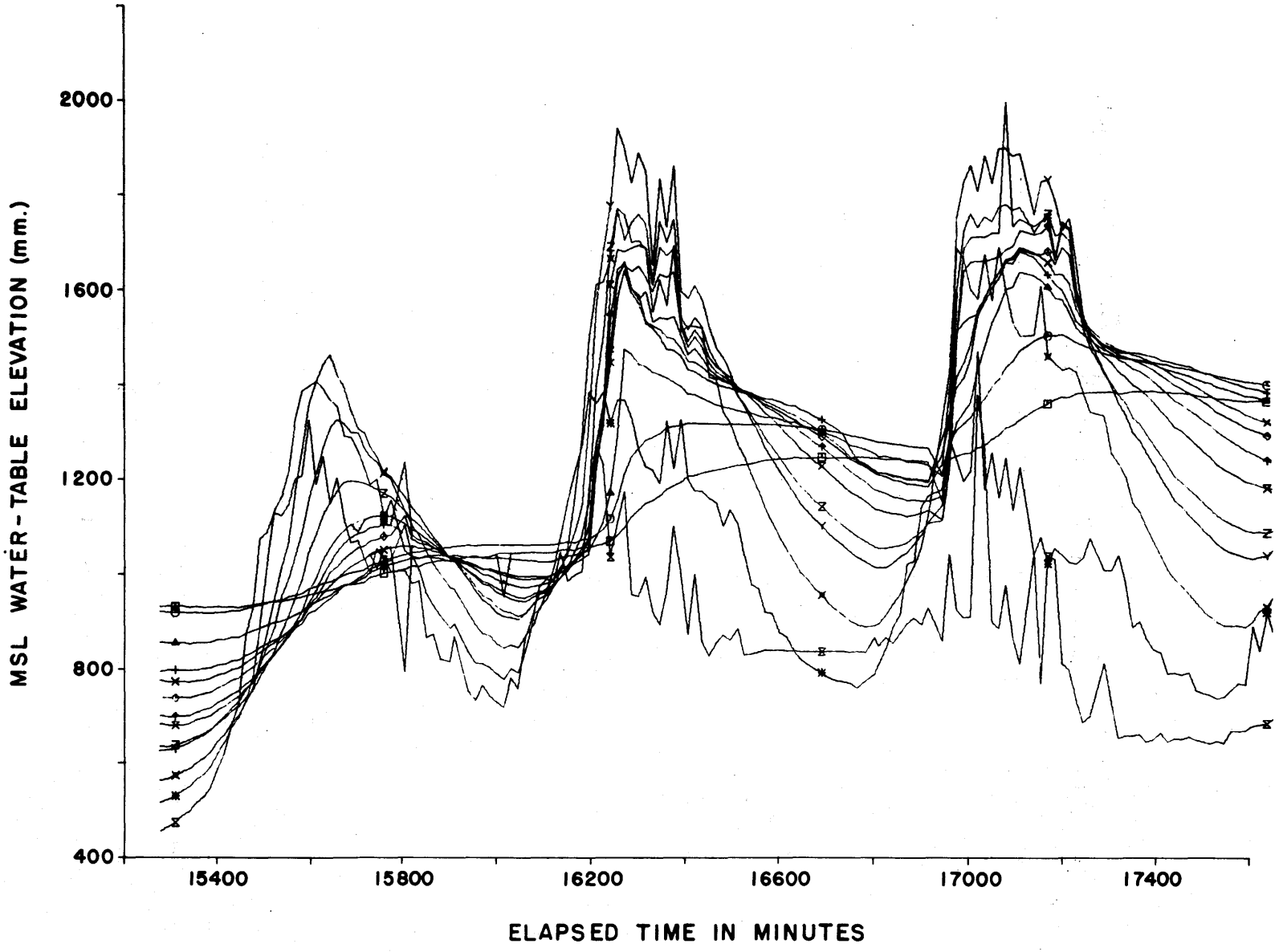

FIG. 6. Water table elevations as a function of time. (Onset of storm and storm conditions).

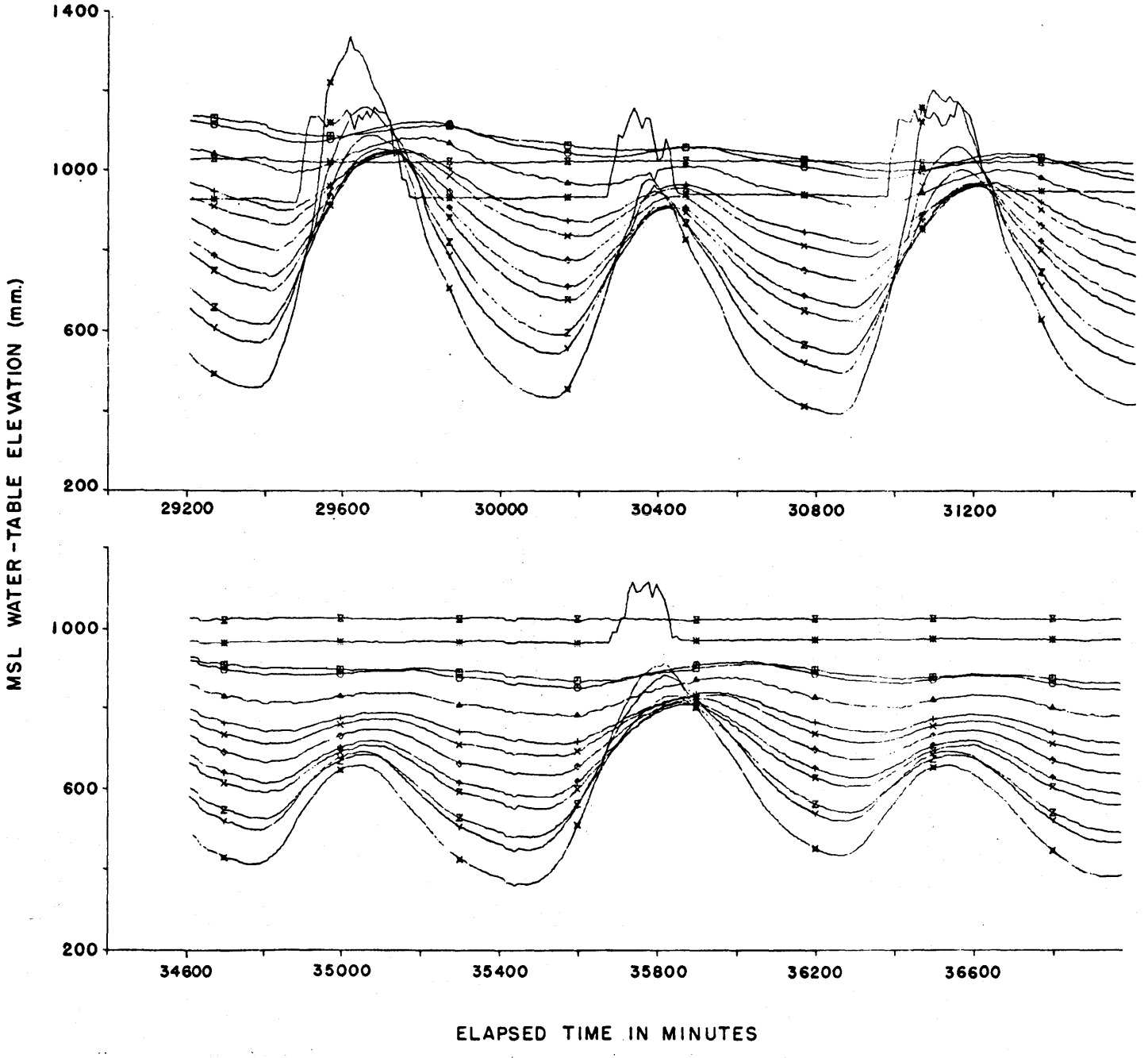

FIG. 7. Water table elevations as a function of time. (Post-storm conditions).

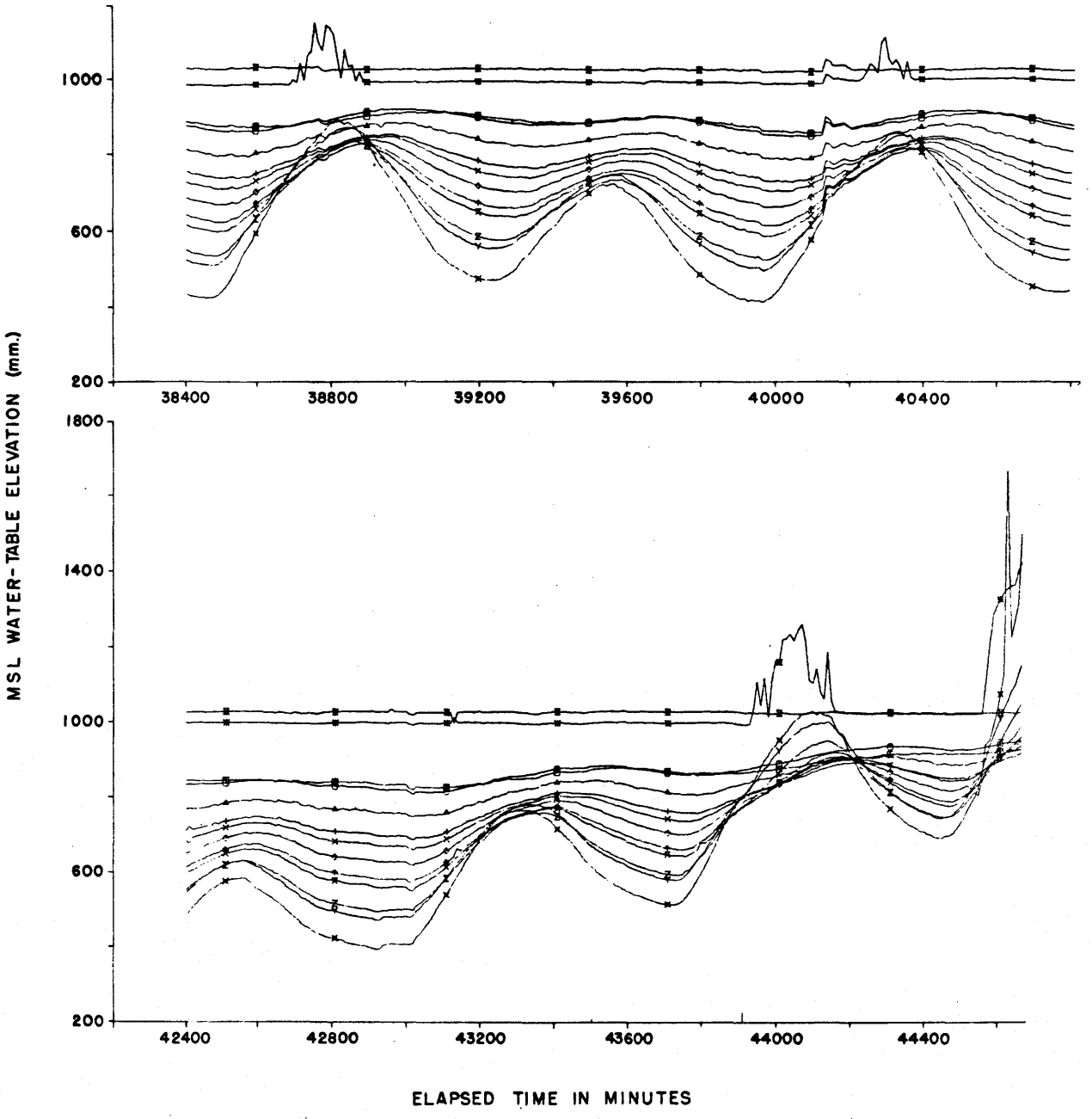

FIG. 8. Water table elevations as a function of time. (Post-large storm and onset of small storm conditions). Wells 12 and 13 are broken and give spurious signals (uppermost two traces).

ACKNOWLEDGMENTS

We thank Dr. David DeVries for supervising installation of the well pipes and Mr. David Tyler for assistance in the field. Mr. William Hale assisted in assembly of the float-pulley and electrical systems. Dr. W. G. MacIntyre supervised the mating and operating of the electronic instrumentation.

REFERENCE

Harrison, W., and L. E. Fausak, 1970, A time series from the beach environment - II: Va. Inst. Marine Sci., Data Rept. No. 7, p. 1-96.

THE WATER TABLE AS A RESPONSE VARIABLE OF THE SYSTEM

Leland E. Fausak

ABSTRACT

Fluctuations of the water table of a tidal marine beach over a 30-day period are examined. The relative importance of variations in still water level, swash runup distance, distance of a sampling station from the shoreline, and atmospheric pressure are determined for rising half-tide cycles in each of 13 water table monitoring wells spaced along a transect perpendicular to the shoreline.

Results showed that tidal oscillations exert the strongest influence in all except the two seawardmost wells and in the most landward well. Distance from the shoreline is the most important variable in the seawardmost wells because of the exponential decay of the input wave and the resultant large range of water-table fluctuations near the beach face. Atmospheric pressure becomes the dominant variable influencing water-table fluctuations in the most landward well, due to the relatively slight contribution of the tide and wave inputs. The amplitude of the water-table fluctuations decreases exponentially in a landward direction and the lag time of the input wave increases linearly with distance from the shoreline. The time lag is found to be approximately 60 minutes per 18 meters of beach penetrated.

INTRODUCTION

The primary factors responsible for the size and configuration of beaches are the type and quantity of sediment available, and the action of the wind-generated surface waves which break on the shore. The source materials are generally constant for a given beach and change only very gradually; the waves striking the beach are responsible for the rapidly changing, short-term, and often cyclic, variations in beach characteristics. The interaction between the waves and the beach, however, is regulated by the position and pressure head of the beach water table, which in turn primarily a function of wave input, tidal level, and permeability of the sand body. This paper will focus attention upon the water table of a specific tidal marine beach and attempt to elucidate some interactions of beach process variables and

fluctuations of the beach water table.

The role of the water table in beach processes was noted by Bagnold (1940), who recognized that sand was deposited on an unsaturated beach due to the energy loss accompanying percolation of the swash into the dry sand. Subsequent work by Grant (1948) and Emery and Foster (1948) established that a high water table promotes erosion of the beach face, and that conversely, a low water table may result in pronounced accretion on the foreshore. Issacs and Bascom (1949) examined the water tables of ten Pacific beaches and recognized the damping of the tidal wave as it passes through the sand body. Duncan (1964), Strahler (1964), and Geise (1966) have shown that zones of erosion and deposition migrate up and down the foreshore in response to the relative positions of the water table and still water level. The relationship of water table position and the movement of sand on the foreshore was defined in quantitative terms by Harrison (1969), who found that the strongest predictors of foreshore erosion and deposition were (1) the breaker steepness, and (2) the ratio of the hydraulic head of the water table to the swash runup distance. Given the demonstrated importance of the water table to beach stability, the present study was undertaken in order to investigate the response of the water table to waves, tides, and atmospheric conditions.

The site chosen for the study is a marine beach located on the seaward side of Cape Henry, Virginia (Figs. 1 and 2), adjacent to the mouth of Chesapeake Bay. The beach is composed of quartzose sand with an average median diameter of 0.41 mm. The average width of the beach, from shoreline to dune ridge, is approximately 60 meters; the average slope is approximately 6°. The offshore zone is gently shoaling and has few bottom irregularities. Figure 3 shows a typical beach profile with the location and spacing of the water table monitoring wells and profile station-markers. The mean range of the astronomical tide is 0.85 m, the spring range is 1.04 m. The nearshore current system is influenced by the ebb and flood of the tide through the adjacent mouth of Chesapeake Bay, but the dominant direction of flow is northerly, due to the normal southerly wave approach and to a persistent clockwise eddy located south of Cape Henry. The mean breaker height for the study period ranged from 0.6 to 1.0 m.

The 30-day data collection phase of the study can be divided into three periods, based on weather and sea state conditions (see Fig. 4). The initial ten days

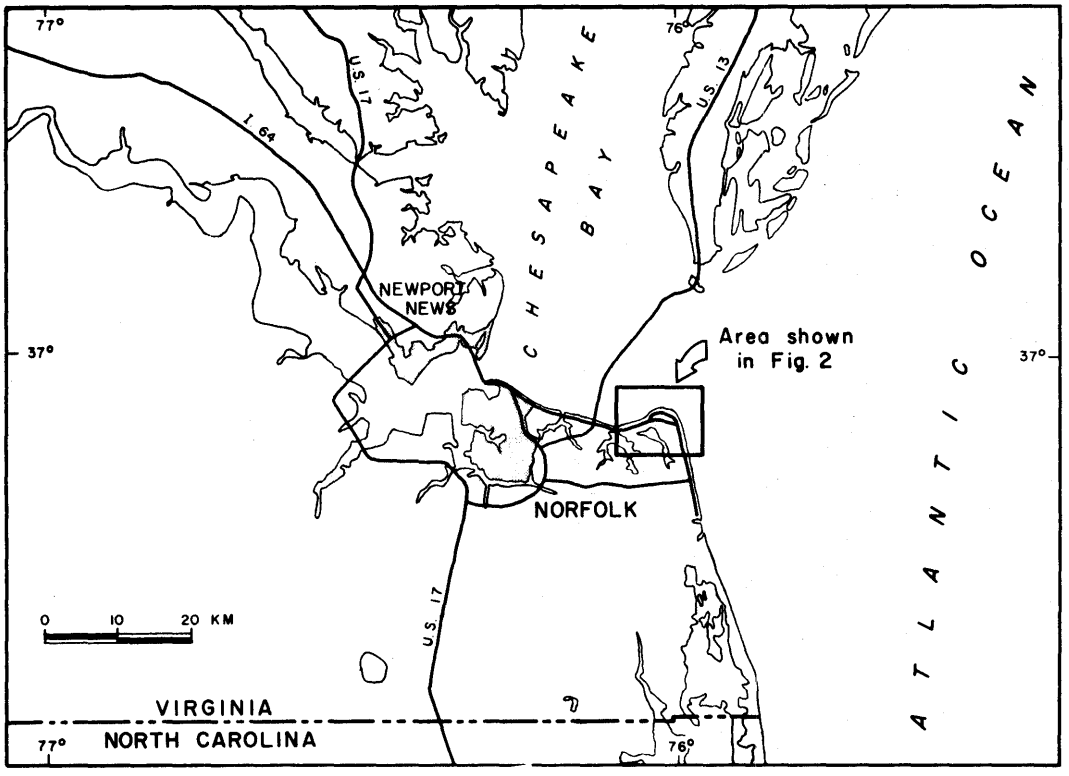

FIG. 1. Regional location map.

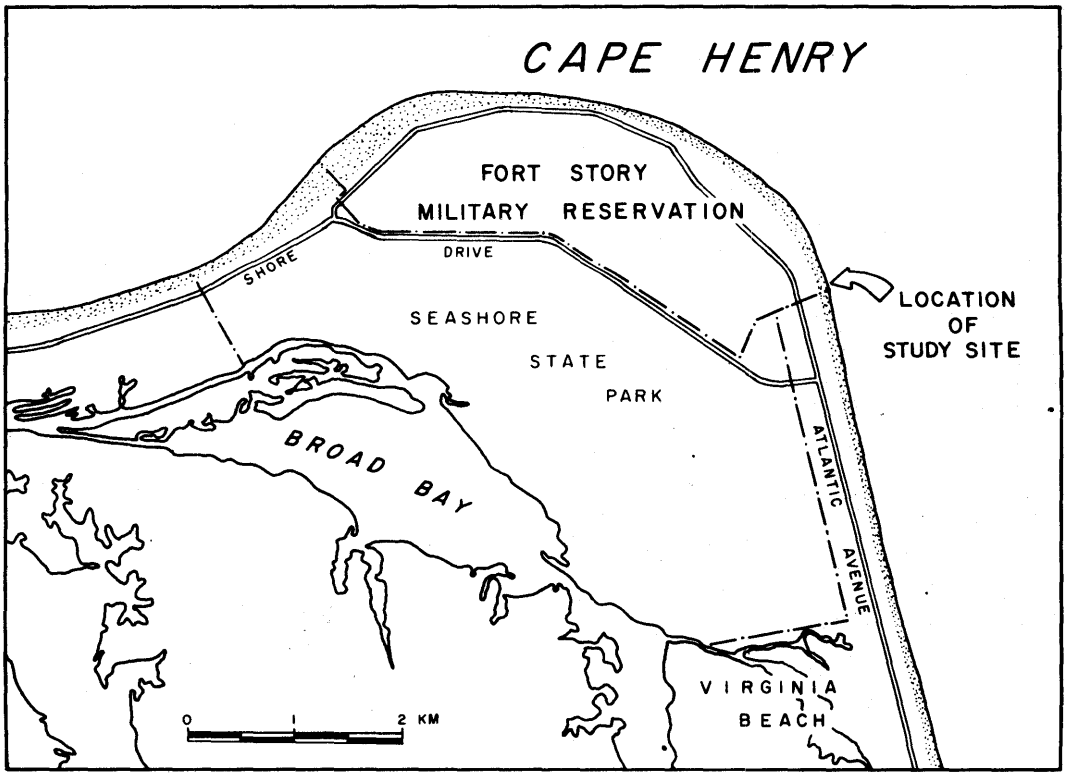

FIG. 2. Location of the Fort Story study site.

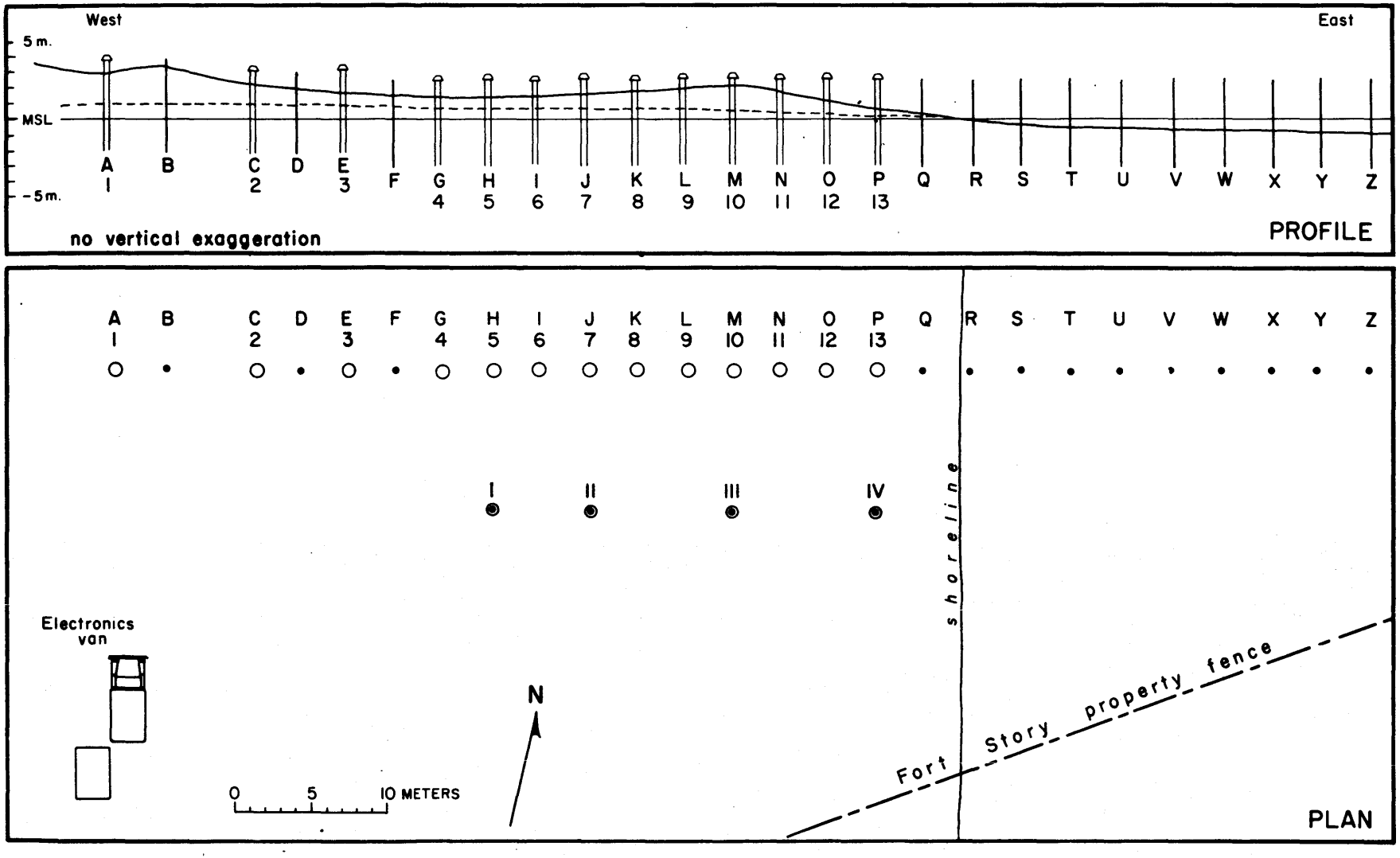

FIG. 3. Plan and profile views of the Fort Story study site, showing typical beach and water table profiles, and the spatial distribution of profile stations (A-Z), water table monitoring wells (1-13), and water table sampling probes (I-IV).

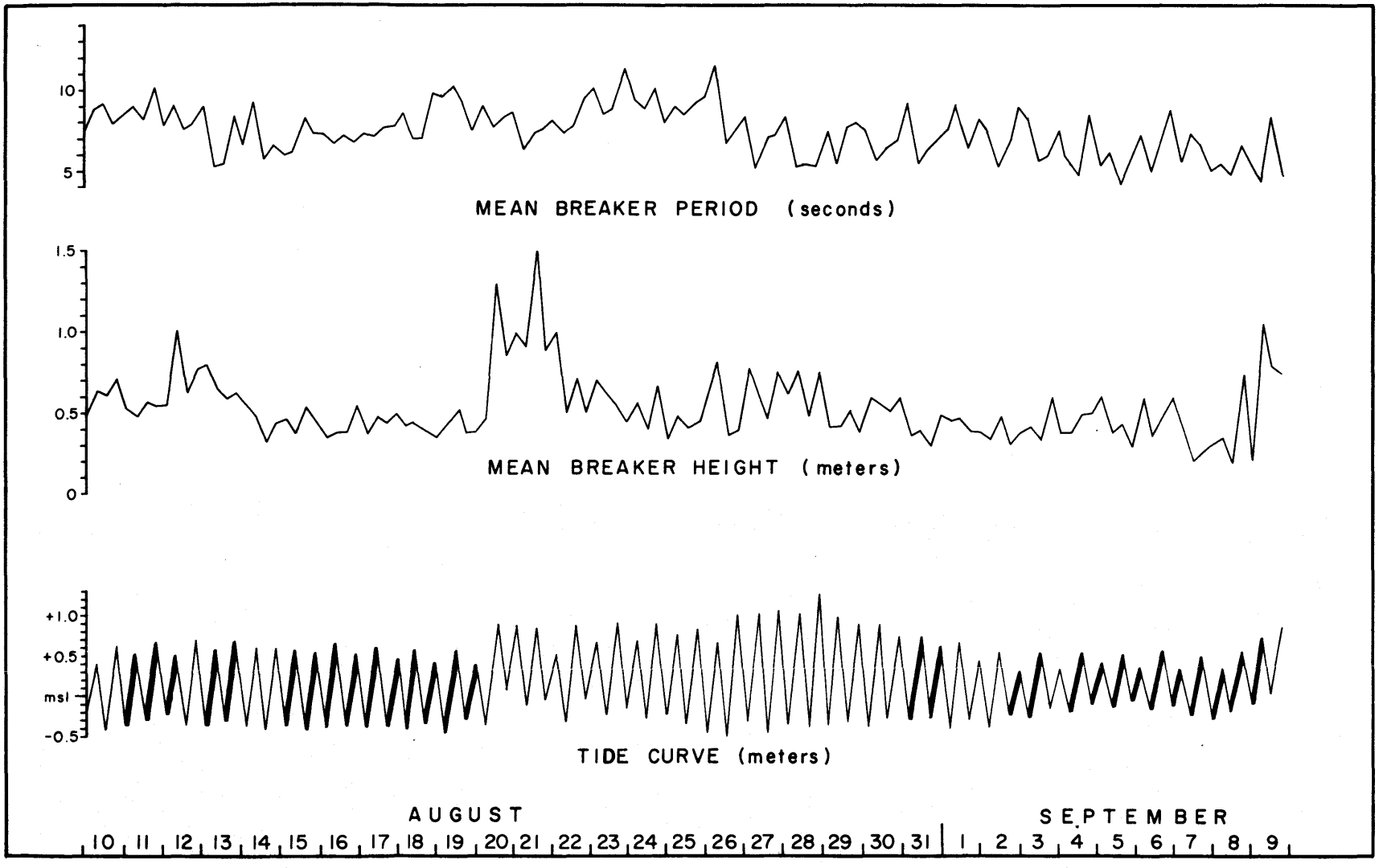

FIG. 4. Wave and tide data for the study period.

were characterized by the normal long, low swell approaching from the south; 3.05 inches of rain fell on the 14th of August, but was not accompanied by a significant change in the sea state. A three-day period of high, short-period waves generated by a local storm followed; rainfall during this period was slight, however, with a total of 0.15 inches. The remaining 17 days saw the return of the normal summer sea conditions; two periods of significant rainfall occurred during this latter period, one of 0.45 inches and one of 0.34 inches, both on September 9th.

PROCESS-RESPONSE MODEL

An intuitive appraisal of the driving forces behind fluctuations of the water table yields the following: 1) the ocean tides will be expected to be the major forcing function, 2) surf conditions should be of considerable importance, 3) distance inland from the ocean free surface has been shown to be a determinant of the water table excursion (e.g., Emery and Foster, 1948; Issacs and Bascom, 1949), and 4) a small but significant factor might be found in atmospheric pressure fluctuations, with regard to both the rhythmic atmospheric tides and to progressive changes associated with the local weather conditions.

These factors were investigated within the conceptual framework of the general process-response model (Krumbein, 1963), in which a given state of the beach is considered to be a response to any number of geologic processes. Transformed into a linear mathematical model, the relationship becomes:

$$Y = f(X_1, X_2, X_3, \ldots, X_n)$$

where Y is designated the response element and X_1 to X_n are termed the process elements. In terms of the present study

$$W = f(T, X, D, P) \quad \text{where}$$

W = the change in elevation of the water table for a rising half-tide cycle

T = the tidal range for a rising half-tide cycle

X = the horizontal distance from a well to a point on the foreshore one half the vertical distance between the preceding low and the

succeeding high still water levels, measured at time of mid-tide

D = the vertical distance between high tide still water level and a horizontal line representing the average position of the swash at its highest level

P = the change in atmospheric pressure over the period of the rising half-tide cycle.

The variables are depicted graphically in Figure 5.

A sequential linear multiple regression analysis was chosen to determine the relative importance of the four process elements determining the magnitude of the water-table fluctuations. This method was developed by Krumbein (Krumbein, Benson, and Hempkins, 1964) and is reviewed and utilized by Harrison and Krumbein (1964). The method consists essentially of first performing a simple regression analysis of the dependent variable against the independent variables, taken one at a time. Regressions are then run using all possible pairs, triplets, etc., until all possible combinations of the variables have been exhausted. The advantages of this method are that interrelationships among the dependent variables themselves become apparent, and that data redundancy, i.e., the degree to which the same information is found in two or more variables, can be determined. Such an approach also may be used to rank the "independent" variables, taken singly and in combination, in order of the relative importance.

In addition, simple linear regression analyses were performed to derive a mathematical expression for the decrease in amplitude of water table fluctuations as a function of distance from the shoreline, and for the lag time of the input tide wave as a function of the distance from the shoreline.

For purposes of simplification, only those factors responsible for a rise in water table level were investigated. Furthermore, only periods of normal conditions were used in the regression analyses; no periods of rainfall or wave overtopping were included. The rising half-tide cycles used are indicated by heavy black lines on the tide curve of Figure 4.

The regression variables were derived from five measured variables of the beach-ocean-atmosphere system. The symbols used for the measured and derived variables, with their dimensions, sampling intervals, and error estimates, are summarized in Table 1.

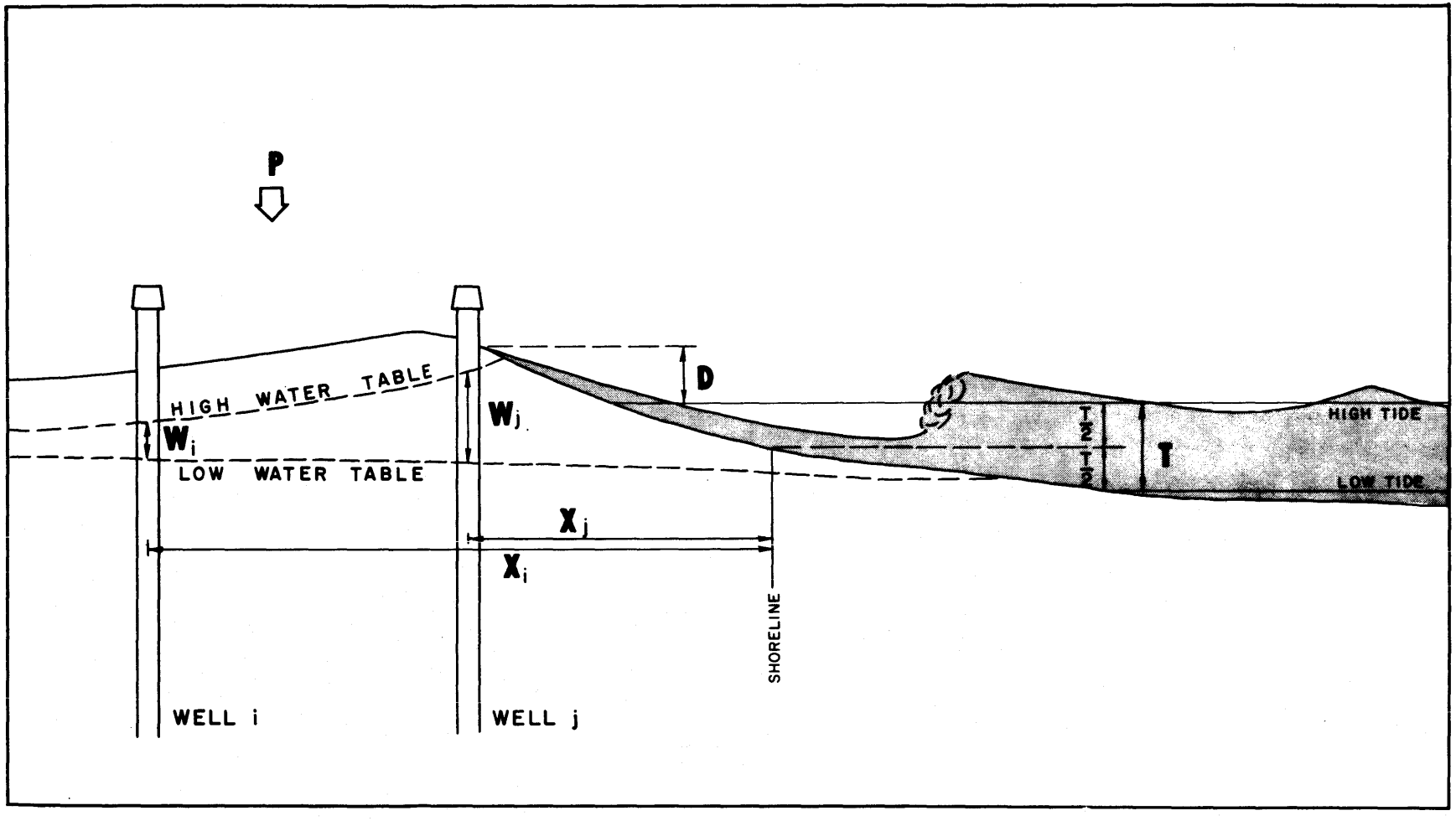

FIG. 5. Diagrammatic representation of the variables W, T, X, D, and P used in the multiple regression analysis.

Table 1.- Measured and Derived Variables, with Their Symbols, Sampling Frequency, Range, and Estimate of Accuracy.

Symbol	Description	Sampling frequency	Range in values	Estimate of accuracy
E_w	Elevation of groundwater table	10 and 15 minutes	0.291 to 1.999 m above msl	±0.01 m
E_t	Elevation of tidal plane	continuous	-0.55 to 1.27 m above msl	±0.05 m
S	Position of limit of swash	hourly and at high, low, and mid-tides	G to Z	±0.25 m
E_b	Elevation of beach profile station	high, low, and mid-tides	-0.940 to 3.693 above msl	±0.05 m above water ±0.10 m below water
P	Atmospheric pressure	continuous	29.550-30.285 in. Hg.	±0.005 in. Hg.
X	Distance of well from datum	Derived	6.83 to 72.62 m	±0.20 m
D	Swash height above still water level	Derived	0.04 to 0.56 m	±0.25 m
W	Change of E_w	Derived for each rising half-tide	0.003 to 0.870 m	±0.005 m
T	Tidal range	Derived for each rising half-tide	0.46 to 0.04 m	±0.05 m

The following assumptions were made: (1) the beach is internally homogeneous in texture and sediment characteristics; (2) changes in temperature, and therefore in the density and viscosity of the sea and ground waters, were not significant; and (3) that the angle of wave approach did not significantly alter the swash runup distance.

RESULTS

General Water-Table Dynamics

Time-dependent fluctuations of the water table for each of the 13 wells are represented by the curves in Figures 6 and 7. These are selected, but typical, parts of the total 30-day record. Figure 6 shows the changes in water level for normal, low-breaker conditions and will be used to illustrate several features of water table dynamics. Of particular interest are the following points:

1) the rise of the water table is generally more rapid than the fall. This phenomenon is due to the seaward-directed head gradient of the groundwater which, on the rising tide, contributes water to a given volume of the beach in addition to the seawater that is being added. Thus, at a point near the foreshore there is a rapid rise due to the addition of water from both directions, while the rate of fall is lessened due to the continuing addition of new, seaward-flowing groundwater;

2) at times of higher high tides, the water-table elevations on the foreshore exceed those on the backshore, resulting in a landward sloping water table. A landward flow of sea water might therefore be expected. Note also that such a slope reversal is uncommon on the lower high tide maxima;

3) the time required for the passage of the damped tidal wave through the sand prism is clearly seen. The time of maximum water table elevation increases for each well in a landward direction. The time required for the wave to pass from the shoreline to well number 1, a distance of approximately 56 meters, is on the order of 4.5 to 5.0 hours;

4) the decrease in amplitude of the tide wave as it passes through the beach is clearly seen. The range of the water table fluctuations in well number 1 is normally less than 5 centimeters; the range of the

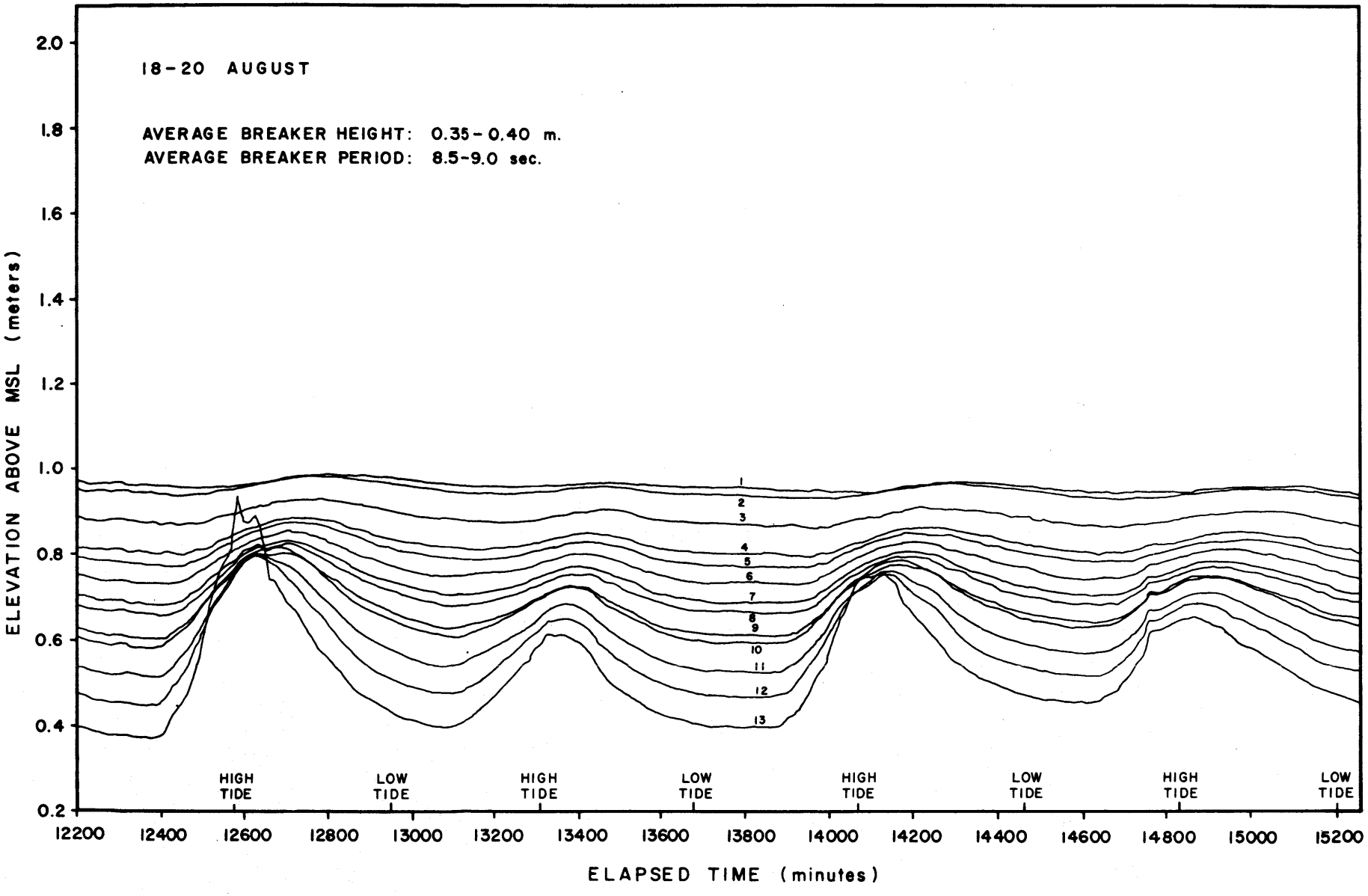

FIG. 6. Time series plot of water table fluctuations for a period of normal wave and tide conditions.

ocean tides is 0.7-0.8 meters. The decay of the tide wave approximates the exponential amplitudinal decay rate which would be expected from classical wave mechanics; and

5) the levels of the water table between certain wells are characteristically closer than between other wells, resulting in the pairing of the traces for wells 1 and 2, 4 and 5, 7 and 8, and 9 and 10. The underlying reasons for these pairings are not clear; there is apparently no relationship, however, between the pairs and the depth of the water table below the beach surface or the distance between wells. Since the phenomenon is stationary in both time and space, it is most likely due to some feature of the sand prism itself, such as the distribution of sand size, sorting, or packing.

In contrast to the normal conditions discussed above, Figure 7 shows the fluctuations in groundwater level for a period of two full tidal cycles during wave overtopping accompanying a local storm. The increase in the water table elevations is due in part to the increase in still water level (the storm surge), in part to the storm waves which reached heights of two meters and overtopped the berm crest, and in part to the decrease in atmospheric pressure accompanying the disturbance. The cumulative effect is a rapid rise in groundwater level; the restoration of the water table to its pre-storm position is seen to be much slower than the rise, taking approximately nine days to return to its original equilibrium position.

The flattening of the trough of the curve for well number 13 near the righthand edge of the figure is due to damage sustained to the well mechanism during the period of high waves; shortly thereafter well 13 ceased to function entirely, followed a short time later by well number 12.

Regression Analyses

The means and standard deviations of the data set used in the sequential multiregression analyses are presented in Table 2. The values for the tide range (T), the swash height (D), and pressure change (P) remain largely the same, since these are not peculiar to an individual well. The 15 sets of measurements obtained for wells 12 and 13 are for the pre-storm period, prior to the failure of these two wells.

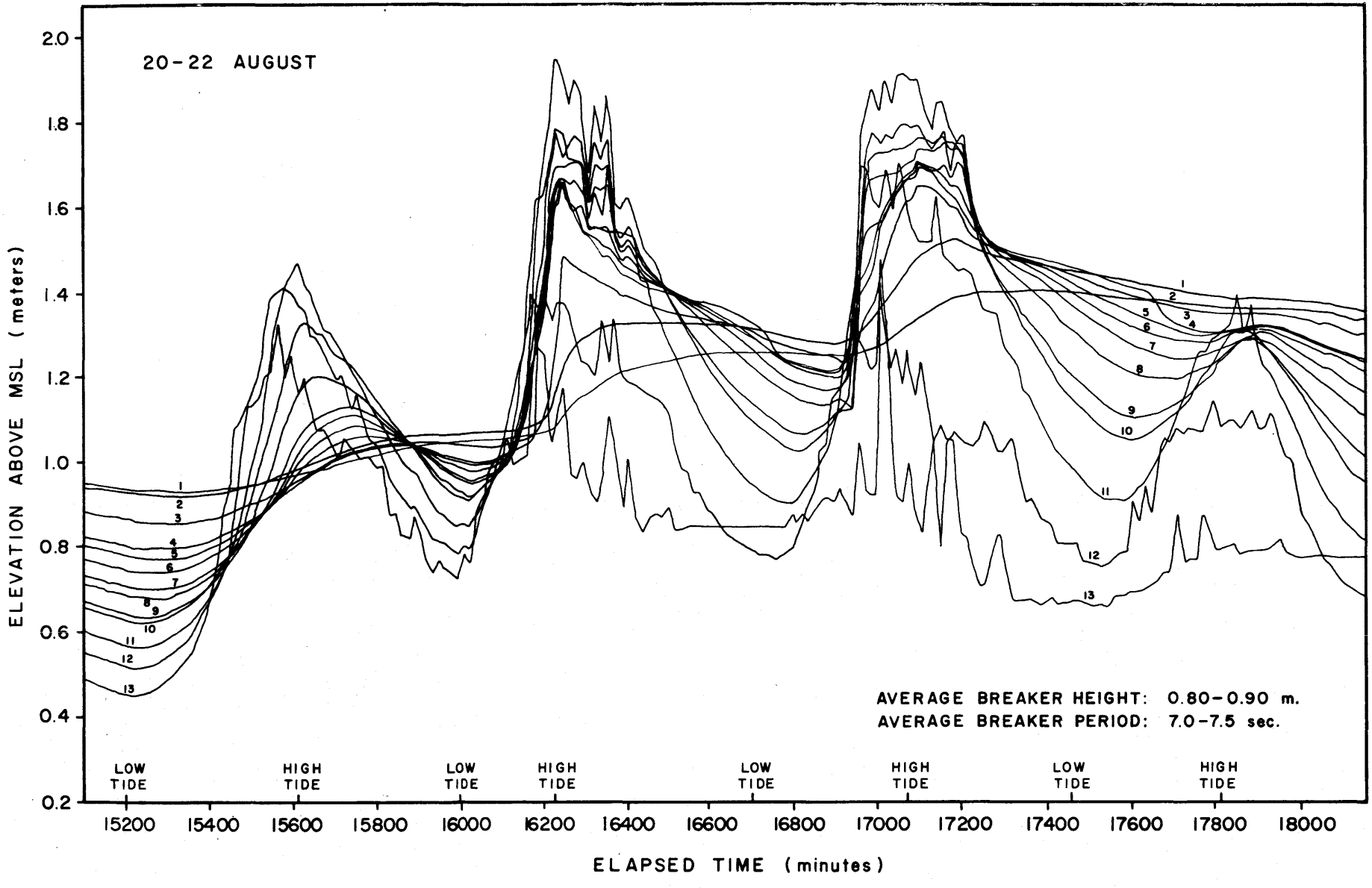

FIG. 7. Time series plot of water table fluctuations for a period of storm conditions.

Table 2.- Means and Standard Deviations for W, T, X, D, and P for Each of the 13 Wells.

Well no.	n	W		T		X		D		P	
		$\bar{x}$	s	$\bar{x}$	s	$\bar{x}$	s	$\bar{x}$	s	$\bar{x}$	s
1	28	0.033	0.020	0.81	0.17	59.37	6.38	0.28	0.14	-0.003	0.040
2	28	0.045	0.023	"	"	50.17	6.39	"	"	"	"
3	28	0.063	0.029	"	"	43.67	6.38	"	"	"	"
4	28	0.089	0.036	"	"	37.28	"	"	"	"	"
5	29	0.107	0.042	"	"	33.95	6.27	"	0.13	"	"
6	29	0.135	0.051	"	"	30.75	"	"	"	"	"
7	29	0.164	0.061	"	"	27.52	"	"	"	"	"
8	29	0.183	0.069	"	"	24.30	"	"	"	"	"
9	29	0.236	0.089	"	"	21.11	6.29	"	"	"	"
10	29	0.284	0.110	"	"	17.97	6.26	"	"	"	"
11	29	0.360	0.148	"	"	14.90	6.27	"	"	"	"
12	15	0.391	0.135	0.89	0.11	16.08	5.84	0.26	0.14	0.011	0.026
13	15	0.517	0.191	"	"	12.82	"	"	"	"	"

The results of the regression analyses for each of the 13 wells are given in Tables 3 and 4. It should be noted that wells 12 and 13 have only 15 samples each; the analyses for these two wells, therefore, lack adequate numbers of observations, and the results are not directly comparable to wells 1 through 11. They are tabulated insofar as they may serve as indicators of trends on the foreshore.

Table 3 lists the predictor equations derived for each well and serves to show the signs of correlation for the process variables. Tidal range (T) and swash height above still water level (D) are positively correlated; i.e., an increase in the magnitude of each independent variable causes an increase in the elevation of the water table in each of the 13 wells. The distance of a well from the foreshore (X), and change in atmospheric pressure (P), on the other hand, are negatively correlated; an increase in either of these variables results in a decrease in the level of the water table in a given well. The correlations are consistent throughout the data set, except for (P) in well number 13, which, as stated above, lacked a sufficient number of data points.

The total percent reductions of the sums of squares of W accounted for by T, X, D, and P taken together are given in Table 4. Also given are the individual contributions of T, S, D, and P, presented as percentages of the total sums of squares reduction for all four process variables; these values are plotted in Figure 8. The results show that the four process variables chosen account for a greater per cent of the variability in the water table fluctuations near the shoreline than they do on the backshore. They show also that the effects of atmospheric pressure on water-table fluctuations are relatively more significant near the dune line, but become less so in a seaward direction; the distance of an individual well from the shoreline and the swash height above still water level become relatively more important toward the shoreline, while the relative importance of the tidal range becomes less.

DISCUSSION

The equations listed in Table 3 are the results of linear multiple regression analyses. It is known, however, that nonlinear relationships exist between the water table fluctuations and certain of the independent variables; e.g., water table changes and distance from

Table 3.- Regression Equations for W for the 13 Wells.

Well no.	Equation
1	W = - 0.0206 + 0.0787(T) - 0.0005(X) + 0.0729(D) - 0.3301(P)
2	W = - 0.0014 + 0.0899(T) - 0.0009(X) + 0.0703(D) - 0.2707(P)
3	W = - 0.0070 + 0.1342(T) - 0.0013(X) + 0.0704(D) - 0.2825(P)
4	W = - 0.0009 + 0.1706(T) - 0.0020(X) + 0.0949(D) - 0.2603(P)
5	W = + 0.0143 + 0.1904(T) - 0.0027(X) + 0.1079(D) - 0.2278(P)
6	W = + 0.0165 + 0.2288(T) - 0.0034(X) + 0.1286(D) - 0.2273(P)
7	W = + 0.0236 + 0.2703(T) - 0.0044(X) + 0.1497(D) - 0.2097(P)
8	W = + 0.0113 + 0.3009(T) - 0.0051(X) + 0.1735(D) - 0.2323(P)
9	W = + 0.0272 + 0.3663(T) - 0.0072(X) + 0.2190(D) - 0.1968(P)
10	W = + 0.0117 + 0.4409(T) - 0.0092(X) + 0.2685(D) - 0.1509(P)
11	W = - 0.0669 + 0.5874(T) - 0.0120(X) + 0.4479(D) - 0.1757(P)
12	W = + 0.0086 + 0.4336(T) - 0.0093(X) + 0.5776(D) - 0.6278(P)
13	W = + 0.2880 + 0.4121(T) - 0.0175(X) + 0.2793(D) + 0.1360(P)

Table 4.- Contributions of T, X, D, and P to Explanation of Variation in W.

Well no.	n	Total % Red. in SS	Percentage of the total sums of squares reduction.			
			T	X	D	P
1	28	50.69	26.94	22.61	22.35	28.08
2	28	48.92	29.09		22.20	23.39
3	28	57.85	35.65	23.78	19.91	20.63
4	28	62.64	35.01	24.90	20.85	19.22
5	29	65.21	33.82	25.71	21.45	19.00
6	29	65.33	33.64	25.86	21.58	18.90
7	29	66.70	32.84	26.59	21.70	18.84
8	29	67.42	32.26	26.93	21.93	18.96
9	29	67.32	30.45	27.27	22.38	18.98
10	29	67.26	29.63	27.61	22.40	18.88
11	29	71.40	28.70	27.95	24.08	19.24
12	15	(85.75)	(23.54)	(28.68)	(27.52)	(20.23)
13	15	(64.55)	(24.47)	(30.76)	(23.35)	(21.40)

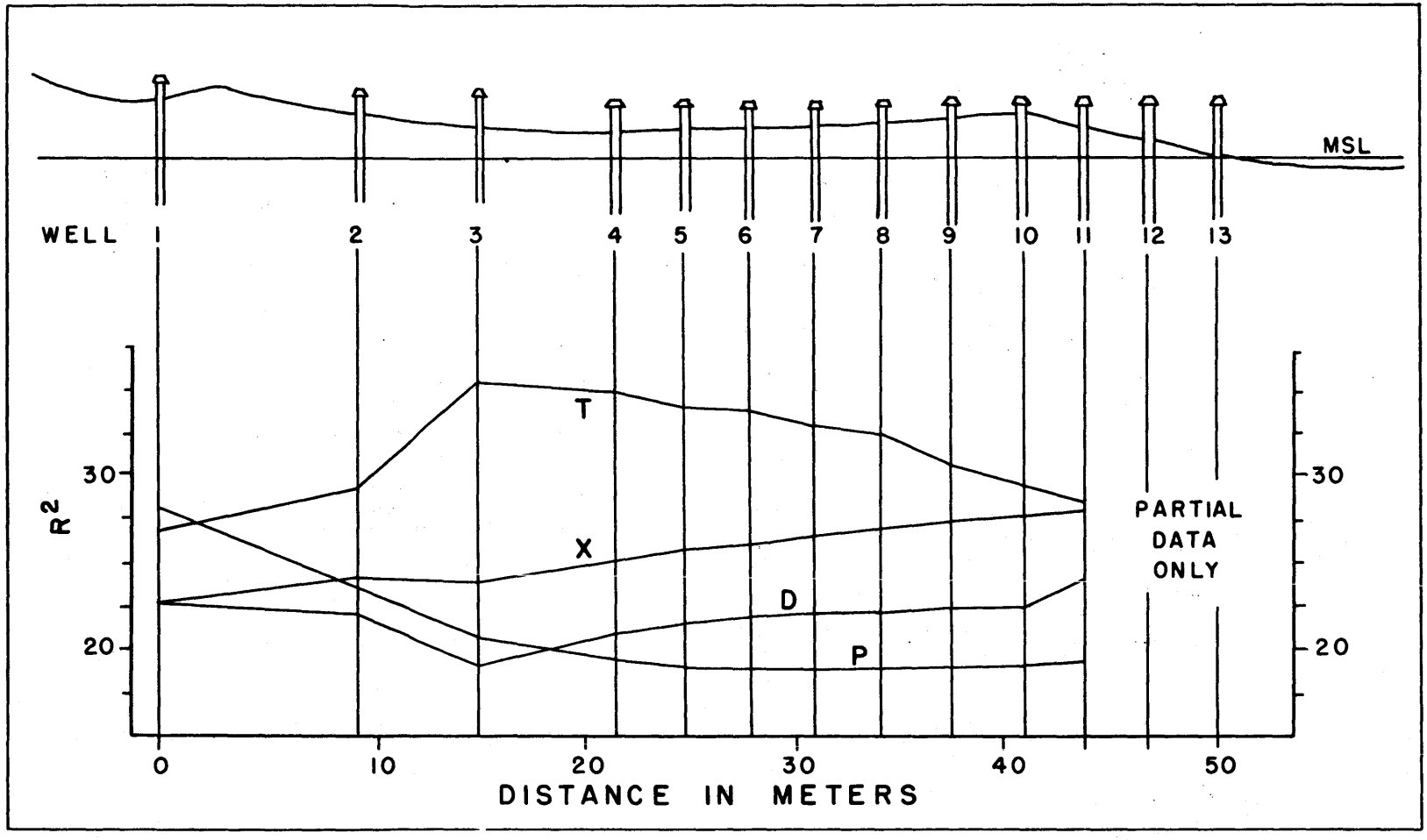

FIG. 8. Relative importance of T, X, D, and P in the reduction of the sums of squares of W.

the shoreline (Fig. 9). A deterministic equation for fluctuations of the water table must account for these nonlinear dependencies; predictive equations based on multiregression analysis for each well, on the other hand, need not account for the nonlinearity if the data are such that they may be satisfied by a linear expression. Scatter diagrams for individual wells indicated that the latter method could be used here. The data plotted in Figure 9 represent the combined data from the 13 wells; these data were in fact analyzed in 13 individual regression analyses, and resulted in predictor equations for water table fluctuations at 13 points on the beach.

The reliability of the predictor equations listed in Table 3, as indicated by the per cent sums of squares accounted for, ranges from fair in the backshore area to good on the foreshore; the sums of squares accounted for generally increases in a seaward direction. It may be concluded from these observations that water-table fluctuations in the backshore and dune areas are significantly influenced by variables not taken into account in the present study. The major factor believed to be of significance in the backshore is the groundwater pressure head, as influenced by local weather conditions in the supply or charging area.

The major forcing function, as shown by the regression analyses, is the action of the tides. The progressive tide wave evident on the free surface is propagated into the sand prism; the amplitude and period of the tidal oscillations at the foreshore are essentially the same as those in open waters; as the wave form passes into the beach, however, and is propagated in the water table, certain fundamental changes take place, which are functions of the porosity and permeability of the sand, of the pressure gradient encountered, and of the amplitude of the tidal fluctuations. The amplitude of the wave is rapidly reduced, as is presented in Figure 9, in which the rise of the water table over a rising half-tide is plotted against distance from shore. A wide range of water level fluctuations are observed at the foreshore, corresponding to the various amplitudes of the input tidal wave; the water table fluctuations are reduced to an essentially constant value of about two to three centimeters at a distance of 60 to 65 meters from the shoreline. The least-squares curve for the data is represented by the following equation:

$$W = f(1/X) = -0.04 + (0.52/X)$$

which resulted from a regression of W on 1/X. Even

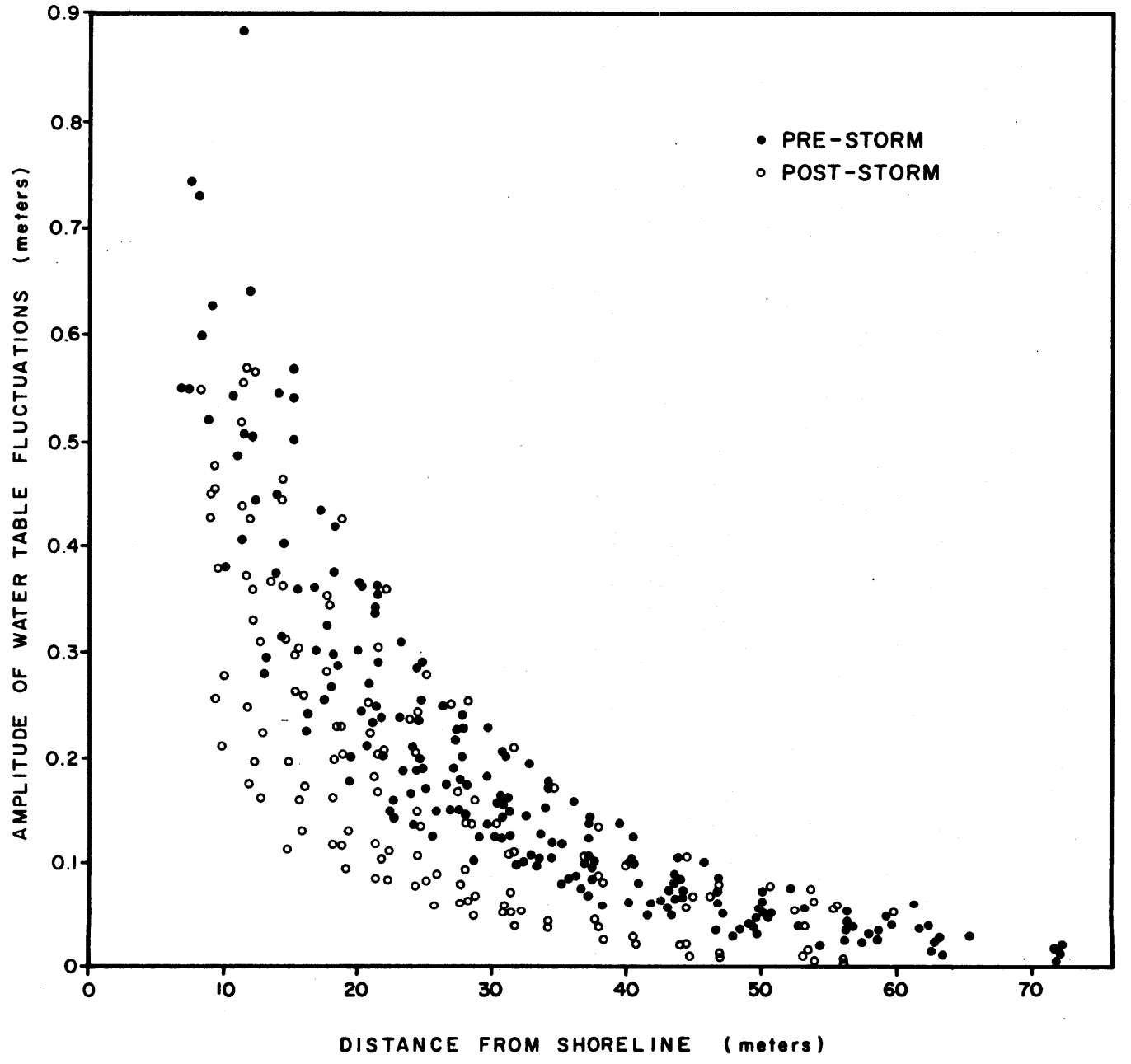

FIG. 9. The amplitude of the water table fluctuations as a function of distance from the shoreline.

though 1/X resulted in a somewhat better fit, an exponential function would physically be more appealing.

The greater variation of the post-storm data exhibited in Figure 9 reflects the greater variability of the tidal amplitudes following the storm (see Fig. 4). A plot of the ratio of the water table rise and the tidal amplitude, W/T, versus distance from the shoreline (Fig. 10) effectively eliminates that variation and shows the rise of the water table as a function of both tidal amplitude and distance from the shoreline.

Lag times of the input tide waves are presented as a function of distance from the shoreline in Figure 11; regression lines are shown for the lag of the high water crest, the low water trough, and for all observations combined. The data are from the sample periods as listed in the appendix. The plot indicates an average lag of the wave of approximately one hour for each 18 meters of beach penetrated; the lag is represented by the equation

$$L = 50.38 + 3.27\ X$$

where

L = lag time in minutes

X = distance from shoreline in meters.

The lag time determined here is somewhat less than those observed by Emery and Foster (1948), who found that the wave lags from one to three hours at a distance of from 20 to 40 feet (approximately 6 to 13 meters) from the shoreline.

The slope of the low water regression line is less steep than the high water line, indicating that the high water crest is propagated through the sand prism somewhat slower than the low water trough; this differential lag phenomenon can also be seen in the time series plot of water table elevation (Fig. 6) by comparing the travel times of the crests and troughts between wells 13 and 1. The lag differential is another manifestation of the seaward-directed pressure head of the ground water, which also causes the water table to rise more rapidly than fall, as was discussed earlier.

The increase in lag time appears to be generally linear throughout the range studied. However, the lag time at the shoreline should, by definition, be

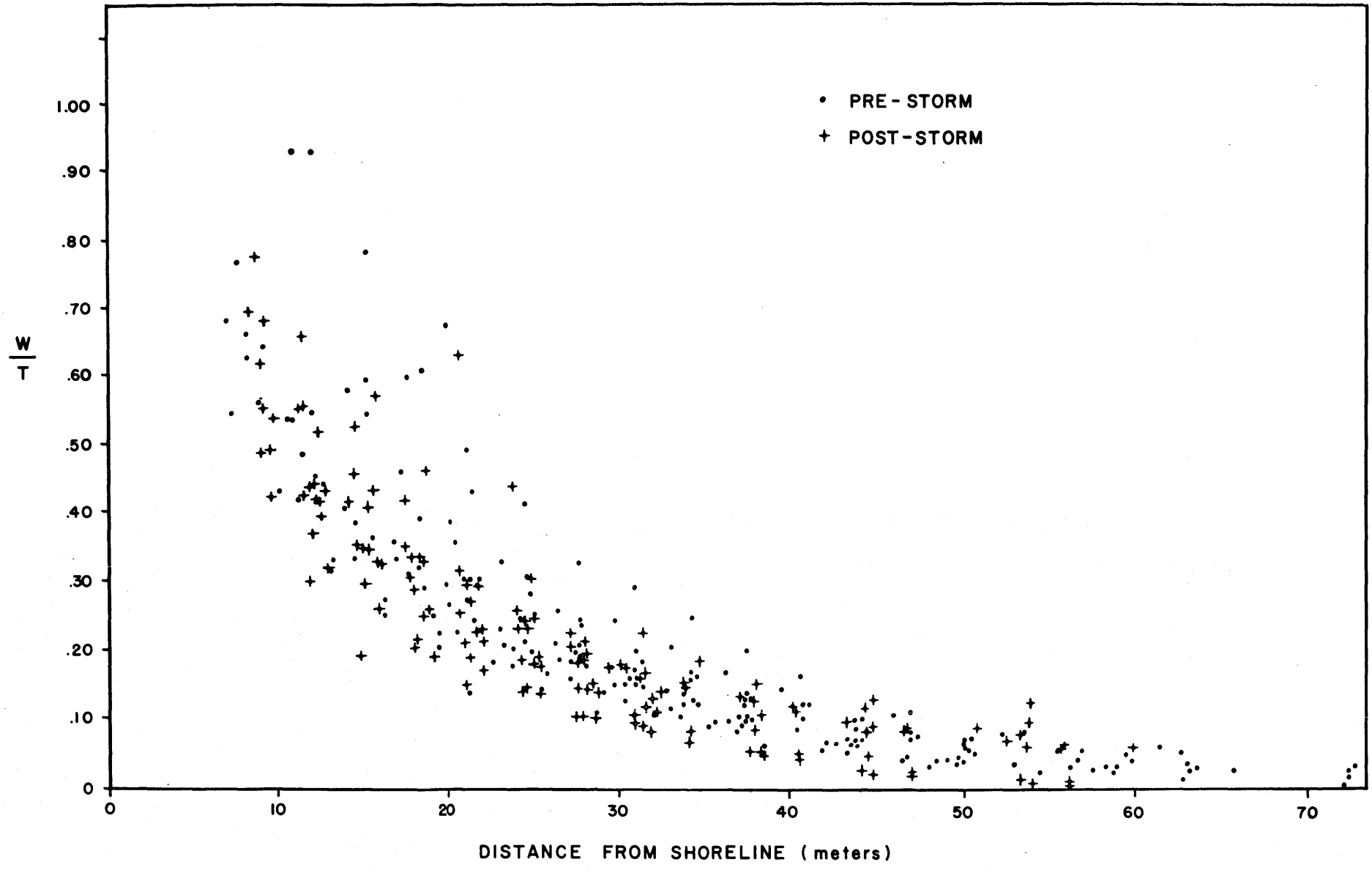

FIG. 10. The ratio of the rise of the water table and the rise in still water level as a function of distance from the shoreline.

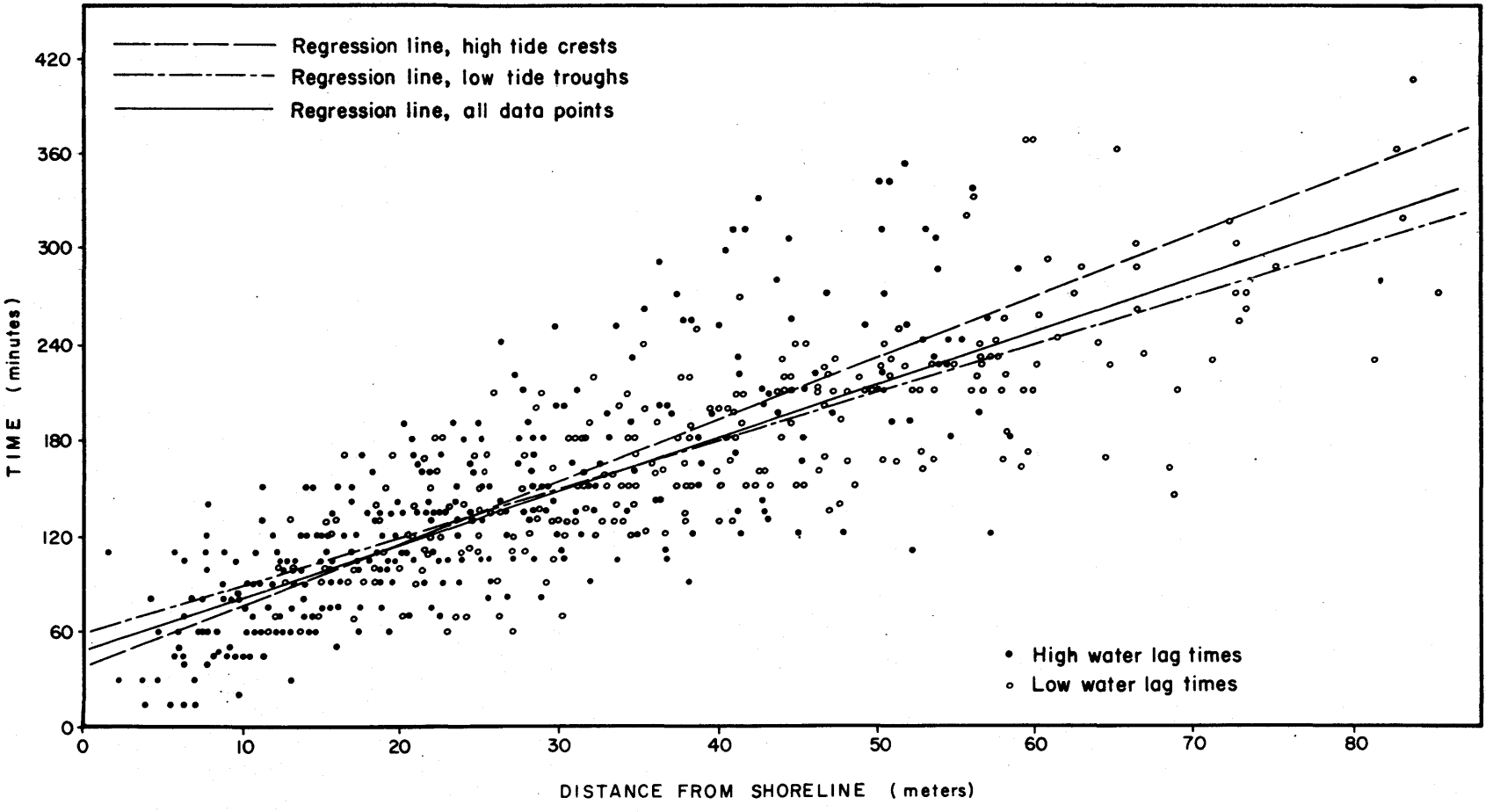

FIG. 11. Lag time of the input tide waves, as a function of distance from the shoreline.

zero, whereas the regression analyses show initial lag times of 38 to 59 minutes. The discrepancy may be due to measurement error; it may on the other hand, be due to a somewhat modified propagation mechanism at work in the first 10-15 meters of the beach. Such an assumption would imply that the rate of energy dissipation is greater during the first 10 to 15 meters of the beach, followed by a lesser rate of dissipation for the backshore area.

The tidal forces predominate throughout the backshore area; near the foreshore, the tidal forces are subordinate to the swash height and the distance from the shoreline; the effects of both die off rapidly in a landward direction. The relative importance of each of the four process variables is graphically depicted in Figure 8.

The effect of rainfall on the level of the water table appeared to be very slight during the study period. The largest period of rainfall for which water table data were obtained amounted to 0.83 inches (2.11 cm). The effect on the water table can be seen (Fig. 12) as an increase of approximately 1.5 cm in water table level; the increase is consistent for all wells in the transect. The rapid and large increase in water table level (Fig. 7) is due mainly to the action of the high waves and the storm surge and possibly to atmospheric pressure effects; atmospheric pressure suddenly dropped 0.735 inches of H_g just prior to the increase in water column of about 18 cm.

A possible source of noise in the data which may account for some part of the low sums of squares reductions may be found in changes in beach configuration which were not due to changing wave or water table conditions. Such changes were observed in the long-shore passage of sand waves, a phenomenon which belies the original assumption of a two-dimensional beach. Such changes are illustrated in Figure 13, which shows the position of the shoreline plotted against time for each rising half-tide of the study period. The fluctuations of the shoreline are quasi-periodic and have a period of six to seven days; no correspondence is seen between the changes in shoreline position and any changes in the wave or tidal characteristics. Similar features are not uncommon along the middle-Atlantic coast and have been investigated by Sonu and Russel (1966) and Dolan (1970) at Nags Head, North Carolina, where they are quite pronounced. Future beach studies along the mid-Atlantic coast will necessarily have to consider the beach as a three-dimensional feature.

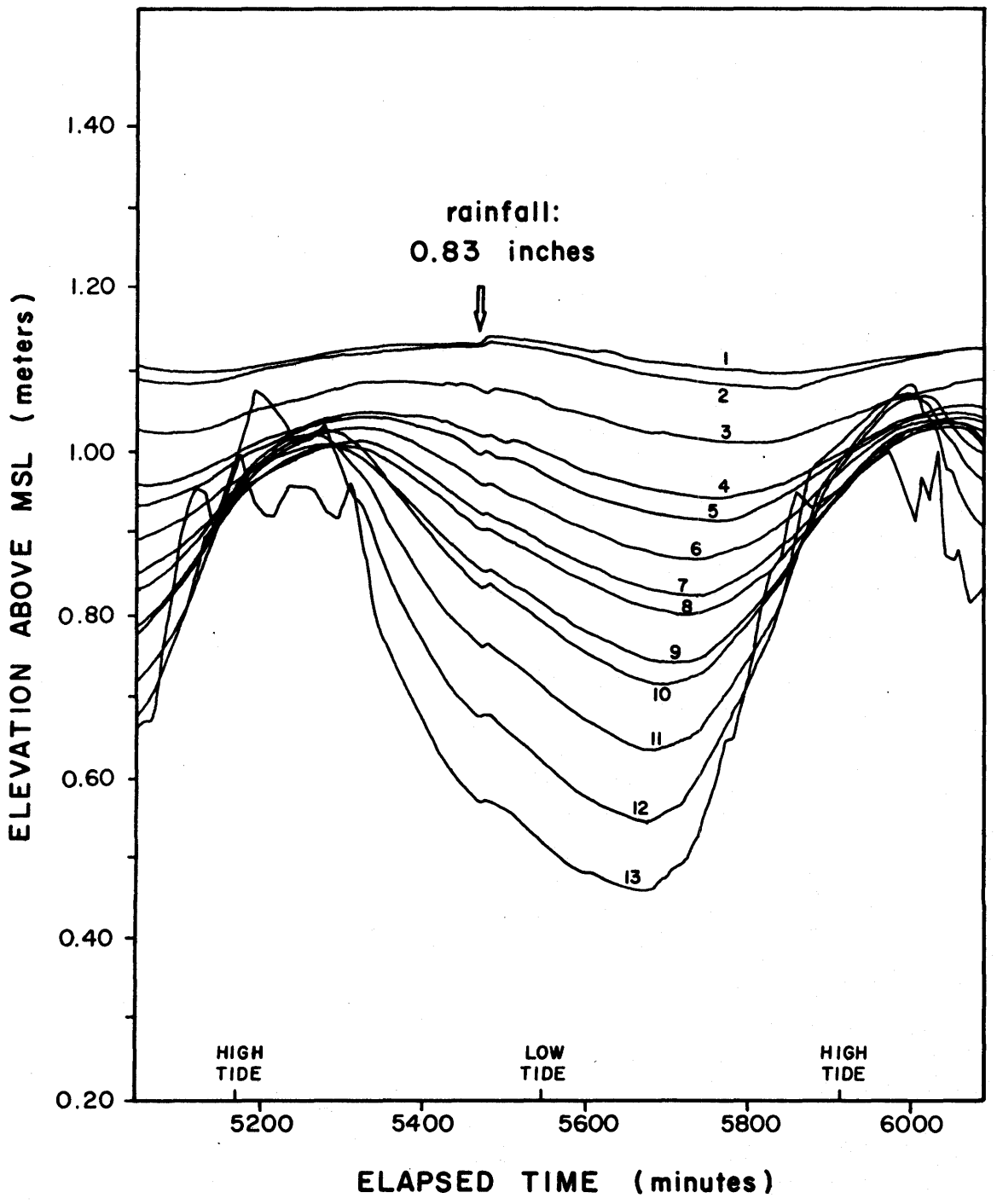

FIG. 12. Effect of rainfall on the level of the water table.

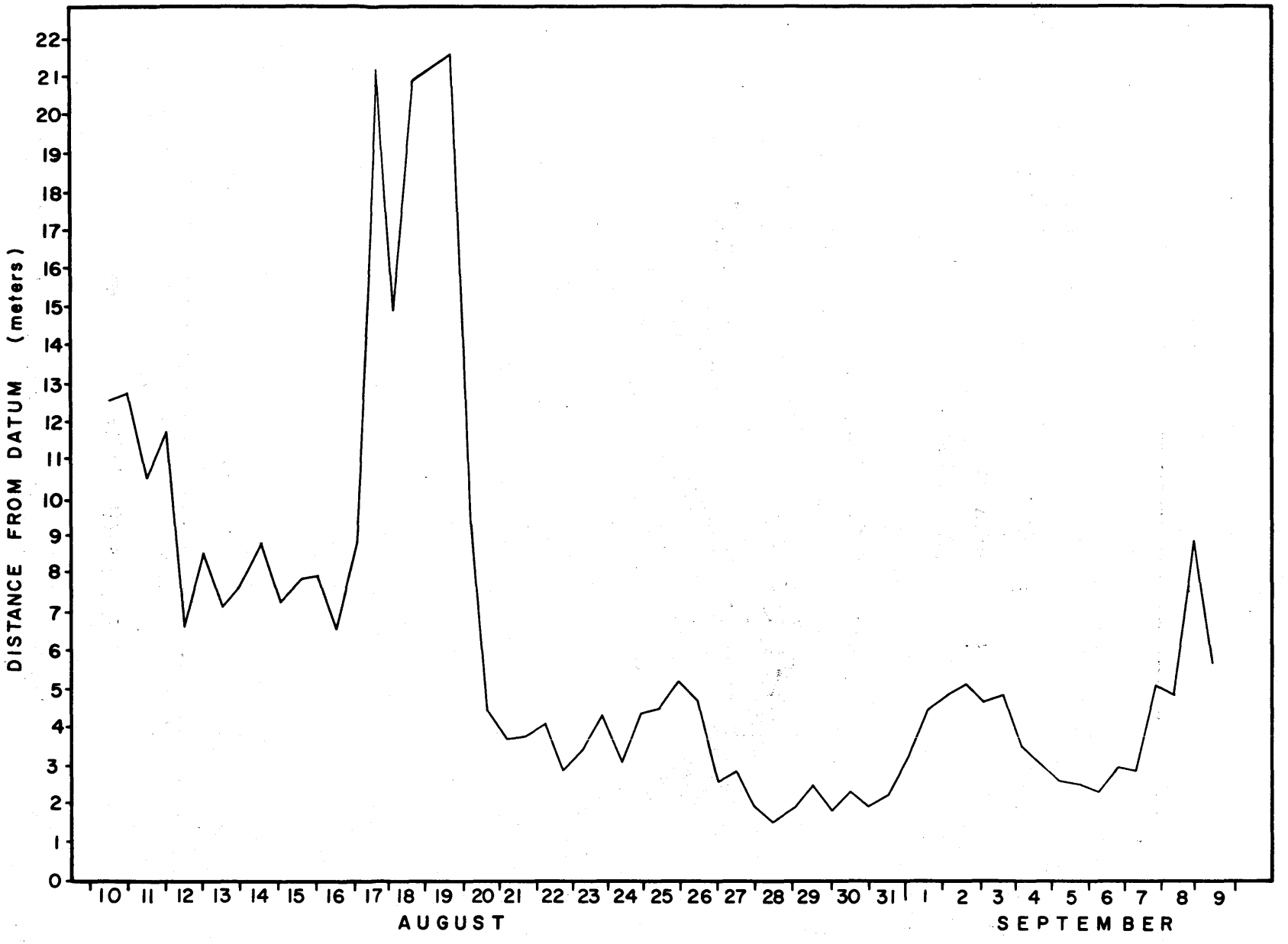

FIG. 13. Position of the shoreline as a function of time for the 30-day study period.

CONCLUSIONS

Quantitative and qualitative consideration has been given to the variations in the level of the water table of a marine beach and to the factors responsible for these variations.

The following conclusions have been drawn from the study:

(1) The tidal fluctuations of the free ocean surface are the major forcing function with regard to water table elevational changes.

(2) The distance from the shoreline (and thus from the source of energy input) is a more important determinant of the level of the water table near the foreshore than is the oscillation of the tidal plane.

(3) The input tide wave decreases rapidly in amplitude upon entering the beach, and dies off exponentially until a semi-constant value of two to three centimeters is attained approximately 60 meters from the shoreline.

(4) The input tide wave exhibits a lag time which increases landward at about the rate of one hour per 18 meters of beach penetrated.

(5) Rainfall did not alter the water table level to a significant degree during the study period.

REFERENCES

Bagnold, R. A., Beach formation by waves; some model-experiments in a wave tank, Jour. Inst. Civil Engrs., 15, 27-52, 1940.

Dolan, R., Sand waves - Cape Hatteras, North Carolina, Shore and Beach, 38(2), 22-25, 1970.

Duncan, J. R., The effects of water table and tide cycle on swash-backwash sediment distribution and beach profile development, Marine Geology, 2(1), 186-197, 1964.

Emery, K. O., and J. F. Foster, Water tables in marine beaches, Jour of Marine Research, 7(3), 644-654, 1948.

Giese, G. S., Beach pebble movements and shape sorting indices of swash zone mechanics, Ph.D. Thesis, of Geophys. Sci., Univ. Chicago, Chicago, Ill., 65 p., 1966.

Grant, U. S., Influence of the water table on beach aggradation and degradation, Jour. of Marine Research, 7(3), 655-660, 1948.

Harrison, W., and W. C. Krumbein, Interactions of the beach-ocean-atmosphere system at Virginia Beach, Virginia, U. S. Army Corps Engrs., Coastal Engineering Research Center, Tech. Memo. 5, 20 p., 1964.

Harrison, W., E. W. Rayfield, J. D. Boon, III, G. Reynolds, R. B. Grant, and D. Tyler, A time series from the beach environment, E.S.S.A. Res. Lab. Tech. Memo. AOL-1, 85 p., 1968.

Harrison, W., Empirical equations for foreshore changes over a tidal cycle. Marine Geology, 7(6), 529-551, 1969.

Issacs, J. D., and W. N. Bascom, Water table elevations in some Pacific Coast beaches, Transactions, Amer. Geophys. Union, 30(2), 293-94, 1949.

Krumbein, W. C., A geological process-response model for analysis of beach phenomenon, Beach Erosion Board Bull., 17, 1-15, 1963.

Krumbein, W. C., B. T. Benson, and W. B. Hempkins, WHIRLPOOL, a computer program for "sorting out" independent variables by sequential linear regression, Northwestern University, Tech. Memo. 14, 1964.

Sonu, C. J., and R. J. Russell, Topographic changes in the surf-zone profile, 10th Conference on Coastal Engineering, Proc. Vol., 1966.

Strahler, A. N., Tidal cycle of changes in an equilibrium beach, Sandy Hook, N. J., Columbia University, Dept. of Geology, ONR Task Rept. 4, 51 p., 1964 (also: Jour. of Geology, 74(3), 247-268, 1966).

CHANGES IN FORESHORE SAND VOLUME ON A TIDAL BEACH: ROLE OF FLUCTUATIONS IN WATER TABLE AND OCEAN STILL-WATER LEVEL

W. Harrison

ABSTRACT

A 30-day-long time series of observations of variables in the beach-ocean-groundwater system was made at Virginia Beach, Virginia, during August and September, 1969. Results of linear multiregression analysis of the data show that the change in ocean still water level, SWL, is the single most important variable influencing changes in quantity of foreshore sand, ΔQ_f, over intervals of half-tidal-cycle to tidal-cycle length. An index of groundwater head, I, is the next strongest predictor of ΔQ_f, followed closely by the number of swash events, S, over the time interval in question. Predictor equations that are presented for ΔQ_f are the strongest yet obtained and when one of the equations was tested upon a completely independent set of data it explained 40 percent of the observed variability.

The importance to ΔQ_f of change in ocean SWL and groundwater head is apparent when it is realized that, statistically, the following equation explains 67 percent of the variability in quantity of foreshore sand eroded or deposited over a tide-cycle interval:

$$\Delta Q_f = -0.9762 - 0.04857(\Delta h) + 0.0021636(I_2)$$

where ΔQ_f is in m^3, Δh is the net change (in cm) in SWL relative to the SWL at initial low water, and $I_2 = (y_{10} - y_{11})\, x$, where Y_{10} and y_{11} are the MSL elevations of the water table, in mm, in two wells, and x is the distance of well 11 from the foreshore surface in m. (The value of x ranged between 2.6 and 12.0 m, the distance between wells 10 and 11 was 3.1 m, and subscript 2 stands for time of rising half tide).

INTRODUCTION

The earliest suggestion of the importance of swash percolation and groundwater flow to beach dynamics seems to have been made by Bagnold (1940). His laboratory experiments were followed by the field studies of Grant (1946, 1948), Emery and Foster (1948), Issacs and Bascom (1949), and Duncan (1964). Although

these studies indicated the importance of water-table fluctuations to beach foreshore changes, they did not quantify the processes involved. Harrison (1969) made some progress toward quantification of the relationship between changes in the water-table and foreshore sand volume. He performed multiregression analysis on a 26-day-long time series of observations collected in 1966 from a beach at Camp Pendleton, Virginia (Fig. 1). The groundwater head was found to be one of the strongest predictors of deposition or depletion of foreshore sand, over a tidal-cycle interval. "Groundwater head" was expressed as the vertical distance between the water-table outcrop on the foreshore and the still-water level in front of the breaking waves.

The present study deals first with data for the beach-ocean-groundwater system that were gathered in 1969 from a beach at Ft. Story, Virginia (Fig. 1). A 30-day-long time series of observations of the variables listed in Table 1 was obtained to document pertinent interactions in the system. Thirteen wells for monitoring the water table (Fig. 1, 1-13), and 26 pipe-stations (Fig. 1, A-Z) for monitoring changes in beach elevation, were positioned along an 83-m-long transect oriented perpendicular to the shoreline and extending seaward from the edge of the foredune. Four multi-tube probes (Fig. 1, I-IV) were installed for extracting small amounts of groundwater for tests of salinity and to facilitate dye tests of flow characteristics. Salinity was determined at the site using a Goldberg refractometer (Behrens, 1965).

The water wells consisted of 1) a #18-slotted PVC pipe, 102-mm in diameter, jetted into the beach to a depth of 3.5 m and 2) a 32-mm-O.D. steel pipe jetted to a depth of 5 m and touching the PVC pipe. A float-pulley system mounted on the pipes drove a potentiometer which provided a DC output voltage that corresponded (linearly) to the instantaneous water level. Water-table elevations were recorded at the site on computer-compatible magnetic tape (after A/D conversion). Details for this and the other measurement systems, as well as the complete time-series of measurements for the variables of Table 1, appear in Harrison and Fausak (1970).

The gently-sloping, quartz-sand beach at Ft. Story (Fig. 1) has a representative porosity of about 34 percent (medium grain diameter of pit samples ranged between 0.37 and 0.59 mm). The mean range of the astronomical tide is about 0.85 m for Cape Henry, the spring range is 1.1 m, and tide is semidiurnal

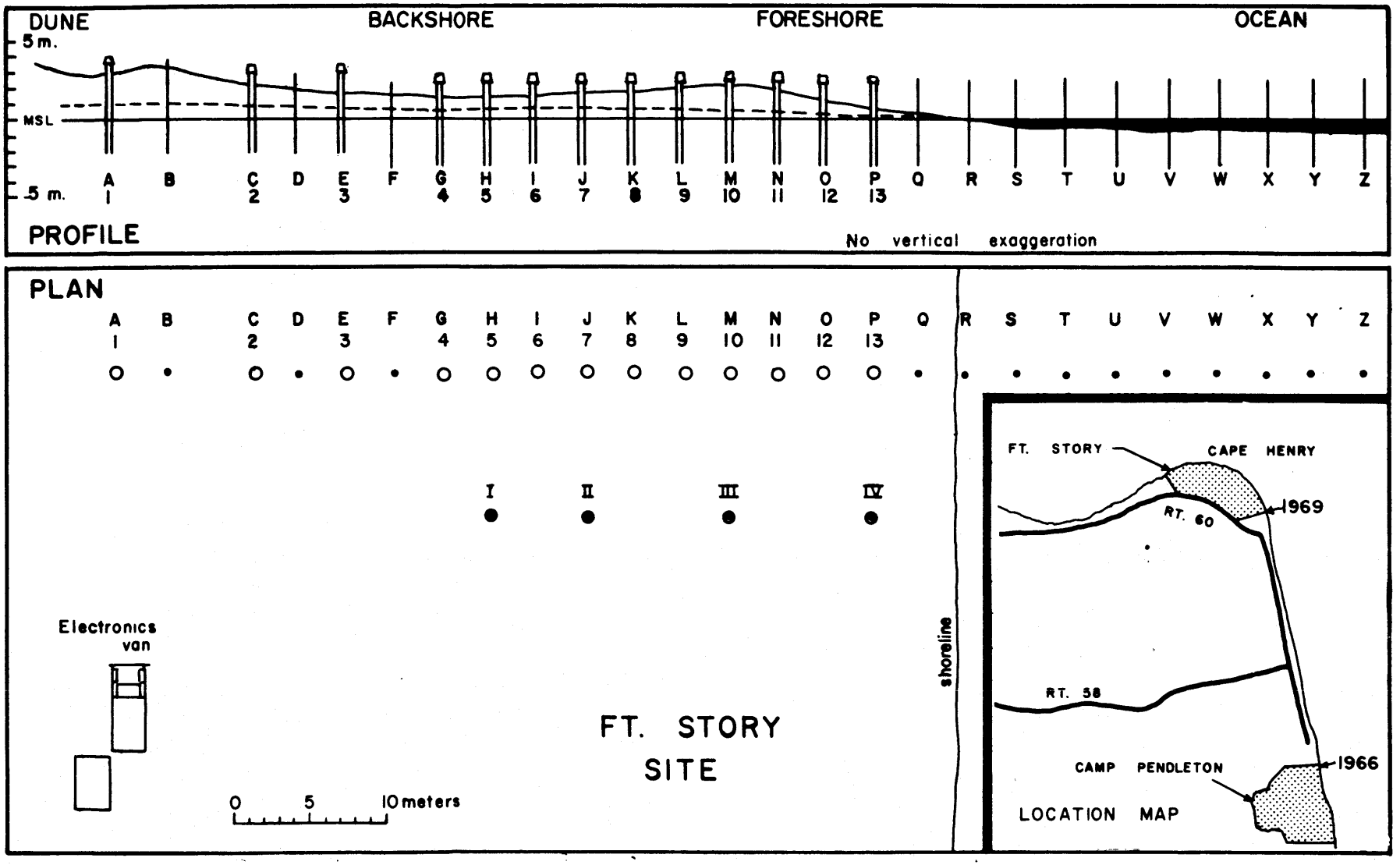

FIG. 1. Plan and profile views of the Ft. Story study site, showing typical beach and water-table profiles, beach profiling stations (A-Z), wells for monitoring water table (1-13), and groundwater sampling probes (I-IV). Inset shows locations of the 1969 and 1966 studies, at Ft. Story and Camp Pendleton, respectively, Virginia Beach, Virginia.

TABLE 1. Measured and Derived Variables for the Beach-Ocean-Groundwater System at Ft. Story, Virginia Beach, Virginia, for the Period 10 August through 9 September, 1969.

Symbol	Description	Sampling Frequency	Range in Values	Estimate of Accuracy
E_b	Elevation of beach surface	High, low, and mid-tide levels	-0.940 to 3.693 m (MSL)	±0.005 m above water, ±0.020 m below water
E_t	Elevation of tidal plane	Continuous	-0.55 to 1.27 m (MSL)	±0.05 m
E_w	Elevation of water table	Either every 10 or every 15 minutes	0.291 to 1.999 m (MSL)	±0.003 m
$\overline{H}_b$	Mean height of 50 successive breaking waves	High, low, and mid-tide levels	0.19 to 1.30 m (MSL)	±0.10 m
$2h_o$	Rise or fall in ocean SWL over half-tide cycle	Derived from E_t	-125 to +128 cm	±0.5 cm
I	Groundwater head index	Derived (high, low, and mid-tide levels)	+1408 to -1234	±3
m	Slope of the foreshore	Derived (high, low, and mid-tide levels)	4.0° to 11.0°	±0.5°

(Continued)

TABLE 1. (Continued)

Symbol	Description	Sampling Frequency	Range in Values	Estimate of Accuracy
p	Barometric pressure	Continuous	29.550 to 30.285 in. of Hg.	±0.005 in Hg.
r	Rainfall	Hourly during storms	Trace to 2.22 cm	±1.0 mm
s	Position of swash limit	Hourly, and at high, low, and mid-tide levels	Sta. G to Sta. Z (Fig. 1)	±0.25 m
S	Total number of swash events over a time interval	Derived from $\overline{T}_b$	2150 to 4861 (½ cycle) 4857 to 8960 (full cycle)	±5
$\overline{T}_b$	Mean period of 50 successive breaking waves	High, low, and mid-tide levels	3.96 to 13.20 sec.	±0.02 sec.
x	Horizontal distance from well no. 11 to point on foreshore ½ vertical distance between successive extremes in SWL	Derived from E_b and E_t	2.6 to 12.0 m	±0.03 m

(Continued)

TABLE 1. (Continued)

Symbol	Description	Sampling Frequency	Range in Values	Estimate of Accuracy
Δh	Net change in ocean SWL over a tidal cycle	Derived from $2h_o$	-13 to +16 cm	±0.5 cm
ΔQ_f	Change in quantity of foreshore sand over a time interval	Derived from E_b	-2.74 to +3.37 m^3 for ½ tide cycle; -1.95 to +1.70 m^3 for entire cycle	±0.04 m^3

with a slight diurnal inequality.

Low, long-period swells characterized the first ten days of the 30-day study period. They were followed by three days of high, short-period waves that, combined with a storm surge, resulted in flooding of the backshore (Fig. 1) for two full tidal cycles. (Nine days were required for the groundwater level to return to its pre-storm position). The remaining 17 days of the study had a wave climate similar to the first 10 days. Rainfall amounted to 10.2 cm during the 30-day period. The greatest hourly rainfall was 2.22 cm, an event that caused an increase of about 1.5 cm in the water level at all wells. The effects of rainfall, as well as sudden fluctuations in atmospheric pressure, can be ignored in what follows.

Figure 2 shows the groundwater salinity structure at Ft. Story for the summer beach (17 August 1969); that is, the normal condition prior to the first "northeaster" of the season. A pronounced salinity gradient is in evidence beneath and to the seaward side of the berm crest. The saline front is seen to move slightly seaward, at low water (1733 hrs., Fig. 2), from the previous high-water position (1200 hrs.). Most of the beach foreshore fluctuations occur either above or seaward of the salt front. Saltier ocean water infiltrates the berm and finds its way into the groundwater at high tide. The seaward-directed head gradient causes the front to move seaward as the tide falls.

The first northeast storm sent ocean water over the berm and onto the backshore. Groundwater salinity increased markedly (Fig. 2, 27 Aug. 69). Flushing of the saline water could be gaged by the distance moved by the 18 ‰ isoline -- about 8 m -- in the 87.5 hours between 1430 hours on 27 August and 0600 hours on 1 September.

MODEL FOR FORESHORE VOLUME CHANGE

Figure 3 shows the change in foreshore sand volume, over a half-tidal cycle, plotted as a function of the change in volume of groundwater in the beach. Both the change in groundwater volume and the change in foreshore sand volume were computed from measured changes in cross-sections plotted for low-tide and high-tide conditions. The groundwater volume change was for a unit distance along the shore that extended landward from the foreshore for a distance of about

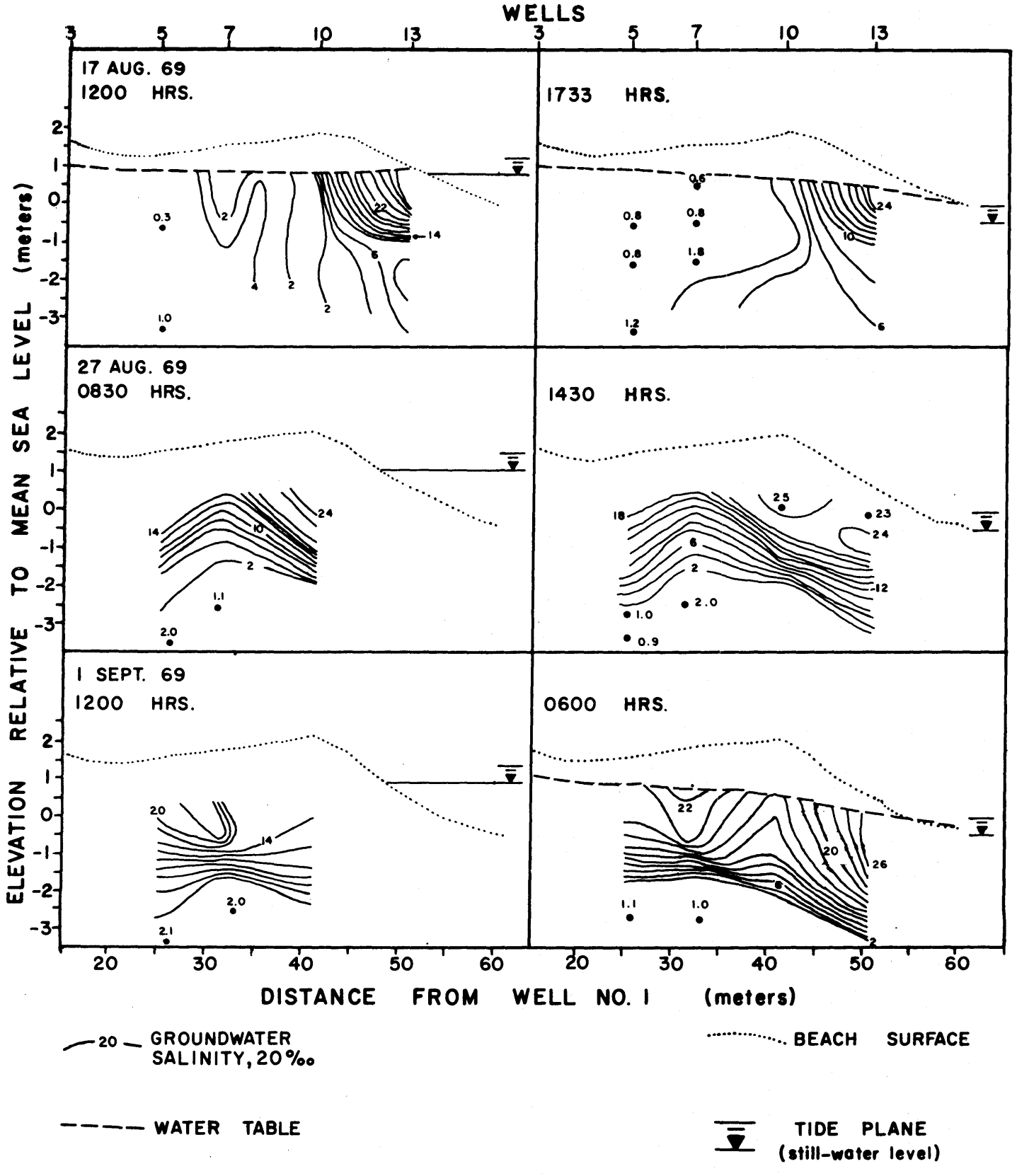

FIG. 2. Salinity structure of the beach groundwater before (17 Aug. 69) and after (27 Aug. 69) storm wave flooding of backshore.

33 m, to well no. 6 (Fig. 1). The "foreshore" for the Ft. Story data extended from the limit of uprush at high water to the significant change in slope (at the toe of the foreshore) that is visible at low water. For the Camp Pendleton data, mentioned below, the inshore margin of the breaking waves was taken as the seaward limit of the foreshore. (Thus, absolute spatial location of the foreshore changed somewhat with each tide cycle).

As indicated by Figure 3, there is a clear relationship that can be stated: "as the volume of groundwater increases (water table rises), the foreshore is depleted of sand; as it decreases (water table falls), sand is deposited on the foreshore." The relationship is clear but the underlying process-response mechanism is not.

The groundwater fluctuations in the Ft. Story and Camp Pendleton beaches were produced by fluctuations of the ocean still water level (SWL) and, intuitively, one would expect changes in the quantity of foreshore sand (ΔQ_f) to be determined, to a large extent, by SWL oscillations.

In modeling the relationship between ocean level and foreshore volume change it is desirable to work with a minimum number of variables, each of which has intuitive physical significance. Imagine a perfectly calm sea whose surface is rising and falling with the frequency of a diurnal tide and amplitude of 1 m. The waveless, slowly-fluctuating sea surface will transfer no grains up or down the foreshore owing to the absence of swash-backwash. The beach water table will rise and fall with tidal periodicity, however.

Now let the energy of breaking waves and swash currents become available for grain transport. As the tide plane falls progressively from its highest level, one would expect sand to be put into suspension in the breaker zone and transported up the foreshore by each successive swash. Much of the sand transported up the foreshore would be deposited because it takes less energy to keep a grain in motion than it does to erode one; that is, the breaker zone is the primary energy source for grain suspension, and the swash zone is the region of upslope and downslope transfer. The still-water level determines the locus of sand deposition by the swash. Throughout a falling tidal half-cycle, therefore, sand will be deposited on the foreshore. The foreshore profile will rise relative to what it was at the time of high water. (At high

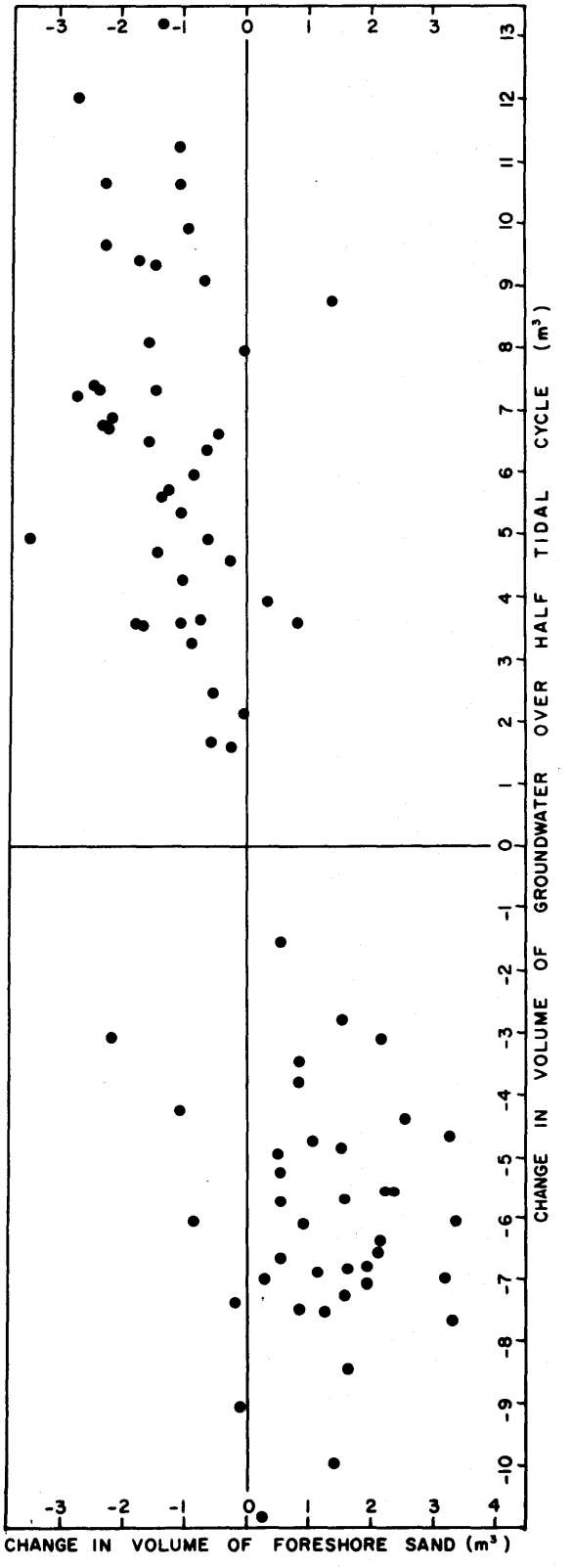

FIG. 3. Change in volume of foreshore sand at Ft. Story versus change in groundwater volume over a rising or falling half-tidal cycle.

water, the breaker zone will be located part way up the foreshore and will lower the profile by sending sand both land and seaward from the zone of maximum dissipation of turbulent energy).

As the still-water level rises from its lowest position, the breaker zone moves up the foreshore. This results in a net lowering of the foreshore profile because, even though some of the eroded foreshore sand is moved upslope and redeposited, a like portion is lost to the offshore side of the breaker zone. Owing to the width of the breaker zone, sand moving to its offshore side will, by the definition of "foreshore" adopted here, be lost from the foreshore profile.

The foregoing describes a symmetry of sand transfer that has been alluded to by others (LaFond, 1939; Strahler, 1964; and Schwartz, 1967) and, indeed, if ΔQ_f is plotted as a function of the change in ocean SWL, a remarkedly symmetrical relationship emerges. The Camp Pendleton data foreshore volume change (ΔQ_f) are plotted in Figure 4 as a function of change in tide level, over a half-tidal cycle. As expected, foreshore depletion occurs almost exclusively during the rising half-tidal cycle; foreshore deposition occurs during the falling half-cycle. The Ft. Story data (Fig. 4) reinforce this finding, the only significant exception to the rule being the large loss of foreshore sand that occurred during a falling half-tidal cycle that coincided with the first storm-wave over-topping of the summer berm. For the rising-tide condition, fully 84 percent of the data from both beaches conform to the rule; 89 percent of the data conform for the falling-tide condition.

Strahler studied an equilibrium beach at Sandy Hook, N. J., and observed (1964, Fig. 9) essentially the same relationship in a series of consecutive beach profiles made over an entire tidal-cycle. The fundamental relationship between ocean SWL fluctuations and foreshore sand-volume changes holds not only for an equilibrium beach, however. As indicated here (Fig. 4), it holds for sandy beaches undergoing overall retreat or advance, for waves as diverse as locally-generated, steep storm waves or long-period hurricane forerunners, and for beaches differing somewhat in mean grain-size and mean foreshore slope. The basic data for the two beaches studied, obtained in August and September of 1966 and 1969, are found in time-series reports for Ft. Story (Harrison and Fausak, 1970) and Camp Pendleton (Harrison, et al., 1968).

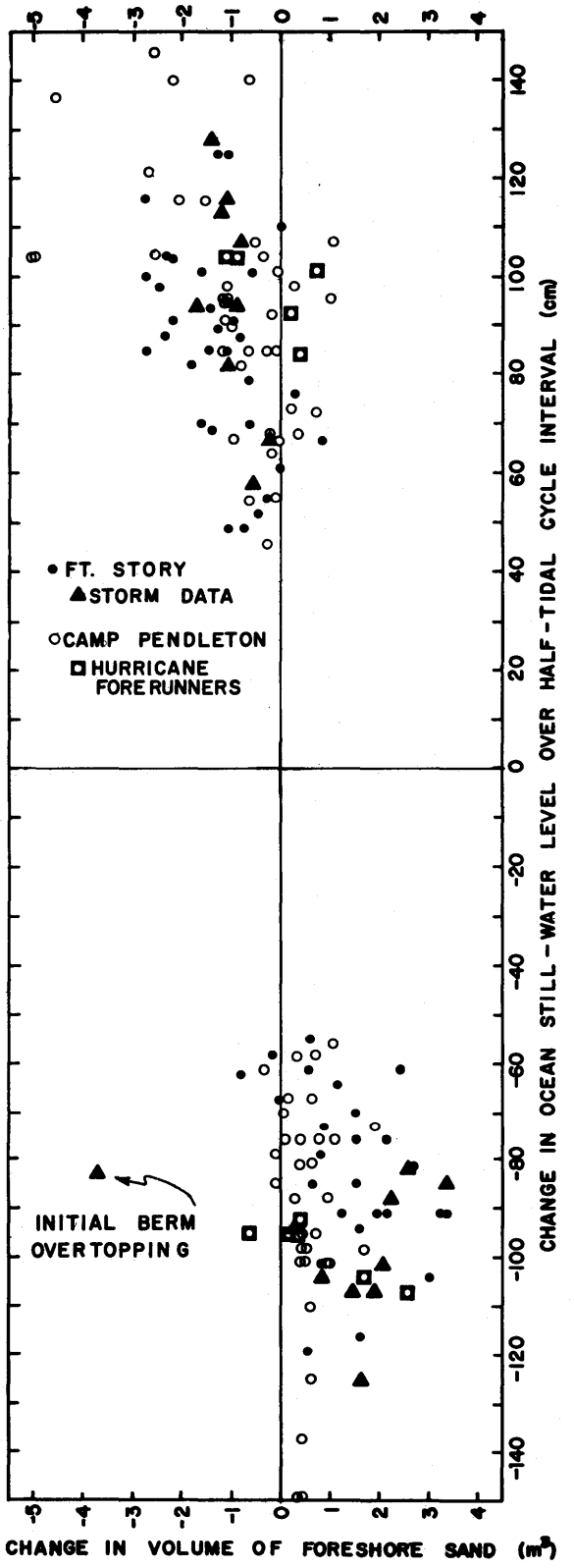

FIG. 4. Change in volume of foreshore sand at Ft. Story and Camp Pendleton (Fig. 1) versus change in ocean still-water level over a rising or falling half-tide cycle.

The relationship of the oceanic SWL to the outcrop of the water table bears special attention. If the SWL is relatively high, the uprush portion of the swash may percolate into the unsaturated sand above the water table outcrop, losing potential energy as it infiltrates. The backwash will not have the same kinetic energy, therefore, as the uprush, leading to sand deposition on the upper foreshore. If the SWL is relatively low, the seaward-directed head gradient will produce lift forces on the sand grains of the lower foreshore, downslope of the outcrop of the water table. These lift forces will assist the backwash in downslope transport of sand.

REGRESSION ANALYSIS

Quantification of the relationship between the ocean SWL and the water-table outcrop is difficult, owing to the problems related to maintenance of wells in the swash zone during storms. It will be assumed that the difference in the head (Fig. 5, Δy) between the two seawardmost wells that remained undisturbed throughout the study (nos. 10 and 11, Fig. 1), is the best descriptor of this relationship. It will also be assumed that Δy adequately reflects a) the swash percolation at high ocean SWL and b) the hydraulic forces exerted on the lower foreshore by the seaward-flowing groundwater at low ocean SWL.

An additional consideration now enters the picture. The foreshore surface moves landward and seaward, relative to the seawardmost well, over several tidal cycles. Δy, being sensitive to the distance from the foreshore at which it is measured, must be corrected for variable x (Fig. 5). The following "head index" will be used, therefore: $I = (\Delta y)\,x$, or $I = (y_{10} - y_{11})\,x$, where y_{10} and y_{11} are the MSL elevations of the water table in wells 10 and 11, in mm, and x is in meters. When $y_{11} > y_{10}$, Δy is negative (landward slope).

The following expressions are now formulated for sequential (linear) multiregression:

$$\Delta Q_f = f(I_1, I_2, I_3, 2h_o, S, \bar{H}_b)_R \qquad (1)$$

$$\Delta Q_f = f(I_3, I_4, I_5, 2h_o, S, \bar{H}_b)_F \qquad (2)$$

$$\Delta Q_f = f(I_1, I_2, I_3, I_4, I_5, \Delta h, S, \bar{H}_b)_C \qquad (3)$$

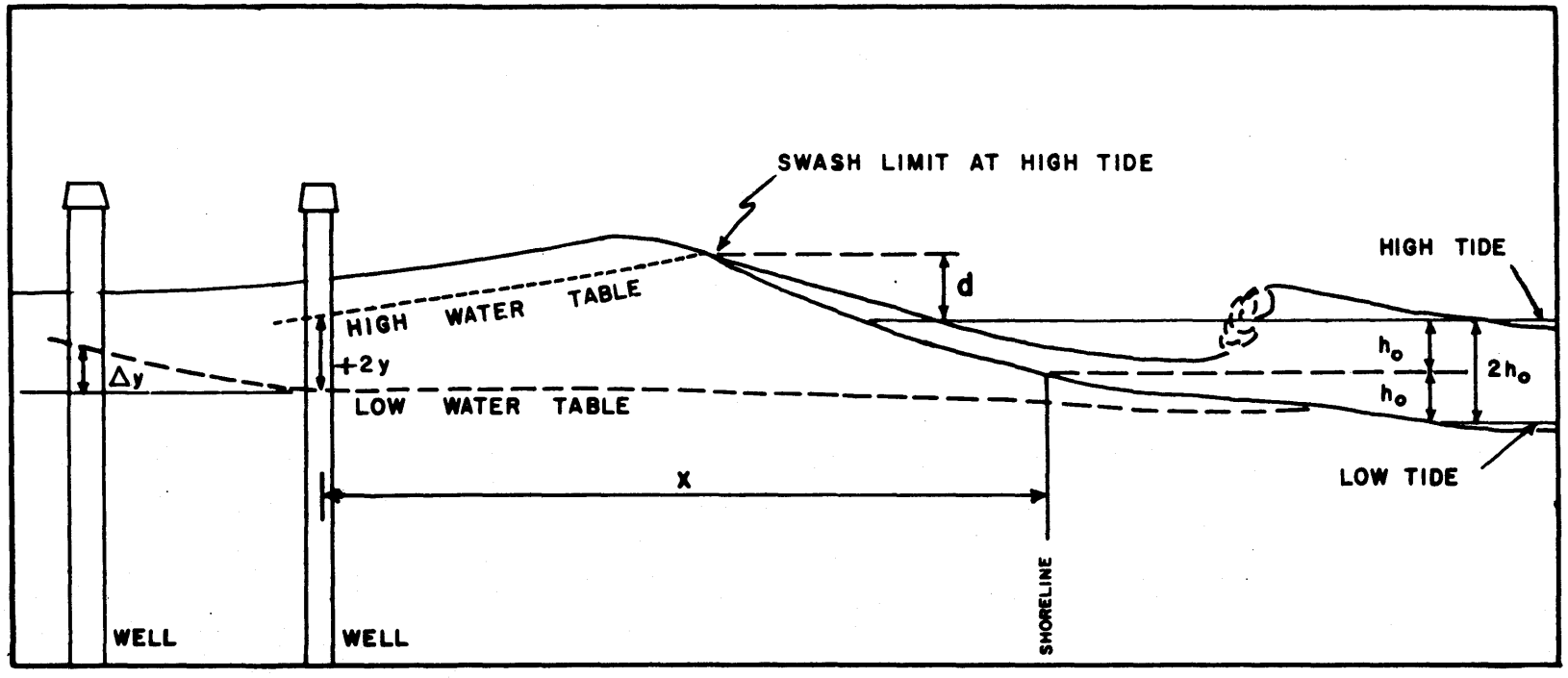

FIG. 5. Definition sketch for variables d, h_o, x, y, and Δy.

where ΔQ_f = change in quantity of foreshore sand (m^3), I = the index of head in the beach water table between wells 10 and 11, $\pm 2h_o$ is the range in rise or fall of the ocean still-water level over a rising or falling half-tidal cycle (in cm), Δh is the net change in ocean still-water level over a complete tide cycle (in cm), S = the total number of swash events over the interval of interest, $\overline{H}_b$ = the mean breaker height (in m) over the interval, the subscripts R, F, and C refer to rising, falling, and complete (low-water to low-water) tidal cycles, and the subscripts 1 through 5 denote times during a tidal cycle corresponding to initial low water, rising half-tide level, high water, falling half-tide level, and final low water, respectively. Total swash events S are assumed equal to the number of breakers occurring over the time interval.

The results of the regression analyses are given in Table 2. They show that, although the groundwater head index (I) is overshadowed by the change in ocean SWL ($2h_o$ or Δh), the head index at various times is, nevertheless, a strong predictor of ΔQ_f. Total swash (S) is the next strongest predictor after I. Somewhat unexpectedly, $\overline{H}_b$ turned out to be the weakest of all predictors.

To the author's knowledge, a predictor equation such as (10) has never before been tested on field data obtained from a different beach, when the data from both beaches were gathered using identical measurement techniques.

Predictor equations for the regressions follow:

Rising half-tide cycle:

$$\Delta Q_f = 0.1758 - 0.015193(2h_o) \qquad (4)$$

$$\Delta Q_f = 1.633 - 0.017471(2h_o) - 0.00040402(S) \qquad (5)$$

$$\Delta Q_f = 2.935 - 0.014474(2h_o) - 0.00052881(S) - 0.0016273(I_1) \qquad (6)$$

Falling half-tide cycle:

$$\Delta Q_f = 0.0479 - 0.016962(2h_o) \qquad (7)$$

$$\Delta Q_f = 0.4209 - 0.022052(2h_o) + 0.00060146(I_3) \qquad (8)$$

$$\Delta Q_f = 3.360 - .03484(2h_o) + 0.0011271(I_3) + 0.00056068(S) \qquad (9)$$

TABLE 2. Selection of Predictors by Regressing Equations 1, 2, and 3.

Condition	N	Regression	Variable	Sign of correlation	R^2	F Value
Rising half-tide cycle (Equ. 1)	38	1	$2h_o$	-	0.39	6.47
		2	S	-	0.51	6.30
		3	I_1	-	0.58	*
Falling half-tide cycle (Equ. 2)	34	1	$-2h_o$	-	0.30	3.21
		2	I_3	+	0.36	*
		3	S	+	0.45	*
Complete tide cycle (Equ. 3)	27	1	Δh	-	0.55	10.60
		2	I_2	+	0.67	*
		3	S	-	0.68	*

*Not valid because of interdependence of $2h_o$ or Δh, and I.

Complete tide cycle:

$$\Delta Q_f = 0.16682 - 0.051067(\Delta h) \quad (10)$$

$$\Delta Q_f = 019762 - 0.04857(\Delta h) + 0.0021636(I_2) \quad (11)$$

To the author's knowledge, a predictor equation such as (10) has never before been tested on field data obtained from a different beach, when the data for both beaches were gathered using identical measurement techniques. This is possible now because the Ft. Story data (Harrison and Fausak, 1970) for ΔQ_f, $2h_o$, and S, from which equation (10) was developed, were obtained with the same measurement techniques as were used at Camp Pendleton (Harrison, et al., 1968), some 9 km to the south (Fig. 1).

Δh emerges as a most significant predictor for sandy beaches like the one studied because R^2 for the regression of ΔQ_f predicted by (10), on the observed values of ΔQ_f, is 0.40, where N = 30. That is, equation (10), developed from the Ft. Story data, and explaining 55 percent of the variation in ΔQ_f there, explains 40 percent of the total variation observed in ΔQ_f at Camp Pendleton. Mean sand-grain diameter at the two beaches is approximately the same.

DISCUSSION AND CONCLUSIONS

Schwartz (1967) analyzed Bruun's (1962) thesis that sea-level rise is the main cause of shore erosion and, after applying his findings (Schwartz, 1968) to three different time and space scales, concluded that sea-level rise is the "common denominator underlying shore erosion on any scale." The multiregression analyses of the present study confirm Schwartz's finding for the rising half-tide situation on sandy beaches; that is, $+2h_o$ is the strongest predictor (Table 2) of ΔQ_f, and ΔQ_f is nearly always negative (Fig. 4) when $2h_o$ is positive. The regression analyses also suggest that $-2h_o$, falling SWL, is the major variable determining foreshore buildup, on the time scale of 6 to 12 hours.

As mentioned previously, this symmetry of foreshore volume change in response to oscillating SWL had been noticed by many others before Schwartz.

(See Schwartz's thorough summary in his 1968 paper). As also mentioned above, however, oscillation of the oceanic SWL, by itself, will not result in beach volume changes. Energy must be available for transport of sand grains and, as a further condition, if the index for available energy is taken as the number of swash events S per unit time, then the diminution of augmentation of that swash energy, by swash percolation into the upper foreshore or groundwater flow through the lower foreshore, must also be taken into account.

Equations 4—9, therefore, are more adequate statements of the processes occurring over a rising or a falling half-tidal cycle than are statements based upon fluctuating SWL alone. Also, the strength (in R^2) of each of the impirical predictor equations is greater than the strength of those previous predictor equations (cf. Harrison, 1969), developed from various other independent variables in the beach-ocean-atmosphere system. Thus, some progress has been made in the attempt to reduce to the lowest possible number the independent variables influencing ΔQ_f in a significant way. The result of testing equation (10) on an independent set of data indicates that ΔQ_f can be reasonably well predicted, over a tidal-cycle interval, knowing only Δh. It was unfortunate that variable I_2 (Table 2 and equ. 11) could not be determined accurately from the Camp Pendleton time series. Had this been possible, equation 11 could have been tested on the independent data from the Camp Pendleton beach study.

The best test of an empirical equation that contains interdependent variables (X_i) is to apply it to a set of independent data and examine the strength (in R^2) of the resulting distribution of observed versus predicted values.

It is hoped that future studies of the dynamics of sandy tidal beaches will be so designed that the variables of Table 1 can be quantified in the same fashion as was done for the present study. In this way, the equations can be tested and improved.

ACKNOWLEDGMENTS

I thank Maurice L. Schwartz and Robert J. Byrne for critical review of the manuscript. Paul Bullock computed the beach volume changes at Camp Pendleton and Mark Stewart made the groundwater salinity determinations at Ft. Story.

REFERENCES

Bagnold, R. A., Beach formation by waves; some model-experiments in a wave tank, Jour. Inst. Civil Engrs., 15, 27-54, 1940.

Behrens, E. W., Use of the Goldberg refractometer as a salinometer for biological and geological field work: Jour. Marine Research, p. 165-171, 1965.

Bruun, P., Sea-level rise as a cause of shore erosion, Jour. Waterways and Harbors Div., Amer. Soc. Civ. Eng. (88), 117-130, 1962.

Duncan, J. R., The effects of water table and tide cycle on swash-backwash sediment distribution and beach profile development, Marine Geology, 2(1), 186-197, 1964.

Emery, K. O., and J. F. Foster, Water tables in marine beaches, Jour. of Marine Research, 7(3), 644-654, 1948.

Fairbridge, R. W., Beach erosion and sea level changes, eustatic and others, Conf. on Coastal Engineering, 9, Lisbon, 1964.

Grant, U. S., Influence of the water table on beach aggradation and degradation, Jour. Marine Research, 7(3), 655-660, 1948.

Harrison, W., et al., A time series from the beach environment, E.S.S.A. Res. Lab., Tech. Memo. AOL-1, 1-85, 1968.

Harrison, W., Empirical equations for foreshore changes over a tidal cycle, Marine Geology, 7(6), 529-551, 1969.

Harrison, W., and L. E. Fausak, A time series from the beach environment—II, Va. Inst. Marine Sci., Data Rept. No. 7, p. 1-96, 1970.

Inman, D. L., and J. Filloux, Beach cycles related to tide and local wind wave regime, Jour. Geology, 68(2), 225-231, 1960.

Issacs, J. D., and W. N. Bascom, Water table elevations in some Pacific coast beaches, Transactions, Amer. Geophys. Union, 30(2), 293-94, 1949.

LaFond, E. C., Sand movements near the beach in relation to tides and waves, Contrib. Scripps Inst. Oceanog., New Ser. 107, 795-799, 1939.

Schwartz, M. L., The Bruun theory of sea level rise as a cause of shore erosion, Jour. Geology, 75(1), 76-92, 1967.

_____, The scale of shore erosion, Jour. Geology, 76, 508-517, 1968.

Strahler, A. N., Tidal cycle of changes in an equilibrium beach, Sandy Hook, N. J., Jour. of Geology, 74(3), 247-268, 1966.

GROUNDWATER FLOW IN A SANDY TIDAL BEACH. 1. ONE-DIMENSIONAL FINITE-ELEMENT ANALYSIS

W. Harrison, C. S. Fang, and S. N. Wang

ABSTRACT

A 31-day-long time series of observations of beach water-table and tidal fluctuations was obtained from 13 wells along a profile perpendicular to the shoreline at Virginia Beach, Virginia. Finite-element techniques were applied to solve the one-dimensional, unsteady-state, nonlinear equation for groundwater movement. For the finite-element analysis, the semi-infinite mass (unconfined aquifer) had to be replaced by a finite mass. The boundary conditions were found from the field data by directly solving the flow equation with a finite-difference technique. The finite-element method, utilizing the variational principle, provided a reasonable solution and afforded economy in computer time. Field data were compared with the corresponding finite-element solution. Results indicate general accuracy of the methodology.

INTRODUCTION

Several workers (e.g., Grant, 1948; Emery and Foster, 1948; and Duncan, 1964) have shown, in a qualitative way, the importance of the slope of the beach water table, and its elevation above tide level, to the stability of sandy foreshore slopes. The goal of this work was to carefully document fluctuations in a beach water table and then develop models of the fluctuations for application to the foreshore stability problem. The present study was directed toward determining the feasibility of a one-dimensional model, using finite-element techniques.

The finite-element method of analysis was developed by the aircraft industry about 15 years ago to calculate stress and strain in complicated aircraft structures. It was not extensively applied to engineering or mechanical problems until two text books—the first edited by Zienkiewicz and Holister and the second authored by Zienkiewicz and Cheung (1967)—became available. These furnished considerable background, application, and research material on the finite-element method.

Extension of the method to cover unsteady-state, free-surface flow has been slow in development, with difficulties encountered in the case of triangular elements. The primary limitation of the finite element method is that it requires access to large computers for solutions to problems of any degree of complexity. Where such computers have been made available, the finite-element method has been widely applied in a variety of engineering fields. The method was first applied to the analysis of fluid flow in porous media by Taylor and Brown (1967). Recently, Neuman and Witherspoon (1970) applied the method to the problem of transient groundwater flow. Guymon (1970) applied finite-element methods to solve the one-dimensional, unsteady, diffusion-convection equation. The numerical technique employed variational principles, and triangular elements were very helpful in that study.

A 31-day-long time series of observations of the variables listed in Table 1 was obtained to document pertinent interactions in the beach-ocean-groundwater system. Thirteen wells for monitoring the water table (Fig. 1, 1-13) and 26 pipe-stations (Fig. 1, A-Z) for monitoring changes in beach elevation were positioned along an 83-m-long transect oriented perpendicular to the shoreline and extending from the edge of the foredune to the low-water line. Four multi-tube probes (Fig. 1, I-IV) were installed for extracting small amounts of groundwater for tests of salinity and to facilitate dye tests of flow characteristics. The wells consisted of 1) a #18-slotted PVC pipe, 102-mm in diameter, jetted into the beach to a depth of 3.5 m and 2) a 32-mm-O.D. steel pipe jetted to a depth of 5 m and touching the PVC pipe. A float-pulley system mounted on the pipes drove a potentiometer which provided a DC output voltage that corresponded (linearly) to the instantaneous water level. Water-table elevations were recorded at the site on computer-compatible magnetic tape (after A/D conversion). Details for this and the other measurement systems, as well as the complete time-series of measurements for the variables of Table 1, appear in Harrison and Fausak (1970).

The gently-sloping, quartz-sand beach that was studied (Fig. 1, "study site"), has a representative porosity of about 34 percent (median grain diameter of pit samples ranged between 0.37 and 0.59 mm). The mean range of the astronomical tide is about 0.85 m for Cape Henry, the spring range is 1.1 m, and the tide is semidiurnal with a slight diurnal inequality.

TABLE 1. Measured and Derived Variables for the Beach-Ocean-Groundwater System at Ft. Story, Virginia Beach, Virginia, for the Period 10 August through 9 September, 1969.

Symbol	Description	Sampling Frequency	Range in Values	Estimate of Accuracy
E_b	Elevation of beach surface	High, low, and mid-tide levels	-0.940 to 3.693 (MSL)	±0.005 m above water, ±0.020 m below water
E_t	Elevation of tidal plane	Continuous	-0.55 to 1.27 m (MSL)	±0.05 m
E_w	Elevation of water table	Either every 10 or every 15 minutes	0.291 to 1.999 m (MSL)	±0.003 m
$\overline{H}_b$	Mean height of 50 successive breaking waves	High, low, and mid-tide levels	0.19 to 1.30 m (MSL)	±0.10 m
m	Slope of the foreshore	Derived (high, low, and mid-tide levels)	4.0° to 11.0°	±0.5°
p	Barometric pressure	Continuous	29.550 to 30.285 in. of Hg.	±0.005 in Hg.
r	Rainfall	Hourly during storms	Trace to 2.22 cm	±1.0 mm

(Continued)

TABLE 1. (Continued)

Symbol	Description	Sampling Frequency	Range in Values	Estimate of Accuracy
s	Position of swash limit	Hourly, and at high, low, and mid-tide levels	Sta. G to Sta. Z (Fig. 1)	±0.25 m
$\overline{T}_b$	Mean period of 50 successive breaking waves	High, low, and mid-tide levels	3.96 to 13.20 sec.	±0.02 sec.

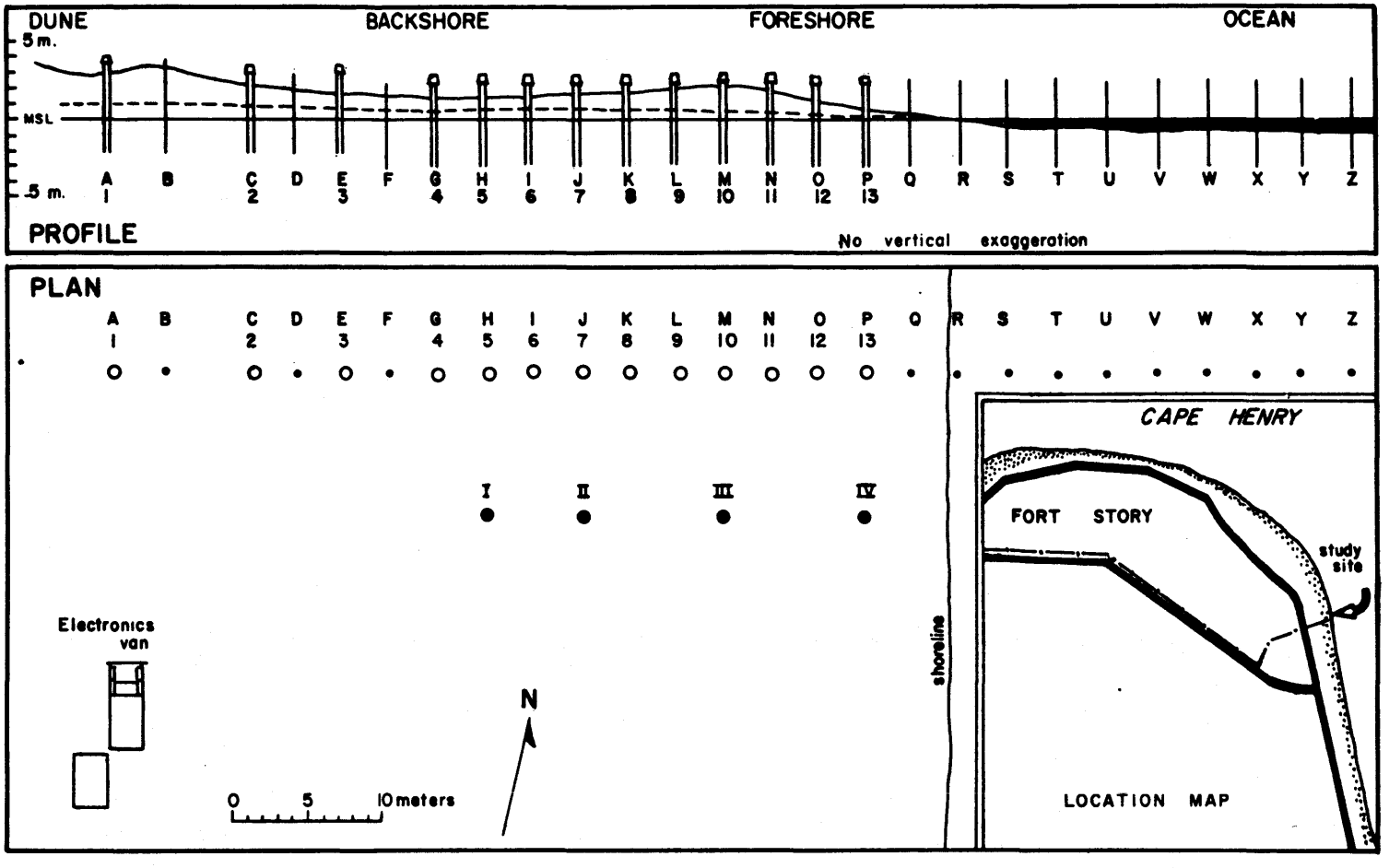

FIG. 1. Plan and profile views of the Fort Story Study site (inset), showing typical beach and water-table profiles, the spatial distribution of profile stations (A-Z), water-table monitoring wells (1-13), and groundwater sampling probes (I-IV).

Low, long-period swells characterized the first ten days of the 30-day study period. They were followed by three days of high, short-period waves that, combined with a storm surge, resulted in flooding of the backshore (Fig. 1) for two full tidal cycles. (Nine days were required for the groundwater level to return to its pre-storm position). The remaining 17 days of the study had a wave climate similar to the first 10 days. Rainfall amounted to 10.2 cm during the 30-day period. The greatest hourly rainfall was 2.22 cm, an event that caused an increase of about 1.5 cm in the water level at all wells. The effects of rainfall, as well as sudden fluctuations in atmospheric pressure, can be ignored in what follows.

WATER TABLE RESPONSE CHARACTERISTICS

It is commonly assumed (see Chow, 1964, p. 13-37) that for an unconfined aquifer connecting with the ocean, the tide wave will damp exponentially as it is propagated inland, so that, if the water table fluctuations are small relative to the saturated thickness, the amplitude y at any distance x inland is

$$y = h_o e^{-x(\pi S/t_o T)^{\frac{1}{2}}} \sin \frac{2\pi t}{t_o} - x \frac{\pi S}{t_o T} \qquad (1)$$

where $y = h_o \sin \omega t$ at $x = 0$, and $y = 0$ at $x = \infty$; t_o = tide period, T = coefficient of transmissibility, t = time, and S = the storage coefficient. A seaward-directed head gradient is almost invariably present in beach aquifers and the beach water table is also affected by tidal forces. Field data indica e that these two factors significantly affect water-table fluctuations. The overall effect is for the water table to rise too rapidly during rising tide and fall slowly during falling tide. Equation 1 cannot be used, therefore, to model the tide-wave response of the water table in a natural beach.

To gain insight into the response characteristics of the beach water table Fausak (1970) performed the following linear multiregression analysis on the water table elevation data for each well:

$$2y = f(2h_o, d, x, p) \qquad (2)$$

where $+2y$ = the total change in elevation of the water table for a rising half-tidal cycle, $+2h_o$ = the total increase in elevation of the tide plane in a well for a rising half-tidal cycle, x = the horizontal distance from a given well to a point on the foreshore lying one-half the vertical distance between the preceding low water and the succeeding high water levels, d = the vertical distance between high-tide still-water level and a horizontal line passing through the average position of the swash at its highest level, and p = the change in atmospheric pressure over a rising half-tidal cycle. (See Figure 2).

The results of the regression analysis (Fig. 3) indicate the significance of the tidal forcing function throughout most of the 50-meter width of instrumented beach. As could be expected, the variable x, or the distance of a well from the foreshore, is the most significant factor in water table fluctuations for wells closest to the ocean. The regression analysis suggests that positive water table fluctuations in wells 12 and 13, closest to the shore, are as strong a function of x and d as they are of the rise in the tide, $2h_o$. At the landwardmost well (Fig. 3, no. 1), the increase in water level is as much a function of p as it is of $2h_o$. In general, however, Figure 3 indicates that we may feel confident in using the tidal fluctuation as the primary forcing function when attempting to model water table fluctuations between wells 1 and 13. A certain amount of noise (unexplained variability) will be present in the output of any model, especially for the seawardmost end of the water table, due to the unaccounted effects of the swash and the variable distance of the wells from the foreshore surface as sand is eroded and deposited. These variables contribute noise which is independent of that due to the two factors mentioned earlier. The total noise contributed by all of the foregoing effects will be lumped into the "drainage velocity," V, in what follows. This is because the groundwater head is the most significant factor of all of the noise effects.

GROUNDWATER FLOW EQUATION

A differential equation of groundwater movement was derived in accordance with the following assumptions:

1) the flow is one-dimensional, 2) the density of the fluid is constant, 3) Darcy's law is valid, 4) the groundwater occurs in a homogenous sand body, and

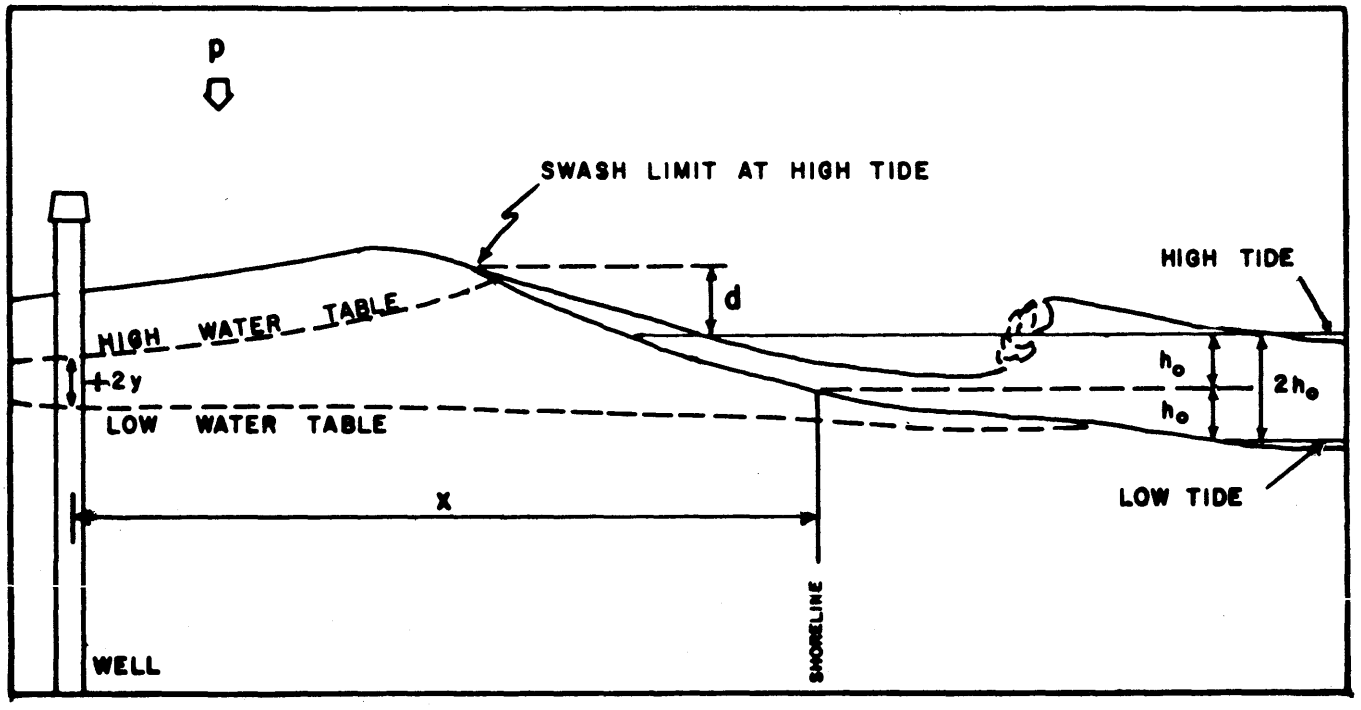

FIG. 2. Definition sketch for variables y, x, d, h_o, and p used in the regression analysis.

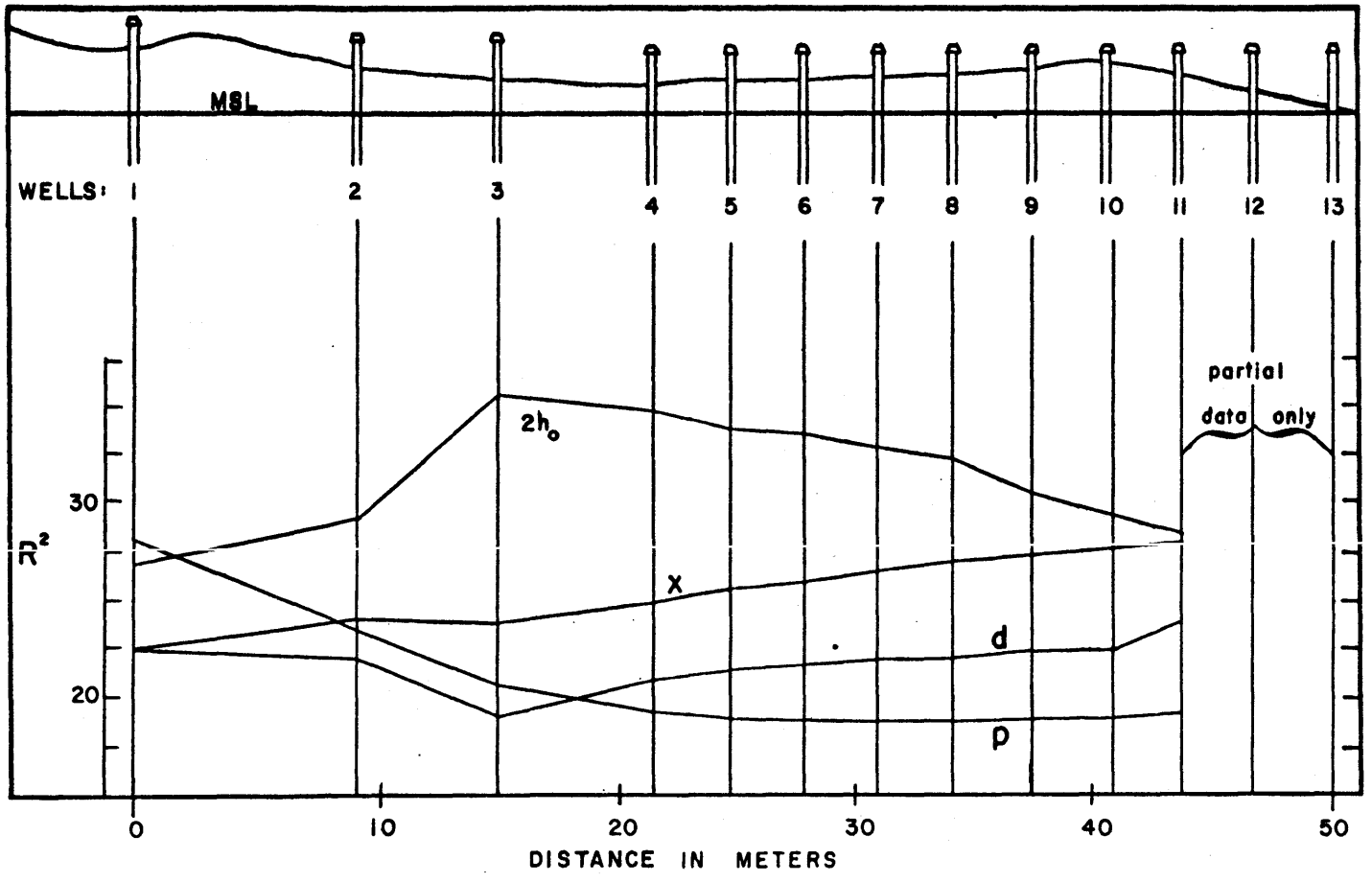

FIG. 3. Relative importance of $2h_o$, x, d, and p, as indicated by percent reduction in sums of squares (R^2) of 2y (after Fausak, 1970, fig. 8).

5) the beach sand drains instantaneously.

Based on the principle of conservation of mass, the continuity equation of groundwater within a homogenous sand body can be written as

$$-\frac{\partial}{\partial x}\left(Kh\frac{\partial h}{\partial x}\right) + f\frac{\partial h}{\partial t} - V = 0 \qquad (3)$$

where $V = V(x,t)$ is a function describing the bottom mass flux of the groundwater

x = direction normal to the shoreline
f = porosity
t = time
K = hydraulic conductivity
h = total head

Applying the variation principle to equation (3), for conditions at a particular instant, the functional of the minimizing function of h for each element is:

$$I^m = \int_{x_n}^{x_{n+1}} \left[\frac{1}{2} Kh \left(\frac{\partial h}{\partial x}\right)^2 + \left(f\frac{\partial h}{\partial t} - V\right) h\right] dx \qquad (4)$$

for all inner elements, and

$$I^1 = \int_{x_1}^{x_2} \left[\frac{1}{2} Kh \left(\frac{\partial h}{\partial x}\right)^2 + \left(f\frac{\partial h}{\partial t} - V\right) h\right] dx + \left[Kh\left(\frac{\partial h}{\partial x}\right)\delta h\right]_{x=0} \qquad (5)$$

and

$$I^M = \int_{x_N}^{x_{N+1}} \left[\frac{1}{2} Kh \left(\frac{\partial h}{\partial x}\right)^2 + \left(f\frac{\partial h}{\partial t} - V\right) h\right] dx - \left[Kh\left(\frac{\partial h}{\partial x}\right)\delta h\right]_{x=L} \qquad (6)$$

for boundary elements.

In deriving the above equations, the assumption was made that equation (3) could be treated as a Sturm-Liouville problem (Weinstock, 1952), when applying the variational principle; i.e., Kh in the

term $\frac{\partial}{\partial x}$ (Kh $\frac{\partial h}{\partial x}$) is taken as function of x only (Volker, 1969).

The boundary was applied to the prescribed value of h for each time step in this study; therefore, equations (5) and (6) are identical to equation (4).

The general concept of the method is to imagine the surface subdivided into a group of subassemblages or elements which are interconnected only at the element joints. Thus, the 1-dimensional region is divided into many subregions (Fig. 4).

By assuming that the linear function of h passes through two end points of each element, and representing equation (4) in local-element coordinates, the contribution over the mth element for the (n-1)th node is given by

$$\frac{\partial I^m}{\partial h_{n-1}} = \frac{3k^m}{4y^m} h_{n-1}^2 - \frac{k^m}{2y^m} h_{n-1} h_n - \frac{k^m}{4y^m} h_n^2 + \frac{f^m y^m}{3} \frac{\partial h_{n-1}}{\partial t} + \frac{f^m y^m}{6} \frac{\partial h_n}{\partial t} - \frac{V^m y^m}{2} \tag{7}$$

where y^m is the length of the mth element, subscripts indicate nodal counters, and superscripts indicate element counters.

Considering the over-all contribution on nodal point n due to all elements, and setting equal to zero:

$$\frac{\partial I}{\partial h_n} = \frac{\partial \left(\sum_{m=1}^{M} I^m \right)}{\partial h_n} = \sum_{m=1}^{M} \frac{\partial I^m}{\partial h_n} = 0$$

That is:

$$\frac{\partial I^{m+1}}{\partial h_n} + \frac{\partial I^m}{\partial h_n} = 0 \tag{9}$$

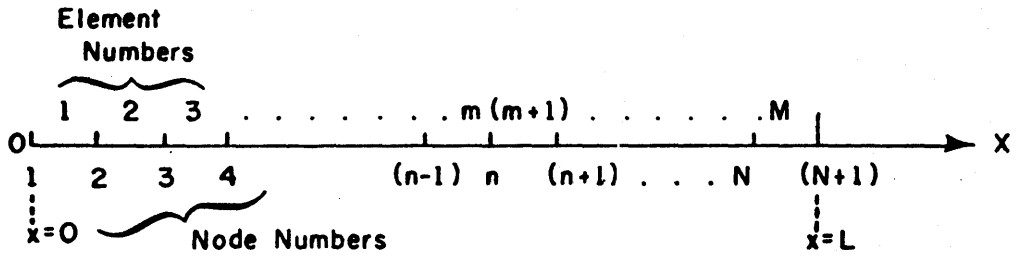

FIG. 4. Definition sketch for elements and nodes.

Substituting equation (8) into equation (9), and expressing the results in matrix form,

$$\begin{bmatrix} -\frac{k^m}{4y^m} & (\frac{3k^m}{4y^m} + \frac{3k^{m+1}}{4y^{m+1}}) & -\frac{k^{m+1}}{4y^{m+1}} \end{bmatrix} \begin{bmatrix} h^2_{n-1} \\ h^2_n \\ h^2_{n+1} \end{bmatrix}$$

$$+ \begin{bmatrix} -\frac{k^m}{2y^m} & -\frac{k^{m+1}}{2y^{m+1}} \end{bmatrix} \begin{bmatrix} h_{n-1} & h_n \\ h_n & h_{n+1} \end{bmatrix} \qquad (10)$$

$$+ \begin{bmatrix} \frac{f^m y^m}{6} & (\frac{f^m y^m}{3} + \frac{f^{m+1} y^{m+1}}{3}) & \frac{f^{m+1} y^{m+1}}{6} \end{bmatrix} \begin{bmatrix} \partial h_{n-1}/\partial t \\ \partial h_n /\partial t \\ \partial h_{n+1}/\partial t \end{bmatrix}$$

$$+ (-V^m y^m/2 - V^{m+1} y^{m+1}/2) = 0$$

Equation (10) represents a system of non-linear functions of h_{n-1}, h_n, h_{n+1} for every node.

In order to handle easily, equation (10) is defined as:

$$f = (h_2, h_3, \cdot\cdot, h_{n-1}, h_n, h_{n+1}, \cdot\cdot, h_N) = 0 \qquad (11)$$

where $n = 2, 3, 4, \cdot\cdot, N$, but $n \neq 1$, and $n \neq N+1$.

Thus:

$$f_n = A_1 h^2_{n-1} + A_2 h^2_n + A_3 h^2_{n+1} + A_4 h_{n-1} h_n \qquad (12)$$

$$+ A_5 h_n h_{n+1} + A_6 h_{n-1} + A_7 h_n + A_8 h_{n+1} + A_9 = 0$$

Relating equations (10) and (12), the coefficients (A's) are:

$$A_1 = - k^m / 4y^m$$

$$A_2 = 3k^m / 4y^m + 3k^{m+1} / 4y^{m+1}$$

$$A_3 = - k^{m+1} / 4y^{m+1}$$

$$A_4 = - k^m / 2y^m$$

$$A_5 = - k^{m+1} / 2y^{m+1}$$

$$A_6 = f^m y^m / 6\Delta t$$

$$A_7 = (f^m y^m/3 + f^{m+1} y^{m+1}/3) \frac{1}{\Delta t}$$

$$A_8 = f^{m+1}\, y^{m+1} / 6\Delta t$$

$$A_9 = (-V^m\, y^m /2 - V^{m+1} y^{m+1}/2) - \frac{f^m y^m}{6\Delta t} h_{n-1}^{6-\Delta t} - (\frac{f^m y^m}{3} + \frac{f^{m+1} y^{m+1}}{3}) \frac{h_n^{t-\Delta t}}{\Delta t} - \frac{f^{m+1} y^{m+1}}{6\Delta t} h_{n+1}^{t-\Delta t}$$

NUMERICAL ANALYSIS

Basic steps.- The basic steps in the formulation of the finite-element method can be summarized as follows:

1) development of the element-equation coefficient matrix,
2) generation of the matrix for the entire system,
3) calculation of nodal head values due to imposed forces and boundary conditions, and
4) calculation of the water-table elevation in each element, from the nodal displacement.

The Newton-Raphson method was chosen to solve the system of nonlinear equations given by equation (10). Fang (1968) has given a detailed description of this method. Only a brief discussion will be given here.

Denote the kth approximation of iteration for the actual roots $[h_i]$ i = 1, 2, - - - I, as $[h_i^{(k)}]$, then equation (11) may be expanded in Taylor series about $[h_i^{(k)}]$, truncating higher order other than first-derivative terms,

$$F_i\left(h_i^{(k+1)}\right) = F_i\left(h_i^{(k)}\right) + \sum_{j=1}^{I} \frac{\partial F_i(h_i^{(k)})}{\partial h_j} \left[h_j^{(k+1)} - h_j^{(k)}\right] \tag{13}$$

If $h_i^{(k+1)}$ are found close to the actual root, then $F_i\left(h_i^{(k+1)}\right) = 0$. Equation (13) represents a system of linear equations that can be expressed in matrix form as

$$[J]\left[h_j^{(k+1)} - h_j\right] = -\left[F_i\left(h_i^{(k)}\right)\right] \tag{14}$$

where [J] is the Jacobian matrix.

The Jacobian matrix has the form

$$[J] = \begin{pmatrix} \frac{\partial F_1}{\partial h_1} & \frac{\partial F_1}{\partial h_2} & & & & & 0 \\ \frac{\partial F_2}{\partial h_1} & \frac{\partial F_2}{\partial h_2} & \frac{\partial F_2}{\partial h_3} & & & & \\ & \frac{\partial F_3}{\partial h_2} & \frac{\partial F_3}{\partial h_3} & \frac{\partial F_3}{\partial h_4} & & & \\ & & \text{---} & \text{---} & \text{---} & & \\ & & & \text{---} & \text{---} & \text{---} & \\ 0 & & & & \frac{\partial F_{I-1}}{\partial h_{I-2}} & \frac{\partial F_{I-1}}{\partial h_{I-1}} & \frac{\partial F_{I-1}}{\partial h_I} \\ & & & & & \frac{\partial F_I}{\partial h_{I-1}} & \frac{\partial F_I}{\partial h_I} \end{pmatrix}$$

It should be noted that each row of the Jacobian matrix contains, at most, three non-zero elements. For large I, the matrix is spare and one can take advantage of the large number of zeros. The modified

subroutine from the IBM System 360 subroutine package entitled SIMQ takes advantage of the large number of zeros in the matrix of coefficients by using the Gaussian elimination method which gives a rapidly convergent procedure with the generalized Newton-Raphson iteration method.

That is, all the non-zero elements of [J] are placed on the diagonal region. There are only three non-zero elements for each row, except for the first and final row where there are two non-zero elements.

The iterative steps may be summarized as follows:

1) $[h_i^{(k)}]$ is found. (It must be a close approximation to the root, otherwise the equation may not converge). For the first iteration, the value of the previous time step is used as an approximation; if $k > 0$, the result of the previous iteration is used.

2) Compute

$$\Delta h_j = h_j^{(k+1)} - h_j^{(k)} \qquad (15)$$

by solving the system of linear equations (14).

3) Find $h_j^{(k+1)}$, using a reasonable convergent criterion.

Boundary conditions.- The prescribed values of h obtained from the field experimental data are applied to the boundary nodal points, $n = 1$ and $n = N + 1$.

The most confused boundary condition occurs on the bottom side of the control region. It is difficult to handle the drainage velocity function, V(x,t), in proper mathematical form because this boundary is a function of both space and time, due to the combined effects of the tide, waves, foreshore changes, and rainfall.

Fourier series analysis for drainage velocity.- Assume that V(x,t) is constant over each interval $x_i \leq x \leq x_{i+1}$, and can be calculated from actual field data by the Eulerian finite-difference formulation, where $i = 1, 2, \ldots, 12$, and the x_i are the coordinates of the wells.

From the results of the Eulerian finite-difference method, we find that $V(x,t)$, $x_i \leq x \leq x_{i+1}$, has much fluctuation from time to time. To simplify the Fourier series analysis, we take the time average first.

$$\bar{V}(x,t) = \frac{\sum_{n=1}^{N} V(x,t_n)}{N} \qquad x_i \leq x \leq x_{i+1} \qquad t_1 \leq t \leq t_n \qquad (16)$$

In our example, we take 100 time cycles (1 cycle = 15 minutes) as the period. Taking the time average for each 20 cycles, three average values in each average interval give a more accurate Fourier series.

The average value of two different intervals is taken as the value at the point of discontinuity. We then find the Fourier series

$$\bar{V}(x,t) = \sum_{n=1}^{N} a_n \cos \frac{2\pi nt}{T} + b_n \sin \frac{2\pi nt}{T} \qquad (17)$$

for each well interval. Results are given in Table 2. The Fourier series coefficients are used in the subroutine to find the drainage velocity for each time step.

APPLICATION OF THE METHOD

The analytical method was applied to the field data as follows (refer to Fig. 5). The prescribed values of h were applied at C and O for every time step. The drainage velocity $V(x,t)$ was applied on the bottom boundary $\overline{OC}$. Also, the following data were used in the example: total nodes = 21, porosity = 34%, hydraulic conductivity = 0.014 cm/sec, length of each element = 250 cm, time increment for each step = 15 minutes.

RESULTS AND CONCLUSION

The finite-element method was applied to solve the nonlinear equation for treating the complicated case of beach water-table fluctuations. The finite-element method, based on the variational principle, provides an accurate solution with an economy of computer time. A compromise decision was made as to

TABLE 2. Fourier Series Coefficients for Each Well Interval. (x_i = well coordinates; i = 1, 2, ... 13).

interval	coeff.	n = 1	2	3	4	5	6
$x_1 \le x \le x_2$	a	0.2060E-04	-0.2555E-04	0.3933E-04	-0.1161E-04	0.7523E-04	-0.2118E-05
	b	0.0000E 00	-0.4224E-05	-0.1677E-05	0.6999E-05	-0.1689E-04	-0.9095E-05
$x_2 \le x \le x_3$	a	0.3689E-04	-0.1483E-04	0.7028E-04	-0.2182E-04	0.1646E-04	0.3183E-05
	b	0.0000E 00	-0.6800E-05	-0.2002E-04	0.6440E-05	-0.2374E-04	-0.1631E-04
$x_3 \le x \le x_4$	a	0.3666E-04	-0.1003E-04	0.1005E-03	-0.4412E-04	0.2276E-04	0.3765E-05
	b	0.0000E 00	-0.8123E-05	-0.5320E-04	0.1999E-05	-0.3054E-04	-0.2445E-04
$x_4 \le x \le x_5$	a	0.4971E-04	-0.9646E-05	0.1261E-03	-0.6833E-04	0.2999E-04	0.6248E-05
	b	0.0000E 00	-0.7289E-05	-0.8863E-04	-0.8633E-06	-0.3150E-04	-0.2679E-04
$x_5 \le x \le x_6$	a	0.6418E-04	-0.8761E-05	0.1453E-03	-0.9076E-04	0.3359E-04	0.6758E-05
	b	0.0000E 00	-0.7440E-05	-0.1177E-03	-0.2665E-05	-0.3154E-04	-0.2828E-04
$x_6 \le x \le x_7$	a	0.5345E-04	-0.7978E-05	0.1637E-03	-0.1162E-03	0.3628E-04	0.6731E-05
	b	0.0000E 00	-0.3818E-05	-0.1470E-03	-0.2576E-05	-0.2888E-04	-0.2791E-04
$x_7 \le x \le x_8$	a	0.7328E-04	-0.4882E-05	0.1783E-03	-0.1286E-03	0.4556E-04	0.1265E-04
	b	0.0000E 00	-0.1082E-05	-0.1770E-03	-0.8028E-05	-0.2667E-05	-0.2772E-04
$x_8 \le x \le x_9$	a	0.8153E-04	0.7425E-05	0.2038E-03	-0.1508E-03	0.5643E-04	0.1902E-04
	b	0.0000E 00	-0.1136E-05	-0.2246E-03	-0.1760E-04	-0.2682E-04	-0.3179E-04

(Continued)

TABLE 2. (Continued)

interval	coeff.	n = 1	2	3	4	5	6
$x_9 \leq x \leq_{10}$	a	0.1070E-03	0.1214E-04	0.2185E-03	-0.1908E-03	0.5860E-04	0.2009E-04
	b	0.0000E 00	-0.6813E-05	-0.2331E-03	-0.2555E-04	-0.1887E-04	-0.2813E-04
$x_{10} \leq x \leq_{11}$	a	0.1245E-03	0.8425E-05	0.2222E-03	-0.2390E-03	0.5734E-04	0.2059E-04
	b	0.0000E 00	-0.1079E-04	-0.3439E-03	-0.2934E-04	-0.5645E-06	-0.1428E-04
$x_{11} \leq x \leq_{12}$	a	0.1214E-03	0.2163E-04	0.2230E-03	-0.2915E-03	0.6012E-04	0.2998E-04
	b	0.0000E 00	-0.2396E-04	-0.4261E-03	-0.3836E-04	0.2684E-04	0.5779E-05
$x_{12} \leq x \leq_{13}$	a	0.7925E-04	-0.7718E-04	0.1126E-03	-0.4094E-03	0.2125E-04	0.3222E-04
	b	0.0000E 00	-0.1256E-04	-0.4542E-03	0.3179E-04	0.1628E-03	0.1422E-03

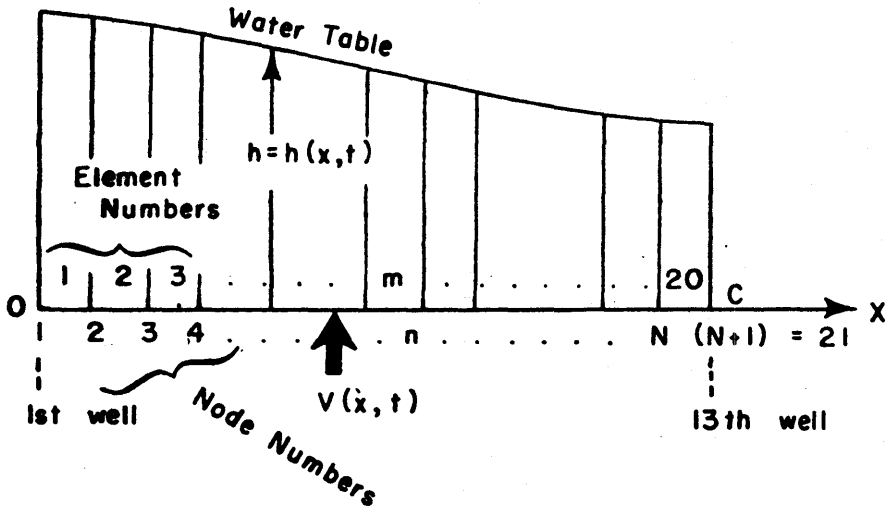

FIG. 5. Definition sketch for application of finite-element model to field data.

the assumed position of the boundaries. In the finite-element analysis, the semi-infinite mass (unconfined aquifer) was replaced by a finite mass. The drainage velocities were found from the field data by directly calculating the pertinent differential equation with a finite-difference technique. Then, a Fourier function was used to describe the mean regional drainage-velocity characteristics and the beach water-table's response to the input tidal fluctuation. Comparing the results (Fig. 6) between this procedure and the field data indicates that the finite-element method is accurate enough to solve the problem of fluctuations of the beach ground-water table.

The fact that small differences exist between the field data and the theoretical results can be explained as due to the effects of variables x and d (equation 2) mentioned earlier. Also of importance will be effects due to capillarity and groundwater density gradients. (These effects possess a complex relationship to space and time). Density gradients in the groundwater will be due to variations in water temperature and salinity (cf. Jansson, 1967). As shown in Figure 7, the groundwater salinity for the summer beach (17 Aug. 69) ranged from near zero at well 3 to 26‰ (parts per thousand) at well 13 at time of high water (1200 hrs). At low tide (1733 hrs) the saline groundwater had migrated slightly seaward. At the end of a storm that sent ocean water over the berm and onto the backshore, however, salinity of the groundwater increased markedly (Fig. 7, 27 Aug. 69). (Flushing of the saline water can be gaged by the distance moved by the 18‰ isoline—about 8m—in the 87.5 hours between 1430 hrs on 27 August and 0600 hrs on 1 September). The point here is that a normal, horizontal density gradient in the beach groundwater changed to a vertical density gradient, as a result of storm flooding.

The procedure developed in this study can be applied to noneven elements and nonhomogenous materials. It makes it possible to predict water-table fluctuations in any sandy, two-dimensional tidal beach knowing only the drainage velocity (obtained from two wells) and the predicted fluctuations in ocean level.

The Fortran computer programs used for the one-dimensional analysis are described and listed in a special section following the References.

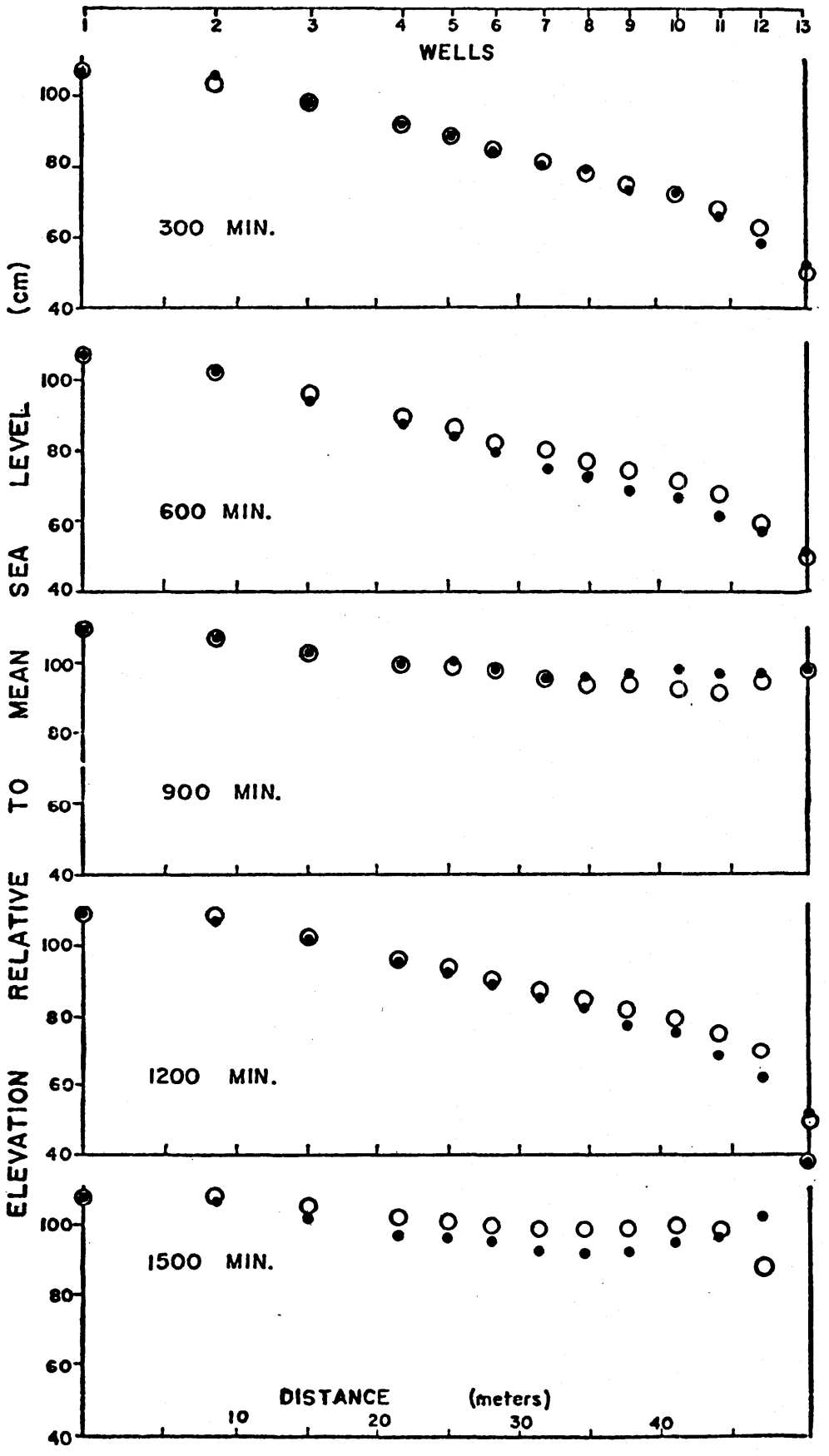

FIG. 6. Comparison between field data (solid circles) and computer results (open circles).

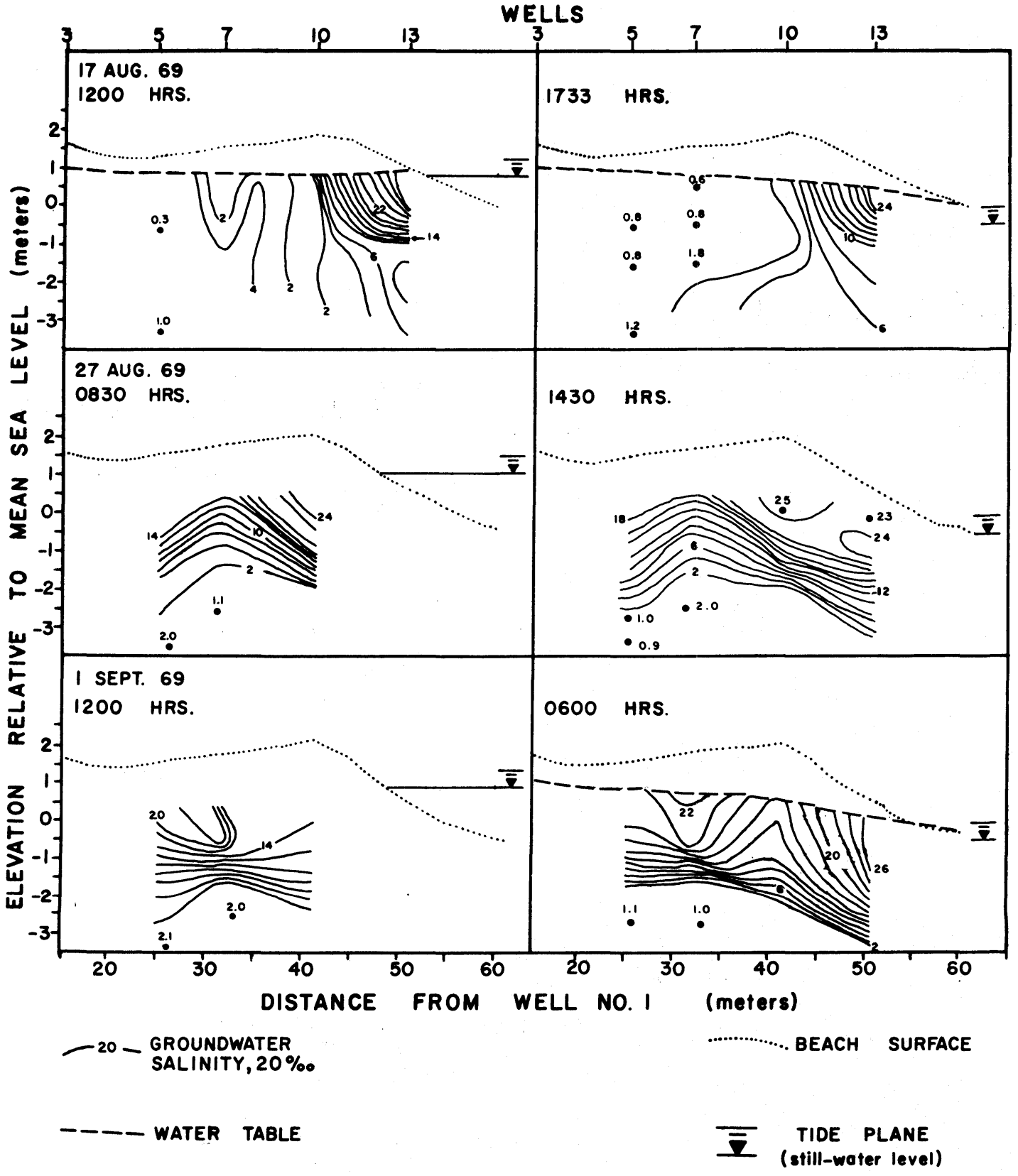

FIG. 7. Salinity structure of the beach groundwater before (17 Aug. 69) and after (27 Aug. 69) storm wave flooding of backshore.

ACKNOWLEDGMENTS

We thank Drs. John Bredehoeft and George Pinder for critical review of the manuscript.

REFERENCES

Chow, Ven Te, Handbook of Applied Hydrology, McGraw-Hill, New York, 1964.

Duncan, J. R., The effects of water table and tide cycle on swash-backwash sediment distribution and beach profile development, Marine Geology, 2(1), 186-197, 1964.

Emery, K. O., and J. F. Foster, Water tables in marine beaches, Jour. Marine Research, 7(3), 644-654, 1948.

Fang, C. S., Mathematical Solution of the Complete Equations of Unsteady Flow in Open Channels, Ph.D. Thesis, N. C. State Univ., 1968.

Fausak, L. E., The Beach Water Table as a Response Variable of the Beach-Ocean-Atmosphere System, Master's Thesis, Univ. of Virginia, 51 p., 1970.

Grant, U. S., Influence of the water table on beach aggradation and degradation, Jour. Marine Research, 7(3), 655-660, 1948.

Harrison, W., and L. E. Fausak, A time series from the beach environment—II, Va. Inst. Marine Sci., Data Rept. No. 7, 1970, p. 1-96.

Jansson, B-O., Diurnal and annual variations of temperature and salinity of interstitial water in sandy beaches: Ophelia 4, 173-201, 1967.

Neuman, S. P., and P. A. Witherspoon, Variational principles for confined and unconfined flow of groundwater, Water Resources Res., 6(5), 1376, 1970.

Taylor, R. L., and C. S. Brown, Darcy flow solutions with a free surface, Amer. Soc. Civ. Eng., Jour. Hydraulics Div., 93(2), 25-33, 1967.

Volker, R. E., Nonlinear flow in porous media by finite elements, Amer. Soc. Civil Eng., Hydraul. Div., 94(HY6), 2093-2114, 1969.

Weinstock, R., Calculus of Variations with Application to Physics and Engineering, McGraw-Hill, New York, 1952.

Zienkiewicz, O., The finite element method in structure and continuum mechanics, McGraw-Hill, New York, 1967.

FORTRAN PROGRAMS FOR THE ONE-DIMENSIONAL, FINITE-ELEMENT ANALYSIS

Main Program & Subroutine DRANV

Following this description the reader will find the main program and a subroutine, DRANV, which was designed to find the bottom drainage velocity with Fourier coefficients for drainage velocity. Definitions of all of the variables can be found from the comment cards in the programs. Also included are comment cards describing the purposes of various sections of the programs. All data that are needed should be prepared in card form; no other input device is used. This program takes 2.38 minutes CPU time, per 100 cycles, in mode 50/IBM 360. Input cards are listed in the following groups:

1) First card: FORMAT(216, 5E12.4)

   (1) NPOIN: total number of nodal points
   (2) NELEM: total number of line elements
   (3) DT: time increment of time step
   (4) TL: total time to quit
   (5) XK: hydraulic conductivity
   (6) POROS: porosity
   (7) DX: length of even line elements

2) Second card: FORMAT(E12.4)

   (1) EPS: the convergent criteria of Newton-Raphson method

3) 3rd to 15th card: FORMAT(I6, 2E12.4)

   Each card contains three initial well's characteristics defined as:

   (1) I: integre counter to specify well number
   (2) XW(I): x-coordinate of well No. 1
   (3) YW(I): water table of well No. 1

4) 16th to (15+ NPOIN)th card: FORMAT(I10,12X,E12.4)

   Each card contains two initial nodal characteristics defined as:

   (1) I: integre counter to specific node number
   (2) Y(I): water tables of node I

5) $(16 + NPOIN)^{th}$ to $(39 + NPOIN)^{th}$ card:
FORMAT (A7, 6E12.4)

This group, containing 24 cards, can be thought of as 12 sets, each set consisting of two cards. Fourier cosine coefficients of drainage velocities are punched on the first card, which may be described as:

(1) CDUMY: variables for A-field, to be identified as Fourier Cosine coefficients
(2) A(I,1): first Fourier cosine coefficient of well number I
(3) A(I,2): second Fourier cosine coefficient of well number I
(4) A(I,3): third Fourier cosine coefficient of well number I
(5) A(I,4): fourth Fourier cosine coefficient of well number I
(6) A(I,5): fifth Fourier cosine coefficient of well number I
(7) A(I,6): sixth Fourier cosine coefficient of well number I

Fourier sine coefficients are punched on the second card which may be described as:

(1) SDUMY: Variables for A-field, to be identified as Fourier sine coefficients
(2) B(I,1): first Fourier sine coefficient of well number I
(3) B(I,2): second Fourier sine coefficient of well number I
(4) B(I,3): third Fourier sine coefficient of well number I
(5) B(I,4): fourth Fourier sine coefficient of well number I
(6) B(I,5): fifth Fourier sine coefficient of well number I
(7) B(I,6): sixth Fourier sine coefficient of well number I

6) $(29 + NPOIN)^{th}$ card on: FORMAT(4F10.4)

Each card contains left- and right-hand-side boundary conditions obtained from field data. The total number of cards in this group is equal to the total number of time steps desired:

(1) Y(1): water table for left-hand-side boundary
(2) Y(NPOIN): water table for right-hand-side boundary

(3) The third and fourth variable of each card are dummy variables.

```
C     PROGRAM OF ONE-DIMENSIONAL UNDERGROUND WATER FLOW,SOLVED BY FINITE
C     ELEMENT METHOD WITH EVEN SPACING,AND NEWTON-RAPHSON METHOD,WRITTEN
C     BY SOU-NAN WANG, UNDER ONR GRANTS
C
C
C     NPOIN=TOTAL NUMBER OF NODAL POINT
C     NELEM=TOTAL NUMBER OF FINITE ELEMENT
C     DT=TIME INCREAMENT
C     TL=TIME TO QUIT
C     XK=HYDRAULIC CONDUCTIVITY
C     POROS=POROSITY
C     DX    =THE LENGTH OF ELEMENT M
C     EPS=THE CONVERGENT CRITERIA OF NEWTON-RAPHSON METHOD
C     A1    =COEFF. OF THE TERM Y(N-1)**2 IN THE NONLINEAR FUNCTION F(N)=0
C     A2    =COEFF. OF THE TERM Y(N)**2 IN THE NONLINEAR FUNCTUIN F(N)=0
C     A3 =COEFFF. OF THE TERM Y(N+1)**2 IN THE NONLINEAR FUNCTUIN F(N)=0
C     A4    =COEFF. OF TERM Y(N-1)*Y(N) IN THE NONLINEAR FUNCTION F(N)=0
C     A5    =COEFF. OF TERM Y(N)*Y(N+1) IN THE NONLINEAR FUNCTION F(N)=0
C     A6    =COEFF. OF TERM Y(N-1)      IN THE NONLINEAR FUNCTION F(N)=0
C     A7    =COEFF. OF TERM Y(N)        IN THE NONLINEAR FUNCTION F(N)=0
C     A8    =COEFF. OF TERM Y(N+1)      IN THE NONLINEAR FUNCTION F(N)=0
C     A9(I)=THE CONSTANT TERM           IN THE NONLINEAR FUNCTION F(N)=0
C     F(I)=NONLINEAR FUNCTION F(N) AT EACH NODAL POINT
C     FDY(I)=JACOBIN MATRIX
C     Y(I)=THE HEIGHT OF FREE SURFACE MEASURED FROM DATUM LINE AT NODES
C     YW(I)=THE HEIGHT OF FREE SURFACE MEASURED FROM DATUM LINE AT WELLS
C     XW(I)=X-COORDINATES OF EACH WELL
C     V(I)=DRAINAGE VELOCITY OF EACH ELEMENT
C     DYB1,DYB2=DUMMY VARIABLE
C     YOLD(I)=ORIGINAL VALUE OF (I) AT EACH TIME STEP FOR COMPARING
C             WITH EACH ITERATED VALUE OF Y(I)
C     NITER=COUNTER OF TOTAL NUMBER OF ITERATION IN NEWTON-RAPHSON
C           METHOD AT EACH TIME STEP,WHEN Y(I) REACHES CONVERGENCE
C     NLEPS=COUNTER OF TOTAL NUMBER OF NODAL WHICH SATISFIES THE
C           CONVERGENT CRITERIA AT EACH ITERATION
C     YP(I)=EQUIVALENT TO Y(I)
C     NPRIN=CONTROL COUNTER OF PRINTING
C     A(I,J)=FOURIER COSINE COEFFICIENTS
C     B(I,J)=FOURIER SINE COEFFICIENTS
C
C
      DIMENSION Y(21),YOLD(21),F(19),FDY(19,19),A9(21),V(20),
     *YP(21),YW(13),XW(13)
      DIMENSION A(12,6),B(12,6)
      DIMENSION VW(12)
      COMMON DX,NPOI1,A,B,VW
      EQUIVALENCE (Y(1),YP(1))
C
      IR=5
      IW=6
    1 FORMAT(2I6,5E12.4)
    2 FORMAT(2X,6HNPOIN=,I6,2X,6HNELEM=,I6,2X,3HDT=,E12.4,2X,3HTL=,E12.4
     1,2X,3HXK=,E12.4,2X,7HPOROS =,E12.4,2X,3HDX=,E12.4)
    3 FORMAT(I10,12X,E12.4)
    4 FORMAT(E12.4)
    5 FORMAT(5X,6HNITER=,I6,2X,6HNLEPS=,I6,2X,4HEPS=,E12.4)
    6 FORMAT(I10,2X,E12.4)
    7 FORMAT(1H0,2X,2HT=,E12.4)
    8 FORMAT(4F10.4)
    9 FORMAT(I6,5E12.4)
   10 FORMAT(I6,E12.4)
   11 FORMAT(8X,1HI,6X,4HY(I),9X,6HY(I+1),9X,6HY(I+2),9X,
```

```
     16HY(I+3),9X,6HY(I+4),9X,6HY(I+5))
   12 FORMAT(2X,I7,6E15.7)
   13 FORMAT(2X,I7,E15.7)
   14 FORMAT(2X,4HEPS=,E12.4///)
   15 FORMAT(I6,3E12.4)
   16 FORMAT(I6,2E12.4)
   17 FORMAT(2X,8E12.4)
   18 FORMAT(A7,6E12.4)
   21 FORMAT(1H1,2X,83HPROGRAM TO SOLVE 1-D UNDERGROUND WATER BY FINITE
     *ELEM-ENT AND NEWTON-RAPHSON METHOD)
   22 FORMAT(2X,22HSTOP DUE TO DIVERGENCE)
   23 FORMAT(2X,60HCHANGE OF Y(I) DUE TO EFFECT OF CAPILLARY AND OTHER
     *FACTORS)
   24 FORMAT(10X,1HI,6X,5HDY(I),8X,7HDY(I+1),8X,7HDY(I+2),8X,7HDY(I+3),
     *8X,7HDY(I+4),7HDY(I+5))
   25 FORMAT(2X,41HYW(I) HEIGHT OF FREE SURFACE AT EACH WELL)
   26 FORMAT(5X,1HI,5X,5HYW(I),8X,7HYW(I+1),8X,7HYW(I+2),8X,7HYW(I+3),8X
     *,7HYW(I+4))
   27 FORMAT(1HO,2X,42HINITIAL HEIGHT OF WATER TABLE AT EACH NODE//)
   28 FORMAT(1HO,2X,46HFOURIER COEFFICIENTS OF WELL DRAINAGE VELOCITY//)
C
C
      WRITE(IW,21)
      READ(IR,1) NPOIN,NELEM,DT,TL,XK,POROS,DX
      WRITE(IW,2)NPOIN,NELEM,DT,TL,XK,POROS,DX
      READ(IR,4)EPS
      WRITE(IW,14)EPS
      READ(IR,16)(I,XW(I),YW(I),I=1,13)
      DO 55 I=1,NPOIN
   55 READ(IR,3) I,Y(I)
      WRITE(IW,27)
      WRITE(IW,11)
      NDIV=NPOIN/6
      NMAX=NDIV*6
      DO 56 I=1,NPOIN,6
      IF(I-NMAX) 211,211,210
  211 WRITE(IW,12) I,Y(I),Y(I+1),Y(I+2),Y(I+3),Y(I+4),Y(I+5)
      GO TO 56
  210 DO 212 J=I,NPOIN
  212 WRITE(IW,13) J,Y(J)
   56 CONTINUE
      NPOI1=NPOIN-1
      NPOI2=NPOIN-2
      DDT=1.0/DT
      T=0.0
      NDV=NPOI1/5
      NMA=NDV*5
      NMA1=NMA+1
C
C     KNOWING THE RELATION BETWEEN NUMBERING SYSTEM OF ELEMENTS AND
C     NODES ,WE EXPRESS THE COEFFICIENTS OF NONLINEAR FUNCTION IN TERMS
C     OF NUMBER SYSTEM OF NODALS
C
      A1=-0.25*XK/DX
      A2=1.5*XK/DX
      A3=A1
      A4=2.0*A1
      A5=A4
      DDTPR=0.166667*DDT*POROS
```

```
      A6=CCTPR*CX
      A7=4.0*A6
      A8=A6
      DC 91 I=1,NPCIN,NPCI1
   91 A9(I)=0.0
      DC 58 I=2,NPCI1
      AA=0.0
      BB=A6*Y(I-1)
      A9(I)=AA-BB
      BB=A7*Y(I)
      AA=A8*Y(I+1)
   58 A9(I)=A9(I)-BB-AA
      DC 61 I=1,NPCI2
      DC 62 J=1,NPCI2
   62 FDY(I,J)=0.0
      V(I)=0.0
   61 F(I)=0.0
      V(NPCI1)=0.0
C
C     READ FCURIER CCEFFIENTS OF WELL DRAINAGE VELOCITY
C
      DC 50 I=1,12
      READ(IR,18)CCUMY,A(I,1),A(I,2),A(I,3),A(I,4),A(I,5),A(I,6)
   50 READ(IR,18)SCUMY,B(I,1),B(I,2),B(I,3),B(I,4),B(I,5),B(I,6)
      WRITE(IW,28)
      DC 290 I=1,12
      WRITE(IW,18)CCUMY,A(I,1),A(I,2),A(I,3),A(I,4),A(I,5),A(I,6)
      WRITE(IW,18)SCUMY,B(I,1),B(I,2),B(I,3),B(I,4),B(I,5),B(I,6)
  290 CCNTINUE
      NREDV=0
C
C     PRISCRIBE BCUNDARY OF Y AT EACH TIME STEP
C
      NPRIN=0
  400 T=T+DT
      NITER=0
      YCLD(NPCIN)=Y(NPCIN)
      DC 116 I=1,NPCI1
  116 YCLD(I)=Y(I)
      READ(IR,8) Y(1),Y(NPCIN),DYB1,DYB2
      NREDV=NREDV+1
      IF(T-2.0*DT) 280,280,281
  280 IF(NREDV-1) 283,282,283
C     FIND DRAINAGE VELCCITY BY CALLING SUBRCUTINE DRANV
  282 CALL DRANV(T,XW,V)
  283 IF(NREDV-2)285,284,285
  284 NREDV=0
      GC TC 285
  281 IF(NREDV-1) 287,286,287
  286 CALL DRANV(T,XW,V)
  287 IF(NREDV-5) 285,288,285
  288 NREDV=0
  285 CONTINUE
      DC 110 I=2,NPCI1
      XV1=V(I-1)
      XV2=V(I)
      AA=-0.5*XV1*CX-0.5*XV2*CX
  110 A9(I)=A9(I)+AA
C
C      FIND BEST FIRST APPRCXIMATION VALUE SET FCR Y(I)
C
```

```
      AA=Y(NPCIN)-YCLD(NPCIN)
      XN=NPCI1
      BB=XN*DX
      BB=1/BB
      DO 250 I=2,NPCI1
      XII=I-1
  250 Y(I)=YCLD(I)+AA*BB*XII*DX*C.5
C     FIND RESIDUE AND JACOBIN MATRIX
  300 DO 66 I=2,NPCI2
      F(I-1)=A1*Y(I-1)*Y(I-1)+A2*Y(I)*Y(I)+A3*Y(I+1)*Y(I+1)
     1+A4*Y(I-1)*Y(I)+A5*Y(I)*Y(I+1)+A6*Y(I-1)+A7*Y(I)
     2+A8*Y(I+1)+A9(I)
      FDY(I-1,I-1)=2.C*A2*Y(I)+A4*Y(I-1)+A5*Y(I+1)+A7
      IF(I-2) 67,68,67
   67 FDY(I-1,I-2)=2.C*A1*Y(I-1)+A4*Y(I)+A6
      FDY(I-1,I)=2.C*A3*Y(I+1)+A5*Y(I)+A8
      GO TO 66
   68 BB=2.0*A3*Y(3)+A5*Y(2)+A8
      FDY(1,2)=BB
   66 CONTINUE
      I=NPCI1
      F(I-1)=A1*Y(I-1)*Y(I-1)+A2*Y(I)*Y(I)+A3*Y(I+1)*Y(I+1)
     *+A4*Y(I-1)*Y(I)+A5*Y(I)*Y(I+1)+A6*Y(I-1)+A7*Y(I)
     *+A8*Y(I+1)+A9(I)
      FDY(I-1,I-1)=2.0*A2*Y(I)+A4*Y(I-1)+A5*Y(I+1)+A7
      FDY(I-1,I-2)=2.C*A1*Y(I-1)+A4*Y(I)+A6
      NDIV=NPCI2/6
      NMAX=NDIV*6
      CALL SIMQ(FDY,F,NPCI2,KS)
      NLEPS=0
      DO 71 I=1,NPCI2
      AA=ABS(F(I))
      AA=AA/YCLD(I+1)
      IF(AA-EPS)72,72,71
   72 NLEPS=NLEPS+1
   71 CONTINUE
      DO 76 I=1,NPCI2
   76 Y(I+1)=Y(I+1)-F(I)
      IF(NLEPS-NPCI2)77,78,77
   77 CONTINUE
      NITER=NITER+1
      IF(NITER-5) 300,402,300
   78 CONTINUE
C
C     FIND YW(I) OF WELLS FROM Y(I) BY LINEAR INTERPOLATION
C
      Yw(1)=YP(1)
      AA=YP(NPCI1)-YP(NPCIN)
      Yw(13)=YP(NPCIN)-77.9*AA/DX
      DO 221 I=2,12
      DO 222 J=1,NPCI1
      AA=Xw(I)
      FJ=J
      X=FJ*DX
      BB=X
      IF(AA-BB)  223,223,222
  223 AA=Xw(I)-X+DX
      BB=X-Xw(I)
      CC=AA*YP(J+1)+BB*YP(J)
```

```
      YW(I)=CC/(AA+BB)
      GO TO 221
  222 CONTINUE
  221 CONTINUE
      NPRIN=NPRIN+1
      IF(NPRIN-10) 226,225,226
  225 CONTINUE
      WRITE(IW,7) T
      WRITE(IW,5) NITER,NLEPS,EPS
      WRITE(IW,25)
      WRITE(IW,26)
      WRITE(IW,9) (I,YW(I),YW(I+1),YW(I+2),YW(I+3),YW(I+4),I=1,10,5)
      I=11
      WRITE(IW,15)  I,YW(I),YW(I+1),YW(I+2)
      NPRIN=0
  226 CONTINUE
      IF(T-TL)201,202,202
  201 CONTINUE
  302 DO 85 I=2,NPOI1
      AA=0.0
      BB=A6*Y(I-1)
      A9(I)=AA-BB
      BB=A7*Y(I)
      AA=A8*Y(I+1)
   85 A9(I)=A9(I)-BB-AA
      GO TO 400
  402 WRITE(IW,22)
      STOP
  202 STOP
      END
```

```
      SUBROUTINE DRANV(T,XW,V)
C     SUBROUTINE DRANV FOR FINDING DRAINAGE VELOCITY OF WELLS AND EVEN ELEMENTS
C     WITH GIVEN FOURIER COEFF. OF WELL DRAINAGE VELOCITY
C     ALL UNITS SHOULD BE IN C.G.S. UNIT SYSTEM
C     INPUT  A(IJ) =FOURIER COSINE COEFFICIENTS OF WELL DRAINAGE VELOCITY
C            B(IJ) =FOURIER SINE COEFFICIENTS OF WELL DRAINAGE VELOCITY
C            XW(I) =X-COORDINATES OF 13 WELLS
C            DX    =LENGTH OF EVEN ELEMENTS
C            T     =CORRENT TIME
C            NPOI1 =TOTAL NO. OF NODAL POINTS MINUS 1
C     OUTPUT VW(I) =DRAINAGE VELOCITY OF WELLS
C            V(I)  =DRAINAGE VELOCITY OF EVEN ELEMENTS
C     A(I,J)=FOURIER COSINE COEFFICIENTS
C     B(I,J)=FOURIER SINE COEFFICIENTS
C     PERIOD = 100*15*60 SECONDS, WHERE 100 MEANS 100 CYCLES, 15 MEANS 15
C              MINUTES PER CYCLE, 60 MEANS 1 MINUTE EQUAL TO 60 SECONDS
      DIMENSION VW(12),V(20),A(12,6),B(12,6),XW(13)
      COMMON DX,NPOI1,A,B,VW
C     FIND DRAINAGE VELOCITY BETWEEN TWO WELLS BY FOURIER SERIES APPROXIMATION
      CC=2.0*3.1416/(15.0*60.0*100.0)
      DO 51 I=1,12
      SUM=A(I,1)
      DO 52 J=2,6
      AA=A(I,J)
      BB=B(I,J)
      FJ=J-1
      DD=FJ*CC*T
   52 SUM=SUM+AA*COS(DD)+BB*SIN(DD)
   51 VW(I)=SUM
C     FIND DRAINAGE VELOCITY FOR EACH ELEMENT WITH EVEN LENGTH
      X=0.5*DX
      DO 60 I=1,NPOI1
      DO 61 J=1,12
      IF(X-XW(J+1))63,65,66
   63 V(I)=VW(J)
      AA=XW(J+1)-X
      IF(AA-0.5*DX) 64,69,69
   64 BB=X+0.5*DX-XW(J+1)
      CC=(0.5*DX+AA)*VW(J)+BB*VW(J+1)
      V(I)=CC/DX
      GO TO 69
   65 V(I)=0.5*VW(J+1)+0.5*VW(J)
      GO TO 69
   66 AA=X-XW(J+1)-0.5*DX
      IF(AA) 67,61,61
   67 BB=X-XW(J+1)+0.5*DX
      CC=XW(J+1)-X+0.5*DX
      V(I)=(BB*VW(J+1)+CC*VW(J))/DX
      GO TO 69
   61 CONTINUE
   69 X=X+DX
   60 CONTINUE
      RETURN
      END
```

INPUT DATA FOR ILLUSTRATED EXAMPLE

NPOIN	NELEM	DT	TL	XK	POROS	DX
21	20	9.000CE+02	9.090CE+04	1.4C00E-02	0.3400E+00	2.5000E+02

EPS
1.0000E-03

INITIAL DATA OF 13 WELLS

I	XW(I)	YW(I)
1	0.0000E+00	1.0590E+02
2	1.0000E+03	1.0390E+02
3	1.5500E+03	0.9710E+02
4	2.2000E+03	0.9100E+02
5	2.5500E+03	0.8880E+02
6	2.8500E+03	0.8540E+02
7	3.1000E+03	0.8170E+02
8	3.5000E+03	0.7980E+02
9	3.8000E+03	0.7630E+02
10	4.0000E+03	0.7590E+02
11	4.5000E+03	0.7160E+02
12	4.8500E+03	0.6880E+02
13	5.0000E+03	0.6700E+02

INITIAL DATA OF WATER TABLE AT EACH NODE

I	Y(I)
1	1.059CE+C2
2	1.054CE+C2
3	1.049CE+C2
4	1.044CE+C2
5	1.039CE+C2
6	1.008CE+C2
7	9.770CE+C1
8	9.530CE+C1
9	9.290CE+C1
10	9.1007E+C1
11	8.9114E+C1
12	8.6147E+C1
13	8.318CE+C1
14	8.149CE+C1
15	7.980CE+C1
16	7.688CE+C1
17	7.590CE+C1
18	7.345CE+C1
19	7.160CE+C1
20	6.960CE+C1
21	6.700CE+C1

FOURIER COEFFICIENTS OF WELL DRAINAGE VELOCITY

ICOS	0.2060E-04	-0.2555E-04	0.3933E-04	-0.1161E-04	0.7523E-05	-0.2118E-05
ISIN	0.0000E 00	-0.4224E-05	-0.1677E-05	0.6999E-05	-0.1689E-04	-0.9095E-05

2CCS	0.3689E-04	-0.1483E-04	0.7028E-04	-0.2182E-04	0.1646E-04	0.3183E-05
2SIN	0.0000E 00	-0.6800E-05	-0.2002E-04	0.6440E-05	-0.2374E-04	-0.1631E-04
3CCS	0.3666E-04	-0.1003E-04	0.1005E-03	-0.4412E-04	0.2276E-04	0.3765E-05
3SIN	0.0000E 00	-0.8123E-05	-0.5320E-04	0.1999E-05	-0.3054E-04	-0.2445E-04
4CCS	0.4971E-04	-0.9646E-05	0.1261E-03	-0.6833E-04	0.2999E-04	0.6248E-05
4SIN	0.0000E 00	-0.7289E-05	-0.8863E-04	-0.8633E-06	-0.3150E-04	-0.2679E-04
5CCS	0.6418E-04	-0.8761E-05	0.1453E-03	-0.9076E-04	0.3359E-04	0.6758E-05
5SIN	0.0000E 00	-0.7440E-05	-0.1177E-03	-0.2665E-05	-0.3154E-04	-0.2828E-04
6CCS	0.5345E-04	-0.7978E-05	0.1637E-03	-0.1162E-03	0.3628E-04	0.6731E-05
6SIN	0.0000E 00	-0.3818E-05	-0.1470E-03	-0.2576E-05	-0.2888E-04	-0.2791E-04
7CCS	0.7328E-04	-0.4882E-05	0.1783E-03	-0.1286E-03	0.4556E-04	0.1265E-04
7SIN	0.0000E 00	-0.1082E-05	-0.1770E-03	-0.8028E-05	-0.2667E-04	-0.2772E-04
8CCS	0.8153E-04	0.7425E-05	0.2038E-03	-0.1508E-03	0.5643E-04	0.1902E-04
8SIN	0.0000E 00	-0.1136E-05	-0.2246E-03	-0.1760E-04	-0.2682E-04	-0.3179E-04
9CCS	0.1070E-03	0.1214E-04	0.2185E-03	-0.1908E-03	0.5860E-04	0.2009E-04
9SIN	0.0000E 00	-0.6813E-05	-0.2831E-03	-0.2555E-04	-0.1887E-04	-0.2813E-04
10CCS	0.1245E-03	0.8425E-05	0.2222E-03	-0.2390E-03	0.5734E-04	0.2059E-04
10SIN	0.0000E 00	-0.1079E-04	-0.3439E-03	-0.2934E-04	-0.5645E-06	-0.1428E-04
11CCS	0.1214E-03	0.2163E-04	0.2230E-03	-0.2915E-03	0.6012E-04	0.2998E-04
11SIN	0.0000E 00	-0.2396E-04	-0.4261E-03	-0.3836E-04	0.2684E-04	0.5779E-05
12CCS	0.7925E-04	-0.7718E-04	0.1126E-03	-0.4094E-03	0.2125E-04	0.3222E-04
12SIN	0.0000E 00	-0.1256E-04	-0.4542E-03	0.3179E-04	0.1628E-03	0.1422E-03

RESULTANT WATER TABLES OF ILLUSTRATED EXAMPLE

C TIME T= 0.9000E 04

NITER= 1 NLEPS= 19 EPS= 0.1000E-02

HEIGHT OF FREE SURFACE AT EACH WELL

I	YW(I)	YW(I+1)	YW(I+2)	YW(I+3)	YW(I+4)
1	0.1067E 03	0.1035E 03	0.9844E 02	0.9227E 02	0.8908E 02
6	0.8595E 02	0.8357E 02	0.8038E 02	0.7778E 02	0.7599E 02
11	0.7087E 02	0.6860E 02	0.6814E 02		

C TIME T= 0.1800E 05

NITER= 1 NLEPS= 19 EPS= 0.1000E-02

HEIGHT OF FREE SURFACE AT EACH WELL

I	YW(I)	YW(I+1)	YW(I+2)	YW(I+3)	YW(I+4)
1	0.1065E 03	0.1033E 03	0.9858E 02	0.9203E 02	0.8857E 02
6	0.8536E 02	0.8276E 02	0.7884E 02	0.7575E 02	0.7361E 02
11	0.6763E 02	0.5900E 02	0.4776E 02		

C TIME T= 0.2700E 05

NITER= 1 NLEPS= 19 EPS= 0.1000E-02

HEIGHT OF FREE SURFACE AT EACH WELL

I	YW(I)	YW(I+1)	YW(I+2)	YW(I+3)	YW(I+4)
1	0.1054E 03	0.1023E 03	0.9744E 02	0.9062E 02	0.8701E 02
6	0.8374E 02	0.8113E 02	0.7722E 02	0.7432E 02	0.7247E 02
11	0.6635E 02	0.5350E 02	0.3770E 02		

C TIME T= 0.3600E 05

NITER= 1 NLEPS= 19 EPS= 0.1000E-02

HEIGHT OF FREE SURFACE AT EACH WELL

I	YW(I)	YW(I+1)	YW(I+2)	YW(I+3)	YW(I+4)
1	0.1044E 03	0.1019E 03	0.9705E 02	0.9031E 02	0.8687E 02
6	0.8377E 02	0.8132E 02	0.7772E 02	0.7537E 02	0.7394E 02
11	0.6750E 02	0.5559E 02	0.4877E 02		

C TIME T= 0.4500E 05

NITER= 1 NLEPS= 19 EPS= 0.1000E-02

HEIGHT OF FREE SURFACE AT EACH WELL

I	YW(I)	YW(I+1)	YW(I+2)	YW(I+3)	YW(I+4)
1	0.1049E 03	0.1044E 03	0.1008E 03	0.9546E 02	0.9331E 02
6	0.9136E 02	0.8974E 02	0.8744E 02	0.8661E 02	0.8625E 02
11	0.7969E 02	0.8705E 02	0.1117E 03		

C TIME T= 0.5400E 05

NITER= 1 NLEPS= 19 EPS= 0.1000E-02

HEIGHT OF FREE SURFACE AT EACH WELL

I	YW(I)	YW(I+1)	YW(I+2)	YW(I+3)	YW(I+4)
1	0.1081E 03	0.1067E 03	0.1040E 03	0.9994E 02	0.9849E 02
6	0.9721E 02	0.9614E 02	0.9486E 02	0.9456E 02	0.9423E 02
11	0.9168E 02	0.9681E 02	0.9892E 02		

C TIME T= 0.6300E 05

NITER= 1 NLEPS= 19 EPS= 0.1000E-02

HEIGHT OF FREE SURFACE AT EACH WELL

I	YW(I)	YW(I+1)	YW(I+2)	YW(I+3)	YW(I+4)
1	0.1098E 03	0.1067E 03	0.1030E 03	0.9794E 02	0.9524E 02
6	0.9286E 02	0.9099E 02	0.8839E 02	0.8608E 02	0.8439E 02
11	0.8175E 02	0.7212E 02	0.5948E 02		

C TIME T= 0.7200E 05

NITER= 1 NLEPS= 19 EPS= 0.1000E-02

HEIGHT OF FREE SURFACE AT EACH WELL

I	YW(I)	YW(I+1)	YW(I+2)	YW(I+3)	YW(I+4)
1	0.1099E 03	0.1066E 03	0.1026E 03	0.9687E 02	0.9374E 02
6	0.9086E 02	0.8857E 02	0.8512E 02	0.8242E 02	0.8078E 02
11	0.7543E 02	0.6327E 02	0.4827E 02		

```
C     TIME T=  0.8100E 05

          NITER=      1  NLEPS=     19  EPS=  0.1000E-02

                      HEIGHT OF FREE SURFACE AT EACH WELL

          I      YW(I)        YW(I+1)      YW(I+2)      YW(I+3)      YW(I+4)

          1  0.1078E 03  0.1063E 03  0.1031E 03  0.9846E 02  0.9648E 02
          6  0.9467E 02  0.9316E 02  0.9111E 02  0.9100E 02  0.9144E 02
         11  0.8922E 02  0.7236E 02  0.5100E 02

C     TIME T=  0.9000E 05

          NITER=      1  NLEPS=     19  EPS=  0.1000E-02

                      HEIGHT OF FREE SURFACE AT EACH WELL

          I      YW(I)        YW(I+1)      YW(I+2)      YW(I+3)      YW(I+4)

          1  0.1081E 03  0.1078E 03  0.1062E 03  0.1031E 03  0.1021E 03
          6  0.1011E 03  0.1004E 03  0.1004E 03  0.1017E 03  0.1024E 03
         11  0.9734E 02  0.9899E 02  0.1125E 03
```

Fortran Program for Obtaining Fourier Coefficients for Drainage Velocities

This program contains one main program and three subroutines whose purposes can be determined from the comment cards. All variables are defined in the program. Input is in the form of punched cards, which can be described in the following groups:

1) First card: FORMAT(4E12.4, I6)

   (1) DT: time increment
   (2) POROS: porosity
   (3) XK: hydraulic conductivity
   (4) TL: total time to quit (end of run)
   (5) NWELL: total number of wells

2) 2nd to (1 + NWELL)th card: FORMAT (I6, 2E12.4)

   Each card has three initial well characteristics defined as:

   (1) I: integer counter to specify well number
   (2) XW(I): x-coordinate of well no. 1
   (3) YW(I): water table of well no. 1

3) (2 + NWELL)th to (1 + NWELL + NSTEP)th card: FORMAT (I5, 12F5.1)

   Each card contains fourteen variables as:

   (1) I: integer to specify time step
   (2) Y(I,1): water table elevation of well no. 1 at time step 1
   (3) Y(I,2): water table of well no. 2 at time step 1

   .

   .

   .

   (14) Y(I,13): water table of well no. 13 at time step 1.

```
C      PROGRAM TO FIND FOURIER COEFFICIENTS OF WELL DRAINAGE VELOCITY
C
C      INPUT
C
C      DT=TIME INCREAMENT
C      POROS=POROSITY
C      XK=HYDRAULIC CONDUCTIVITY
C      NWELL=TOTAL NUMBER OF WELLS, SHOULD BE GREATER THAN 3
C      TL=TIME TO QUIT
C      XW(I)=X-COORDINATE OF EACH WELL
C      YW(I)=Y-COORDINATE OF EACH WELL AT TIME T
C            Y(IJ)=NEW WATER TABLES OF WELLS
C
C      OUTPUT
C
C            A(IJ)=FOURIER COSING COEFF. OF DRAINAGE VELOCITY
C            B(IJ)=FOURIER  SINE  COEFF. OF DRAINAGE VELOCITY
C
C      DEFINITION OF OTHER VARIABLES
C      NSTEP=TOTAL NO. OF TIME STEP
C      YWN(I)=Y-COORDINATE OF EACH WELL AT TIME T+DT
C            V(IJ) =BOTTOM DRAINAGE VELOCITY AT TIME STEP I, ELEMENT J
C            VW(I) =DUMMY V(IJ) FOR CALLING FDRAV
C
      DIMENSION Y(101,13),V(100,12),A(6,2),B(6,2),VW(12),YWN(13),XW(13),
     *YW(13)
C
      IR=5
      IW=6
    1 FORMAT(I5,13F5.1)
    4 FORMAT(4E12.4,I6)
    5 FORMAT(I6,2E12.4)
C
      READ(IR,4) DT,POROS,XK,TL,NWELL
      READ(IR,5) (I,XW(I),YW(I),I=1,NWELL)
      NSTEP=TL/DT+0.1
      DO 50 I=1,NSTEP
      READ(IR,1)I,Y(I,1),Y(I,2),Y(I,3),Y(I,4),Y(I,5),Y(I,6),
     *Y(I,7),Y(I,8),Y(I,9),Y(I,10),Y(I,11),Y(I,12),Y(I,13)
   50 CONTINUE
C
      L=NSTEP
      NJ=NWELL-1
      DO 70 I=2,L
      DO 71 JJ=1,NWELL
   71 YWN(JJ)=Y(I,JJ)
C
C     FIND WELL DRAINAGE VELOCITY BY EULERIAN FINITE DIFFERENCE METHOD
C
      CALL FDRAV(DT,POROS,XK,XW,YW,YWN,VW,NWELL)
      DO 72 JJ=1,NJ
   72 V(I-1,JJ)=VW(JJ)
      DO 73 JW=1,NJ
   73 WRITE(IW,7) JW,VW(JW)
   70 CONTINUE
C
C     FIND FOURIER COEFF. OF WELL DRAINAGE VELOCITY
C
      L=NSTEP-1
      CALL FORAV(L,5,NWELL,21,5,0.0,1.0,V,A,B)
      END
```

```
      SUBROUTINE FDRAV(DT,POROS,XK,XW,YW,YWN,VW,NWELL)
C
C     PROGRAM TO FIND THE TABULATED VALUE OF DRAINAGE VELOCITY
C     BY EULERIAN FINITE DIFFIRENCE METHOD
C
C     V(I)=DRAINAGE VELOCITY OF ELEMENT WITH EVEN SPACING
C     VW(I)=DRAINAGE VELOCITY OF ELEMENT SEPARATED BY WELLS
C
      DIMENSION VW( 1),XW( 1),YW( 1),YWN( 1)
      NJ=NWELL-1
      FDT=0.5*POROS/DT
      DO 50 I=1,NJ
      AA=FDT*(YWN(I+1)+YWN(I)-YW(I+1)-YW(I))
      IF(I-1) 52,51,52
   52 BB=-XK*YW(I)*(Yw(I+1)-YW(I-1))
      DXW=1.0/(XW(I+1)-XW(I-1))
      BB=BB*DXW
      IF(I-NJ) 53,54,53
   53 CC=-XK*YW(I+1)*(YW(I+2)-YW(I))
      DXW=1.0/(XW(I+2)-XW(I))
      CC=CC*DXW
      GO TO 55
   54 CC=-XK*YW(I+1)*(YW(I+1)-YW(I))
      DXW=1.0/(XW(I+1)-XW(I))
      CC=CC*DXW
      GO TO 55
   51 BB=-XK*YW(I)*(YW(I+1)-YW(I))
      DXW=1.0/(XW(I+1)-XW(I))
      BB=BB*DXW
      CC=-XK*YW(I+1)*(YW(I+2)-YW(I))
      DXW=1.0/(XW(I+2)-XW(I))
      CC=CC*DXW
   55 DXW=1.0/(XW(I+1)-XW(I))
      VW(I)=AA-DXW*(BB-CC)
   50 CONTINUE
      DO 75 I=1,NWELL
   75 YW(I)=YWN(I)
      RETURN
      END
```

```
      SUBROUTINE FORAV(NTSPS,NAVER,NWELL,LL,MM,TS,TSTEP,VW,A,B)
C
C     PRCGRAM TC SMCOTH THE FLUCTUATION OF DRAINAGE VELOCITIES BY TAKING AVERAGE
C     OF EACH WELL DRAINAGE VELOCITIES EVERY  NAVER  TIME STEP
C
C     PR & PR1  = 8 CHARACTERS FOR IDENTIFICATION
C     NTSPS     = NC. OF TIME STEPS
C     NAVER     = NC. OF TIME STEPS TO AVERAGE
C     NWELL     = NC. OF WELLS  ( 12 OR 13 )
C     LL        = NC. OF TABULATED DATA POINTS DESIRED  ( FOURIER ANALYSIS
C                   IS PERFORMED ON THESE PCINTS)
C     BE CDC INTEGER, OTHERWISE PROGRAM STOP
C     MM        = NC. OF FOURIER COEFFICIENTS TO GENERATE MINUS ONE
C     TS        = START TIME FOR PLOT ROUTINE
C     TSTEP     = TIME INCREMENT FOR PLOT RCUTINE
C     VW(IJ)=GIVEN ARRAY TO BE PERFORMED FOURIER ANALYSIS
C     SVW(IJ)=ARRAY OF VW(IJ) AFTER TAKING AVERAGE EVERY  NAVER  TIME STEPS
C     IRPT=(NUMBER CF PCINT INTERPOLATED ON EACH AVERAGE REGION)-1
C         = BETTER GREATER THAN OR EQUAL TO ONE
C
C     EXAMPLE
C
C             NPSPS=120
C             NAVER=5 , THEN
C             IN=120/5+1=25=TOTAL NUMBERS OF AVERAGE REGION PLUS ONE
C          IF, NUMBER OF POINT INTERPOLATED CN EACH REGION IS 3 , THEN
C             LL=24*(3+1)+1=97
C        AND, IRPT=3-1=2
C
      DIMENSION SVW(5,2),VW(13,2),A(6,2),B(6,2)
C
C
      IW=6
   51 FORMAT(I10)
   52 FORMAT(2I10,E12.4)
      NJ=NWELL-1
      IN= NTSPS/NAVER +1
      DO 23 I=1,NJ
   23 SVW(1,I)=VW(1,I)
      KMJ=1
      DO 6 J=2,IN
      DO 5 I=1,NJ
    5 SVW(J,I)= 0.0
      DO 47 I=1,NAVER
      KMJ = KMJ +1
      IF(KMJ- NTSPS)11,11,12
   12 KMJ = KMJ -1
   11 DO 47 L=1,NJ
   47 SVW(J,L) = SVW(J,L) + VW(KMJ,L)
      DO 48 I=1,NJ
   48 SVW(J,I) = SVW(J,I)/NAVER
    6 CONTINUE
      IRPT=(LL-IN)/(IN-1)
      IRPT=IRPT-1
      WRITE(IW,51) IRPT
      DO 21 J=1,NJ
      DO 21 I=1,NTSPS
   21 WRITE(IW,52) I,J,VW(I,J)
      DO 22 J=1,NJ
      DO 22 I=1,IN
```

```
22 WRITE(IW,52) I,J,SVW(I,J)
   CALL TABFR(NJ,NTSPS,LL,MM,TS,TSTEP,IRPT,VW,SVW,A,B)
   RETURN
   END
```

```
      SUBROUTINE TABFR(KRD,NTSPS,L,M,TS,TSTEP,IRPT,VWW,SVW,A,B)
C
C     PROGRAM TO PERFORM FOURIER ANALYSIS FOR AVERAGE DRAINAGE VELOCITY
C
C     L SHOULD BE ODD INTEGER
C     NTSPS CAN BE EITHER EVEN OR ODD INTEGER
C        WELLS(JI)=ARRAY OF SVW(IJ) AFTER SETTING INTERPOLATION ON EACH AVERAGE
C                  REGION
C     VW(I)=1-D DUMMY ARRAY OF WELL(JI) FOR CALLING SUBROUTINE FORIT
C        FC(I)=FOURIER COSINE COEFF.
C        FS(I)=FOURIER SINE COEFF.
C        V(I) =ARRAY OF FOURIER SERIES APPROXIMATION
C
      DIMENSION VW(13),FS(6),FC(6),WELLS(2,13),T(13),V(13),VWW(13,2),
     *SVW(5,2),A(6,2),B(6,2)
C
C
   10 FORMAT('ON NOT .GT. OR = TO M')
   11 FORMAT('OM .LT. 0')
   19 FORMAT('ONUMBER OF TABULATED VALUES NOT ODD')
   21 FORMAT(' ',18X,I3,2E15.5)
   63 FORMAT(' WELL NUMBER ',I3,10X,'SINE      COSINE   FOURIER COEF.')
   56 FORMAT(I10,E12.4)
   57 FORMAT(2I10,E12.4)
C
      IR=5
      IW=6
C
C     GENGRATE TIME SCALE
C
      DO 20 I=1,L
   20 T(I)= TS +(I-1)*TSTEP
      MM=M+1
      F= (L-1)/2.0
      FNCR=3.141592/F
      N = F
C
C     CHECK, IF VWW(IJ) HAS ODD NUMBER OF TABULATED DATA, STOP PROGRAM
C
      IF(N-F)18,17,18
   18 WRITE(IW,19)
      STOP
C
C     LET FIRST AND FINAL DATA POINTS OF WELLS(JI) AND VWW(IJ) EQUAL
C
   17 DO 1 J=1,KRD
      WELLS(J,1) = VWW(1,J)
    1 WELLS(J,L    ) = VWW(NTSPS,J)
C
C     SETUP FIRST POINT OF EACH AVERAGE REGION
C
      I=2
      NSVW=1
   34 NSVW=NSVW+1
      DO 3 J=1,KRD
    3 WELLS(J,I) = SVW(NSVW,J)
      DO 41 J=1,KRD
      WRITE(IW,56) NSVW,SVW(NSVW,J)
   41 WRITE(IW,56) I,WELLS(J,I)
      IF(IRPT)30,30,31
```

```
C
C     SETUP 2ND TO (IRPT)TH POINT OF EACH AVERAGE INTERVAL
C
   31 DO 32 K=1,IRPT
      I=I+1
      DO 33 J=1,KRD
   33 WELLS(J,I)=WELLS(J,I-1)
      WRITE(IW,56) (I,WELLS(J,I),J=1,KRD)
   32 CONTINUE
C
C     SETUP INDEX TO SKIP TO NEXT AVERAGE INTERVAL
C
   30 I=I+2
      IF(I-L-1)34,35,35
C
C     TAKE AVERAGE VALUE AT EACH JUMP DISCONTINUITY POINT BETWEEN TWO ADJACENT
C     AVERAGE REGIONS
C
   35 IRPT=IRPT+2
      KK=L-IRPT
      IK=IRPT+1
      DO 36 I=IK,KK,IRPT
      DO 37 J=1,KRD
   37 WELLS(J,I)= (WELLS(J,I-1) + WELLS(J,I+1))/2.0
   36 CONTINUE
C
C     FIND FOURIER COEFF. OF EACH WELL
C
      DO 61 I=1,KRD
      DO 61 J=1,L
   61 WRITE(IW,57) I,J,WELLS(I,J)
      LN=(L-1)/2
      MM= M+ 1
      DO 5 K=1,KRD
      DO 6 J=1,L
    6 VW(J)=WELLS(K,J)
C
C     SUBROUTINE FORIT IS IBM STANDARD SCIENTIFIC SUBROUTINE FOR FOURIER
C     ANALYSIS
C
      CALL FORIT(VW,LN,M,FC,FS,IER)
C
C     CHECK
C
      IF(IER-1)7,8,9
    8 WRITE(IW,10)
      GO TO 12
    9 WRITE(IW,11)
   12 STOP
    7 CONTINUE
      WRITE(IW,63) K
      WRITE(IW,21)(I,FS(I),FC(I),I=1,MM)
      DO 26 I=1,MM
      A(I,K)=FC(I)
   26 B(I,K)=FS(I)
C
C     FIND RESULTANT ARRAY OF FOURIER SERIES APPROXIMATION
C
      DO 13 I=1,L
      G=FNCR*(I-1)
      SUM=FC(1)
```

```
      DO 14 J=2,MM
   14 SUM = SUM +(FC(J)*COS((J-1)* G    )+FS(J) * SIN((J-1)* G    ))
       V(I) = SUM
   13 CONTINUE
C
C  PLOT RAW DATA AND COMPUTED VALUES, IF DESIRED
C
    5 CONTINUE
      RETURN
      END
```

GROUNDWATER FLOW IN A SANDY TIDAL BEACH. 2. TWO-DIMENSIONAL FINITE-ELEMENT ANALYSIS

C. S. Fang, S. N. Wang, and W. Harrison

ABSTRACT

Two-dimensional finite-element techniques are described which model closely the complicated fluctuations observed in the water table of an ocean beach. Use of triangular elements permits specification of more realistic boundary conditions than was possible with the line elements of the one-dimensional model; also, results for the region close to the ocean compare more favorably with the field data than was the case with the one-dimensional, finite-element model.

INTRODUCTION

The object of this study was to remedy deficiencies of the one-dimensional groundwater flow model (Harrison, Fang, and Wang, 1971) and to examine the efficacy of a two-dimensional, finite-element model that uses triangular elements. The use of finite-element methods to attack boundary-value field problems was anticipated by Zienkiewiez and Cheung (1965). Later, Zienkiewiez and Cheung (1967) gave detailed analyses of the theory as well as examples of application of the finite-element method. The application of general variational principles to the groundwater flow equation did not occur until Newman and Witherspoon's studies (1970b, 1971). Application of this method has been limited to steady flow (Newman and Witherspoon, 1970a) until now. To model the movement of beach groundwater, where a free surface is involved, requires complete solution of the unsteady equation. Studies by Javandel and Witherspoon (1969), and France, et al. (1971) were helpful in this aspect of application of the finite-element method.

As mentioned in the one-dimensional model for groundwater flow in a sandy tidal beach (Harrison, et al., 1972), the hydrostatic assumption is critical over the region near the ocean boundary where the effects of tidal forces and seaward-directed head gradient are important. A two-dimensional finite-element model was necessary for modeling the effects of tidal fluctuations in this region.

EQUATIONS OF GROUNDWATER FLOW WITH A FREE SURFACE

Unsteady flow in an elastic porous medium was first studied by Theis (1935). Theis (1938) also introduced the concepts of storage coefficient and aquifer transmissibility.

The equation for unsteady groundwater flow through uniformly thick, horizontally compressible sand was derived by Jacob (1940) as:

$$\frac{\partial^2 h}{\partial x^2} + \frac{\partial^2 h}{\partial y^2} = \frac{S}{T} \frac{\partial h}{\partial t} \tag{1}$$

where the storage coefficient S is defined as:

$$S = \rho g b(\alpha + n\beta) \tag{2}$$

and T = transmissibility, ρ = fluid density, g = gravitational acceleration, b = uniform thickness of aquifer, α = vertical compressibility of the medium, n = porosity of the medium, β = compressibility of the liquid, and h = the piezometer head above the datum, defined as:

$$h = z + \frac{1}{g} \int_{P_o}^{P} \frac{dP}{\rho(P)} \tag{3}$$

where P is pressure head.

The equation for three-dimensional groundwater flow was also derived by Jacob (1950) as:

$$\frac{\partial^2 h}{\partial x^2} + \frac{\partial^2 h}{\partial y^2} + \frac{\partial^2 h}{\partial z^2} = \frac{S_s}{K} \frac{\partial h}{\partial t} \tag{4}$$

where

$$S_s = \rho g(\alpha + n\beta) \tag{5}$$

is called the specific storage, and defined as the volume of water in a unit volume that the aquifer releases from storage under a unit head decline, and K is hydraulic conductivity. Theis's storage coefficient is equal to the product of the specific storage and the thickness of the aquifer, if the aquifer is homogeneous and uniformly thick.

By considering the conservation of mass in a control volume, Dewiest (1966) rederived the equation of groundwater flow as:

$$\frac{\partial^2 h}{\partial x^2} + \frac{\partial^2 h}{\partial y^2} + \frac{\partial^2 h}{\partial z^2} - 2\rho\beta g \frac{\partial h}{\partial z} = \frac{S^*}{K} \frac{\partial h}{\partial t} \quad (6)$$

where DeWiest's specific storage was defined as:

$$S^* = \rho g \left[(1-n)\ \alpha + n\beta\right] \quad (7)$$

Cooper (1966) improved DeWiest's equation of flow by changing the vertical coordinates to deforming coordinates (z')

$$\frac{\partial^2 h}{\partial x^2} + \frac{\partial^2 h}{\partial y^2} + \frac{\partial^2 h}{\partial (z')^2} - 2\rho\beta g \frac{\partial h}{\partial z'} = \frac{S_s}{K} \frac{\partial h}{\partial t} \quad (8)$$

In practical problems, the fourth term on the left hand side of Equ. (8) is always neglected without introducing any significant error. In all problems, then, the flow equation can be written as:

$$\frac{\partial^2 h}{\partial x^2} + \frac{\partial^2 h}{\partial y^2} + \frac{\partial^2 h}{\partial (z')^2} = \frac{S_s}{K} \frac{\partial h}{\partial t} \quad (9)$$

Therefore, Jacob's equation, Equation (4), for three-dimensional flow appears to be exact if one considers the fixed coordinates to be deforming coordinates.

Hence, the governing partial differential equation of an isotropic, homogeneous porous medium in two dimensions can be represented by

$$K \left(\frac{\partial^2 h}{\partial x^2} + \frac{\partial^2 h}{\partial y^2}\right) = S_s \frac{\partial h}{\partial t} \quad (10)$$

For the beach groundwater flow problem the initial and boundary conditions can be specified as follows.

Initial condition:

$$h\ (x,y,o) = h_o\ (x,y) \quad (11)$$

$$\zeta\ (x,o) = \zeta_o(x) \quad (12)$$

Boundary conditions:

A prescribed head on the left boundary, A_1

$$h = H(t) , \tag{13}$$

and a prescribed flux at the bottom boundary, A_2

$$K \frac{\partial h}{\partial y} = - V(x,t) , \tag{14}$$

where V is defined as positive downward, and

(x,t) represents the equation of the free surface. (See Fig. 1).

Two conditions must be satisfied on the free surface

$$\zeta = h \tag{15}$$

$$K \left(\frac{\partial h}{\partial x} n_x + \frac{\partial h}{\partial y} n_y\right) = \left(I - S_y \frac{\partial \zeta}{\partial t}\right) n_y \tag{16}$$

where S_y and I are the specific yield and downward infiltration through the porous medium, and n_x and n_y are x- and y-directional cosines of unit outward normal along the free surface.

Before employing finite-element analysis, the variation principles must be applied to find the minimum value of the functional for a particular function h; thus (Newman and Witherspoon, 1970b and 1971),

$$\Omega = \iint_R \left[\tfrac{1}{2} K \left(\frac{\partial h}{\partial x}\right)^2 + \tfrac{1}{2} K \left(\frac{\partial h}{\partial y}\right)^2 + S_s h \frac{\partial h}{\partial t}\right] dxdy + \int_{A_2} Vh \, dA - \int_{FS} h \left(I - S_y \frac{\partial h}{\partial t}\right) n_y \, dS \tag{17}$$

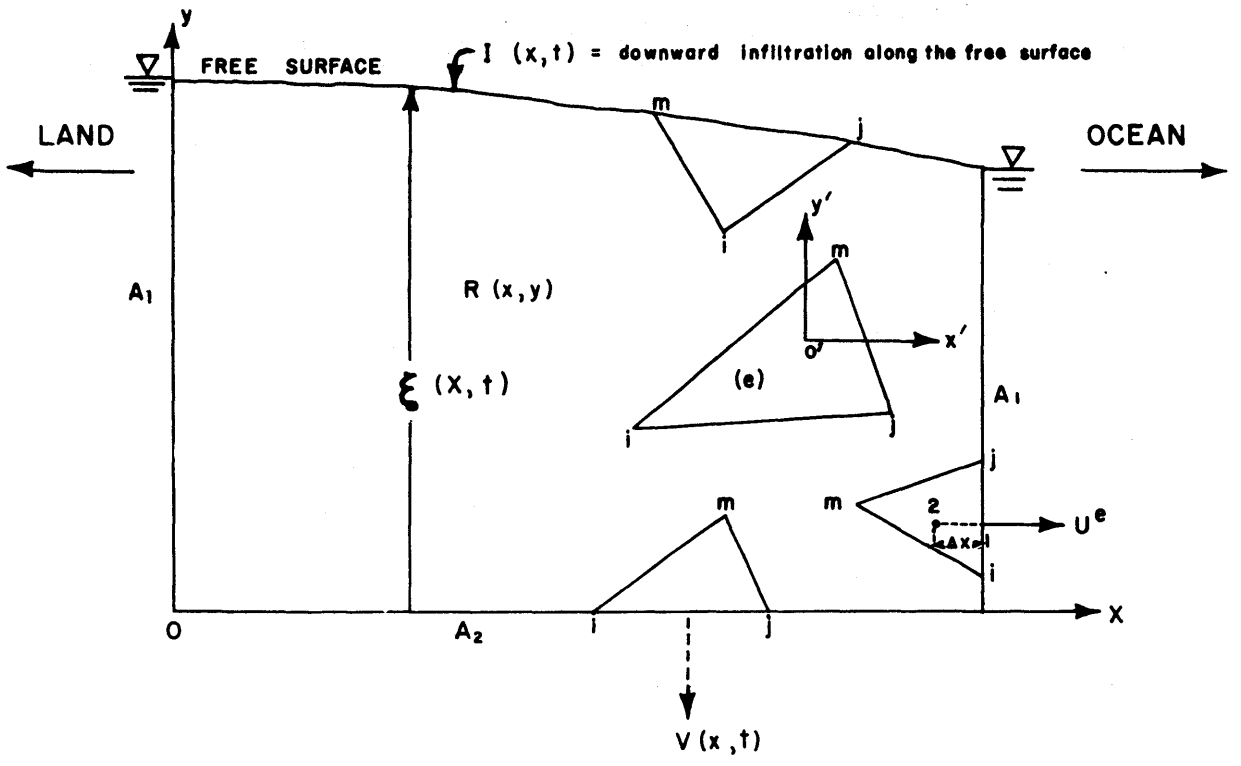

FIG. 1. Definition sketch for triangular elements and nodes, initial conditions, and boundary conditions.

FINITE ELEMENT ANALYSIS

Assume the flow region is divided into many triangular elements, each element shown as in Figure 1, where i, j, and m represent the first, second, and third nodes of an element e. Then o' is the centroid of element e and x' and y' are the element coordinates through the centroid, assuming no transformation angle. The total head, h, within each triangular element can be uniquely defined (linearly) by:

$$h \equiv \alpha_1 + \alpha_2 x + \alpha_3 y \tag{18}$$

Substituting the coordinates and the total heads for the three nodes of each element into Equation (18), h can be represented in terms of coordinates and total head at three nodes, in matrix form, as

$$h = [N] \{h\}^e \tag{19}$$

where

$$\{h\}^e = \begin{Bmatrix} h_i \\ h_j \\ h_m \end{Bmatrix} \tag{20}$$

and

$$[N] = [N_i \quad N_j \quad N_m] \tag{21}$$

where

$$N_I = \frac{1}{2\Delta} (a_I + b_I x + c_I y) \ , \ I = i, j, m, \text{ and } \Delta$$

is the area of the triangular element. Letters a, b, and c, with subscripts i, j, and m, are short notations for

$$\begin{aligned} a_i &\equiv x_j y_m - x_m y_j \\ b_i &\equiv y_j - y_m \\ c_i &\equiv x_m - x_j \ , \end{aligned} \tag{22}$$

and the corresponding coefficients for each element are obtained by a cyclic permutation of the subscripts in the order i, j, and m.

Similarly, time derivatives within each element can be represented by

$$\left\{\frac{\partial h}{\partial t}\right\} = [N] \left\{\frac{\partial h}{\partial t}\right\}^{e} \tag{23}$$

where

$$\left\{\frac{\partial h}{\partial t}\right\}^{e} = \begin{Bmatrix} \left(\frac{\partial h}{\partial t}\right)_i \\ \left(\frac{\partial h}{\partial t}\right)_j \\ \left(\frac{\partial h}{\partial t}\right)_m \end{Bmatrix} \tag{24}$$

Dividing the whole region into many small elements, the minimum function of the overall region can be expressed by the summation of all the element parts of a functional, whose minimizing functions are approximate solutions to the problems, as

$$\Omega = \sum_{e=1}^{K_1} \Omega_{FS}^{e} + \sum_{e=K_1+1}^{K_2} \Omega^{e} + \sum_{e=K_2+1}^{M} \Omega_{A_2}^{e} \tag{25}$$

where Ω_{FS}^{e}, Ω^{e} and $\Omega_{A_2}^{e}$ are the element minimum functionals of the elements along the free surface, of the inside region, and along the boundary of prescribed flux, respectively; K_1 is the total number of elements free surface, $(K_2 - K_1)$ = the total number of inner elements, $(M - K_2)$ = the total number of elements along the prescribed flux boundary, and M = the total number of elements in the whole region.

In Equation (17), the integral along the prescribed flux boundary, $\int_{A_2} VhdA$, existed only in the element minimum functionals $\Omega_{A_2}^{e}$, and the integral along the free surface vanished, except in Ω_{FS}^{e}; therefore, the element minimum functionals can be rewritten as:

$$\Omega^e = \iint_{R^e} \left[\tfrac{1}{2} K^e \left(\frac{\partial h^e}{\partial x}\right)^2 + \tfrac{1}{2} K^e \left(\frac{\partial h^e}{\partial y}\right)^2 + S_s{}^e h^e \frac{\partial h^e}{\partial t}\right] dxdy \tag{26}$$

$$\Omega^e_{A_2} = \iint_{R^e} \left[\tfrac{1}{2} K^e \left(\frac{\partial h^e}{\partial x}\right)^2 + \tfrac{1}{2} K^e \left(\frac{\partial h^e}{\partial y}\right)^2 + S_s{}^e h^e \frac{\partial h^e}{\partial t}\right] dxdy + \int_{A_2} V^e h^e \, dA \tag{27}$$

$$\Omega^e_{FS} = \iint_{R^e} \left[\tfrac{1}{2} K^e \left(\frac{\partial h^e}{\partial x}\right)^2 + \tfrac{1}{2} K^e \left(\frac{\partial h^e}{\partial y}\right)^2 + S_s{}^e h^e \frac{\partial h^e}{\partial t}\right] dxdy - \int_{FS} h^e \left(I^e - S_y{}^e \frac{\partial h^e}{\partial t}\right) n_y{}^e \, dS \tag{28}$$

where the superscript e indicates the parameters of an element e under consideration, and R^e means to take the area integral of the element being considered.

If h is defined uniquely and continuously throughout the region, then the functional can be minimized with respect to all nodal values of the total head, h_i ; that is,

$$\frac{\partial \Omega}{\partial h_i} = \sum_{e=1}^{K_1} \frac{\partial \Omega^e_{FS}}{\partial h_i} + \sum_{e=K_1+1}^{K_2} \frac{\partial \Omega^e}{\partial h_i} + \sum_{e=K_2+1}^{M} \frac{\partial \Omega^e_{A_2}}{\partial h_i} = 0 \tag{29}$$

If there are N nodes in the whole region, then Equation (29) becomes a linear system of N equations at any particular time step; for example,

$$[P]\left[h\right]_t + [Q]\left[\frac{\partial h}{\partial t}\right]_t = [R] \qquad (30)$$

where [P] and [Q], called the overall matrices, are N x N square matrices. $[h]_t$ is an N x 1 row matrix formed by the total head of all nodes at the particular time step being considered, and so is $\left[\frac{\partial h}{\partial t}\right]_t$. R is an N x 1 constant row matrix obtained due to the existence of the prescribed flux and the infiltration flux.

When the central finite-difference approximation for $\left[\frac{\partial h}{\partial t}\right]_t$ is made as

$$\left[\frac{\partial h}{\partial t}\right]_t = -\left[\frac{\partial h}{\partial t}\right]_{t-\Delta t} + \left([h]_t - [h]_{t-\Delta t}\right)\frac{2}{\Delta t} \qquad (31)$$

then Equation (30) becomes

$$[D]\,[h]_t = [E]\,, \qquad (32)$$

where

$$[D] = [P] + \frac{2}{\Delta t}[Q]$$

$$[E] = [R] + [Q]\left(\frac{2}{\Delta t}[h]_{t-\Delta t} + \left[\frac{\partial h}{\partial t}\right]_{t-\Delta t}\right) \qquad (33)$$

and, Δt is the increment of the time step. Then, the total head of all nodes h_i, i = 1, 2, ...N, should be found from Equation (32), instead of Equation (30). If there are just N' nodes (N' < N) with unknown total head, which are numbered first, then, only the first N' non-redundant equations in Equation (32)

useful. The prescribed values of all given h_i should be substituted into Equation (32), and the constant terms moved to the left hand side of the equation to get a new linear system of N' equations as

$$[D'] \; [h]_t = [E'] \tag{34}$$

where

$$\begin{aligned} D_{ij}' &= D_{ij} \qquad i = 1, 2, \ldots, N' \\ & \qquad\quad j = 1, 2, \ldots, N' \\ E_i' &= E_i - \sum_{j=N'+1}^{N} D_{ij} \, h_j \qquad i = 1, 2, \ldots, N' \end{aligned} \tag{35}$$

In order to achieve the purpose of obtaining overall matrices and the total heads of all nodes shown in the above procedures; the terms,

$$\frac{\partial \Omega_{FS}^{e}}{\partial h_i} \qquad \frac{\partial \Omega^{e}}{\partial h_i}, \quad \text{and} \quad \frac{\partial \Omega_{A_2}^{e}}{\partial h_i}$$

obtained first as expressed in equation (29). Equation (29) is the source of element matrices and the reason why element matrices must be found before overall matrices.

The detailed formulation of the element matrices can be obtained in (Zienkiewiez and Cheung, 1967). The results are as follows:

<u>For inner elements</u>:

$$\left[\frac{\partial \Omega}{\partial h}\right]^{e} = \begin{bmatrix} \frac{\partial \Omega^{e}}{\partial h_i} \\ \frac{\partial \Omega^{e}}{\partial h_i} \\ \frac{\partial \Omega^{e}}{\partial h_m} \end{bmatrix} = [BC] \; [h]^{e} + [SKN] \left[\frac{\partial h}{\partial t}\right]^{e}$$

For inner elements along the boundary of prescribed flux:

$$\left[\frac{\partial \Omega}{\partial h}\right]^e_{A_2} = [BC]\,[h]^e + [SKN]\left[\frac{\partial h}{\partial t}\right]^e + \tfrac{1}{2} V^e \Delta x^e \begin{bmatrix} 1 \\ 1 \\ 0 \end{bmatrix} \tag{37}$$

and for elements along the free surface:

$$\left[\frac{\partial \Omega}{\partial h}\right]^e_{FS} = [BC]\,[h]^e + [SKN]\left[\frac{\partial h}{\partial t}\right]^e + \frac{Sy^e}{6}(x_j - x_m) \begin{bmatrix} 0 & 0 & 0 \\ 0 & 2 & 1 \\ 0 & 1 & 2 \end{bmatrix} \left[\frac{\partial h}{\partial t}\right]^e - \frac{I^e}{2}(x_j - x_m) \begin{bmatrix} 0 \\ 1 \\ 1 \end{bmatrix}, \tag{38}$$

where

$$[BC] = \frac{K^e}{4\Delta} \begin{bmatrix} b_i b_i & b_i b_j & b_i b_m \\ b_j b_i & b_j b_j & b_j b_m \\ b_m b_i & b_m b_j & b_m b_m \end{bmatrix} + \frac{K^e}{4\Delta} \begin{bmatrix} C_i C_i & C_i C_j & C_i C_m \\ C_j C_i & C_j C_j & C_j C_m \\ C_m C_i & C_m C_j & C_m C_m \end{bmatrix} \tag{39}$$

and

$$[SKN] = S_s^e \begin{bmatrix} \iint_{R^e} N_i N_i \, dxdy & \iint_{R^e} N_i N_j \, dxdy & \iint_{R^e} N_i N_m \, dxdy \\ \iint_{R^e} N_j N_i \, dxdy & \iint_{R^e} N_j N_j \, dxdy & \iint_{R^e} N_j N_m \, dxdy \\ \iint_{R^e} N_m N_i \, dxdy & \iint_{R^e} N_m N_j \, dxdy & \iint_{R^e} N_m N_m \, dxdy \end{bmatrix} \quad (40)$$

and Δx is the length of the side of an element along the prescribed flux boundary.

In deriving the above element matrices, we numbered the nodes of elements along the free surface and the boundary of the prescribed flux in the manner shown on Fig. 1. Also, it was assumed that h varied linearly from one node to the other.

BOUNDARY CONDITIONS

Mathematical modeling of groundwater flow using the Jacob's equation requires a knowledge of hydraulic conductivity and specific storage, as well as appropriate boundary conditions. The lack of precise measurements of these two geohydrologic parameters will cause an uncertainty in preparing mathematical models. Freeze and Witherspoon (1968) tried to estimate the parameters, by a trial-and-error process of matching calculated and measured data at various points. Kleinecke (1971) attempted to employ linear programming to achieve the same purpose. Hydrologic records over large regions were needed in order to use even the simplest forms of boundary conditions.

There are two types of boundaries: prescribed-head, and prescribed-flux boundaries. Such boundaries of simple form are used in most studies, but for the beach groundwater problem, if a finite region is selected, portions of the boundaries do not possess hydrologic characteristics. Both the bottom boundary and the ocean boundary (right-hand boundary, Fig. 1) are complicated functions of space and time, due to the seaward-directed head gradient and tidal fluctuations. Therefore, it is necessary to replace the semi-infinite, unconfined aquifer with a finite

region. The assumption of the existence of the hydrostatic condition, required for the one-dimensional model on the ocean-side boundary (Harrison, et al., 1971), was somewhat weak; it may be replaced here by a prescribed boundary condition (see below).

The "drainage velocity" V(x,t), calculated (Harrison, et al., 1971) from the field data by the finite-difference method, was used to impose the effects of tide on each element of the bottom boundary. If there is any infiltration in the system it will also be limped into this term.

For the present two-dimensional model, the landward (left) boundary was assumed to be hydrostatic. The ocean boundary was approximated by imposing a uniform horizontal flux along the boundary of each element (Fig. 1).

This horizontal flux could be approximated by Darcy's Law as

$$U^e = - \frac{K^e}{\Delta x} (h_1 - h_2) \qquad (41)$$

where point 1 is any point on the boundary, and Δx is selected as small as possible. Because point 2 has the same altitude as point 1 , and because Equation (19) holds for any element; then, the uniform boundary flux becomes

$$U^e = - \frac{K^e}{\Delta x} [b] \quad [h]^e \qquad (42)$$

Effects of this flux must be considered, as shown in Equation (28), to be expressed implicitly in terms of unknown nodal heads before substituting given nodal heads into Equation (32). The same procedure is also followed for the left boundary, whether a prescribed head or a hydrostatic condition is imposed.

FREE SURFACE

The most difficult problem with the free-surface boundary for the beach groundwater problem lies in treating the free-surface as a moving boundary. All free-surface elements are needed to recalculate element matrices at every time step, otherwise the accuracy of the model will be decreased. The iteration method was chosen for recalculating the free-surface elements. The cumulative change of the free-surface leads to changes in node-element configuration. It is necessary, therefore, to reset nodes and elements or shift nodes during each successive time step.

For simplification, shifting was restricted to vertical coordinates; thus,

$$yN_i = y_i + (yN_j - y_j)$$

where yN_i, and y_i represent the y-coordinate of node i under consideration, before and after shifting, yN_j and y_j represent the new and old y-coordinates of free-surface node j, which is directly above the inner node i. Then, the new total head h_i', after a shift, can be found from equation (19) as (Fig. 2):

$$\begin{aligned} h_i' = {} & \frac{1}{4\Delta^{(e)}} \left[(a_i + b_i x_i + c_i yN_i) h_i \right. \\ & + (a_j + b_j x_i + c_j yN_i) h_j \\ & \left. + (a_m + b_m x_i + c_m yN_i) h_m \right]^{(e)} \\ & + \frac{1}{4\Delta^{(e+1)}} \left[(a_i + b_i x_i + c_i yN_i) h_i \right. \\ & + (a_k + b_k x_i + c_k yN_i) h_k \\ & \left. + (a_m + b_m x_i + c_m yN_i) h_m \right]^{(e+1)} \end{aligned} \tag{43}$$

where the superscripts e and $e+1$ correspond to transformed elements e and $e+1$, respectively.

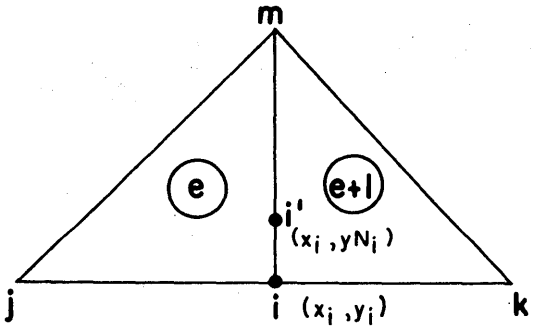

FIG. 2. Definition sketch for shifting vertical coordinates.

APPLICATION OF METHOD

To facilitate computer programming, nodes on the free surface were numbered first (nodes 1 to 19, Fig. 3). Then all nodes with unknown total head were numbered (nodes 20 to 69), after which nodes with given head were numbered (for example, nodes 70 to 74). In like manner, the elements along the free surface were numbered first, from element 1 to element 40, in the element-numbering system. Elements along the free surface should be smaller than other elements to obtain accurate results.

Once the node-element configuration is decided, data cards for such a numbering system should be prepared. Initial total head and coordinates are also needed. Starting time was chosen as 0645 EDT, August 11, 1969 (see Harrison and Fausak, 1970).

The computer program continuously seeks the element matrices, based on Equations (39) and (40), before obtaining the overall matrices equation (Equ. 30); then, it finds time-derivatives of total head at time $(t-\Delta t)$ before reaching Equation (32). The prescribed values of h, obtained from the field data (Harrison and Fausak, 1970), are now applied on the nodes of the landward-side boundary (Fig. 3, nodes 71 to 74), where the hydrostatic state was assumed to exist. A prescribed value of h is also applied at the upper node (node 70) of the ocean-side boundary, where the hydrostatic condition does not exist.

The prescribed head values substituted into Equation (32) to obtain a linear system of simultaneous equations, as Equation (34). The equations were solved by the elimination method, using the largest pivotal divisor, to obtain the total head for all nodes at any time step under consideration. The program then proceeded to consider the effects of the moving free surface. The results of each time step were used as initial values for the next time step. The necessity of resetting the node-element configuration was checked every 5 cycles. This procedure was followed as long as desired.

Fourier coefficients for bottom drainage velocities were read at initial setup, a subroutine being called to find the drainage velocities for the coefficients given at each time step. The following data were also read in: total nodes = 74, total elements = 110, porosity = 34%, hydraulic conductivity = 0.014 cm/sec, specific storage = 0.003125 1/cm, and

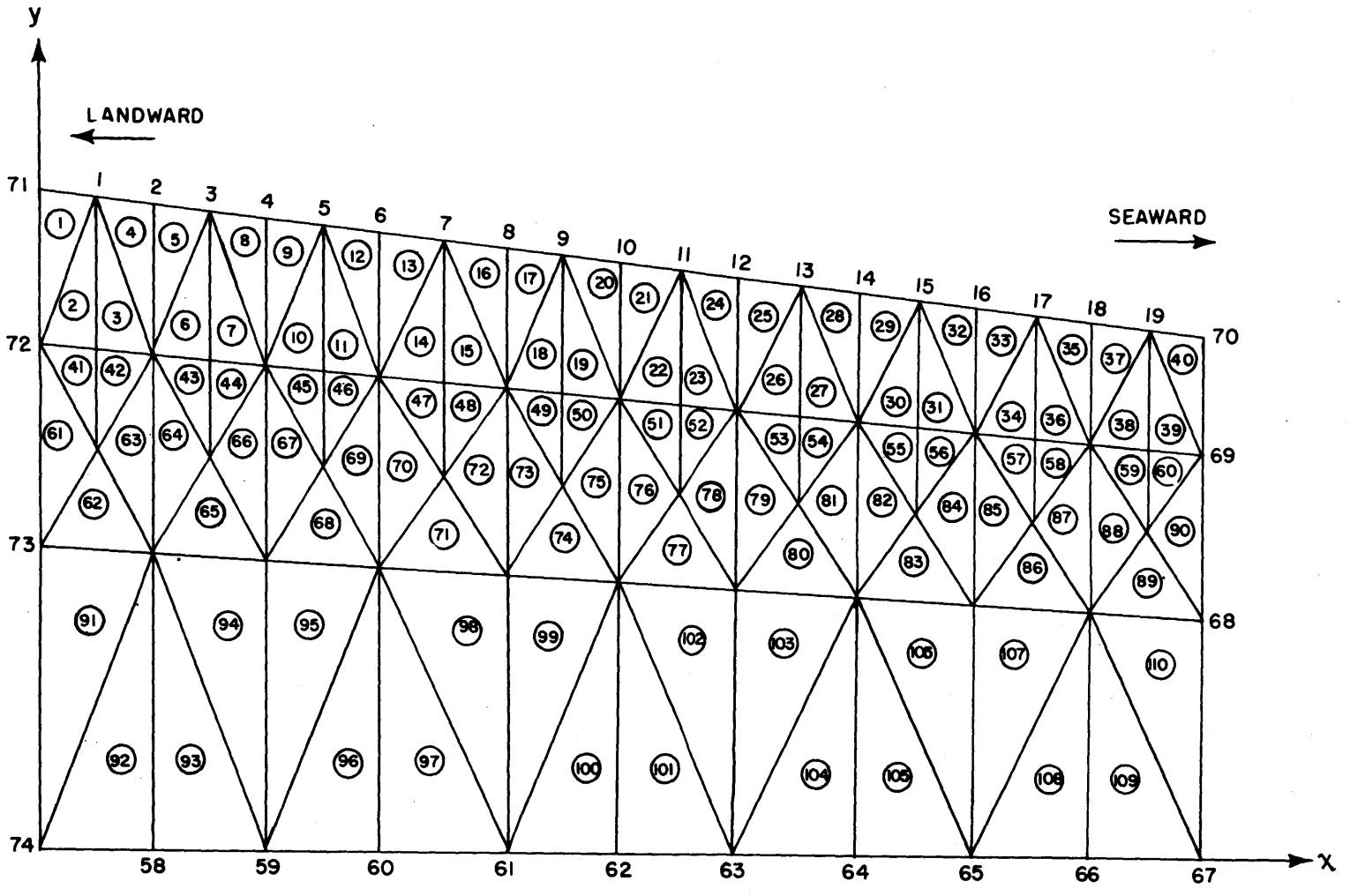

FIG. 3. Definition sketch for numbering nodes and elements.

time increment for each step = 15 minutes.

The storage coefficient may be considered equal to the specific yield for an unconfined flow with a free surface (Chow, 1964). Since only field tests of porosity and hydraulic conductivity were made, the Figure 13-2, in Chow (1964), was chosen to find the specific yield. This was found to be 25% for the given porosity. The specific storage was taken as 0.003125 1/cm, for an average flow region assumed to be 80 cm.

RESULTS AND DISCUSSION

As shown in Figure 4, the two-dimensional finite-element method has provided an accurate solution for groundwater flow with respect to complicated beach water-table fluctuations. A compromise decision was made relative to the assumed positions of the boundaries, the value of the specific storage, and the average drainage velocity. A Fourier series was used to describe the mean regional drainage-velocity characteristics and the beach water-table's response to the input tidal fluctuations. Comparison of the results (Fig. 4) for the two-dimensional case, the one-dimensional case, and the field data indicates that the two-dimensional finite-element method is more accurate for modeling the fluctuations of the beach groundwater table than is the one-dimensional method.

Even though one-dimensional field data were used as the boundary condition for the two-dimensional case, the results still exhibit less fluctuations, after many time steps, near the ocean (right) side boundary (Fig. 4) where the effects of tidal fluctuations are large. The small discrepancies (Fig. 4) can be further reduced by using smaller elements over this region, since no matter what combinations of element sizes are used, a system of linear matrix equations will finally result from the two-dimensional finite-element method. For the one-dimensional case, a system of nonlinear functions was obtained; the equations were solved by the Newton-Raphson iteration method (Harrison, et al., 1971). The Newton-Raphson method, after our testing, seems restricted to even-length elements; otherwise, the iteration solution would easily become divergent.

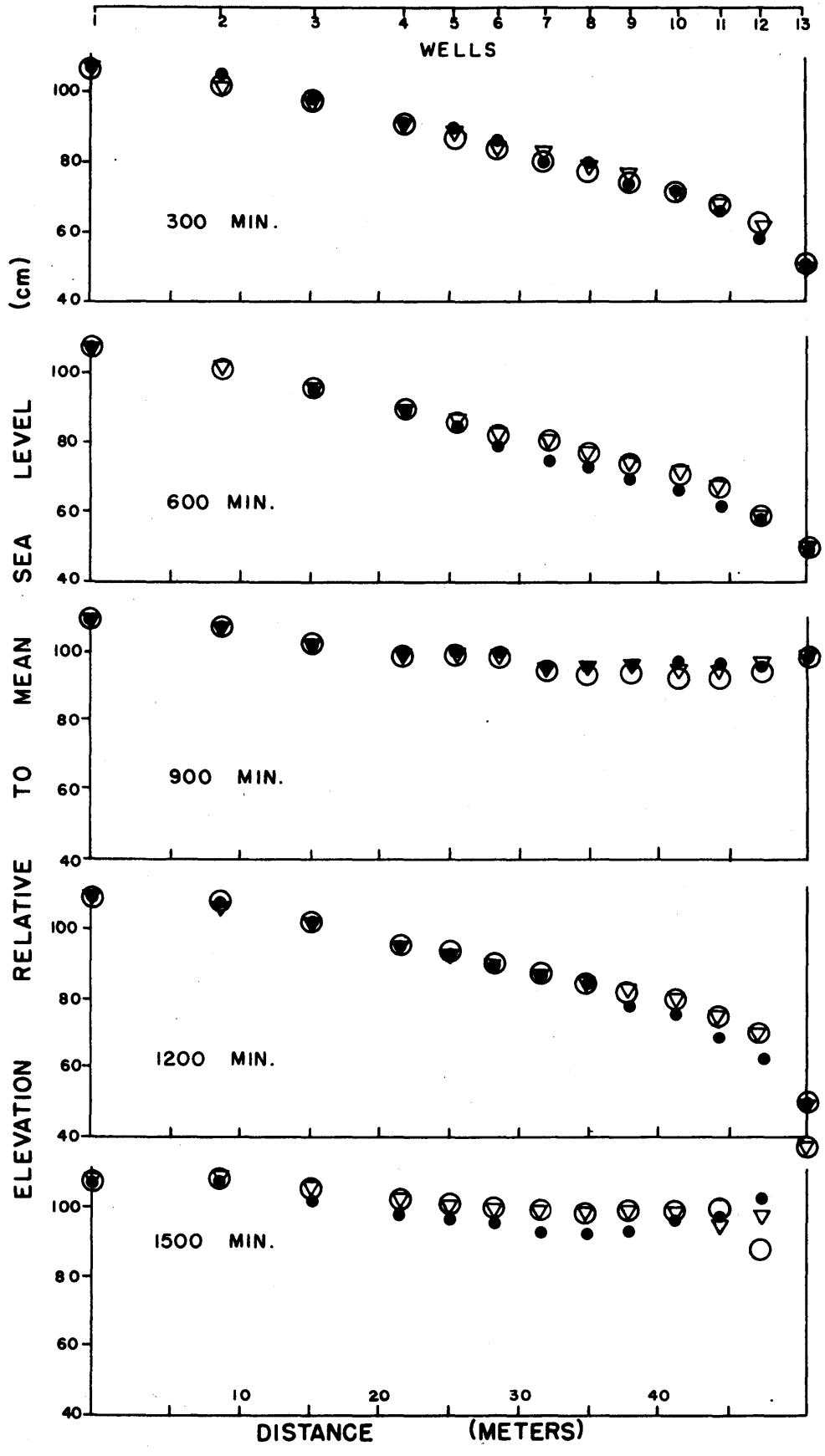

FIG. 4. Comparison between field data (solid circles), one-dimensional model results (open circles), and two-dimensional model output (triangles).

The fact that small differences exist between the field data and the theoretical results can be explained as due to the effects of variables in Equation (2) of Harrison, et al. (1971, p. 1315). The effects of capillarity and groundwater density gradients are probably also important. It also seems certain that if the specific storage can be measured precisely, the model results will more closely parallel the field data.

COMPUTER PROGRAM

A description and listings of the FORTRAN computer programs used in the finite-element analysis are given in a section following the References.

REFERENCES

Chow, Ven Te, Handbook of Applied Hydrology, McGraw-Hill, New York, 1964.

Cooper, H. H., Jr., The equation of groundwater flow in fixed and deforming coordinates, Jour. Geophys. Res., 71, 4785-4790, 1966.

DeWiest, R. J. M., On the storage coefficient and the equations of groundwater flow, Jour Geophys. Res., 71, 1117-1122, 1966.

France, P. W., C. J. Parekh, J. C. Peters, and C. Taylor, Num ical analysis of free surface seepage problems, Amer. Soc. Civ. Eng., Jour. of Irrigation and Drainage Div., 97(1), 165-178,

Freeze, R. A., and P. A. Witherspoon, Theoretical analysis of regional groundwater flow. 3. Quantitative interpretation: Water Resour. Res., 4(3), 581-590, 1968.

Harrison, W., and L. E. Fausak, A time series from the beach environment - II, Va. Institute of Marine Science, Data Report No. 7, 1-96, 1970.

Harrison, W., C. S. Fang, and S. N. Wang, Groundwater flow in a sandy tidal beach. 1. One-dimensional finite-element analysis, Water Resour. Res., 7(5), 1313-1322, 1971.

Jacob, C. E., The flow of water in an elastic artesian aquifer, Trans. Amer. Geophys. Union II, 574-386, 1940.

_____, Chapter 5, Engineering Hydraulics, edited by H. Rouse, John Wiley & Sons, New York, 321-386, 1950.

Javandel, I., and P. A. Witherspoon, A method of analyzing transient fluid flow in multilayered aquifers, Water Resour. Res., 5(4), 1969.

Kleinecke, D., Use of linear programming for estimating geohydrologic parameters of groundwater basins, Water Resour. Res., 7(2), 367-374, 1971.

Newman, S. P., and P. A. Witherspoon, Finite element method of analyzing steady seepage with a free surface, Water Resour. Res., 6(3), 889-897, 1970a.

_____, Variational principles for confined and unconfined flow of groundwater, Water Resour. Res., 6(5), 1376-1382, 1970b.

_____, Variational principles for fluid flow in porous media, Amer. Soc. Civ. Eng., Jour. of the Engineering Mech. Div., 97(2), 359-374, 1971.

Theis, C. V., The relation between the lowering of the piezometer surface and the rate and duration of discharge of a well using groundwater storage, Trans. Amer. Geophys. Union II, 519-524, 1935.

_____, The significance and nature of the cone of depression in groundwater bodies, Econ. Geol., (33), 889-920, 1938.

Zienkiewiez, O., and Y. K. Cheung, Finite elements in the solution of field problems, Engineering, 507-510, 1965.

_____, The Finite Element Method in Structure and Continuum Mechanics, McGraw-Hill, New York, 1967.

FORTRAN PROGRAM
FOR TWO-DIMENSIONAL, FINITE-ELEMENT ANALYSIS

Following this description are the main program, subroutine DRANV (which was designed to find the bottom drainage velocity with given Fourier coefficients of drainage velocity), and subroutine SIMQM (which was obtained by modifying IBM standard scientific subroutine SIMQ, to eliminate an underflow problem). Definitions of all variables can be found on the comment cards of the programs. Also included are comment cards describing the purposes of various portions of the programs. Only punched cards are used for input. This program takes 47.82 minutes CPU time per 100 cycles in MODE 50/IBM 360. Input cards are listed according to the following groups:

1) First card: FORMAT (3I6, 4E12.4)

   This card contains three integer variables, four real variables in sequence as:

   1st variable: NPART
   2nd variable: NPOIN
   3rd variable: NELEM
   4th variable: DT
   5th variable: XK
   6th variable: TL
   7th variable: POROS

2) Second card: FORMAT (14I5)

   This card contains 14 integer variables in sequential order as:

   1st variable: NFSF
   2nd variable: NFSL
   3rd variable: NBSF
   4th variable: NBSL
   5th variable: MFSF
   6th variable: MFSL
   7th variable: MBSF
   8th variable: MBSL
   9th variable: NLEFT
   10th variable: NRIGT
   11th variable: NBOND
   12th variable: LITER
   13th variable: NST
   14th variable: INNER

3) 3rd card: FORMAT (6E12.4)

Contains six real variables as:

1st variable: SYE (0 in this study)
2nd variable: FIE (0 in this study)
3rd variable: YLENS
4th variable: FLEPS
5th variable: FDCON
6th variable: FD

4) 4th to (3 + NPOIN)th card: FORMAT (I10, 3F10.4)

Each card of this group contains four variables as:

1st variable: I = integer to specify nodal number
2nd variable: X(I)
3rd variable: Y(I)
4th variable: H(I)

5) (4 + NPOIN)th card: FORMAT (I10)

Contains variable NCARD only

6) (5 + NPOIN)th to (4 + NPOIN + NELEM)th card:
FORMAT (4I10)

Each card of this group contains:

(1) 1st variable: I = integer to specify element number
(2) 2nd variable: NOD1(I)
(3) 3rd variable: NOD2(I)
(4) 4th variable: NOD3(I)

7) (5 + NPOIN + NELEM)th card: FORMAT (I10)

Contains variable NCARD only

8) (6 + NPOIN + NELEM + INNER)th card: FORMAT (5I5)

Each card of this group contains

(1) 1st variable: I = integer specify nodal number
(2) MNUM (I,1)
(3) MNUM (I,2)
(4) MNUM (I,3)

9) (7 + NPOIN + NELEM + INNER)th to (30 + NPOIN + NELEM + INNER)th card:

FORMAT (A7, 6E12.4)

Contains 12 sets in this group. Each set has 2 cards. The first card is composed of Fourier cosine coefficients as:

(1) 1st variable: CDUMY = variable for A-field to identify as Fourier cosine coefficients
(2) 2nd variable: A(I,1)
(3) 3rd variable: A(I,2)

.
.
.

(7) 7th variable: A(I,6)

Similarly, a second card is composed of Fourier sine coefficients punched in same sequence.

10) FORMAT (I6, 2E12.4)

This group contains 13 cards, each card has:

(1) 1st variable: I = integer to specify well number
(2) 2nd variable: XW(I) = x-coordinates of well I
(3) 3rd variable: YW(I) = water table of well I

11) FORMAT (I6, 6E12.4)

This card contains three variables as:

(1) NPOV
(2) DXV
(3) SSTA

12) FORMAT (4F10.4)

The total number of cards in this group is equal to the total number of time steps desired. Each card contains left and right-hand-side boundary conditions obtained from field data.

(1) 1st variable: YLEFT
(2) 2nd variable: YRIGT
(3) 3rd and 4th variables of each card are dummy variables.

```
//CNRPROJ  JOB  (1005,MV12,29,9),'WANG',MSGLEVEL=(2,0),CLASS=U
// EXEC FSSPCLG
//FORT.SYSIN  DD  *
C
C      PROGRAM TO SOLVE GROUND WATER PROBLEM WRITTEN BY SOU-NAN WANG,
C      DEPT. OF OCEANOGRAPHY
C
C      UNDER GRANT CNR
C
C      TWO-DIMENSIONAL UNSTEADY CASE
C
C
C      NPART=TOTAL NUMBER OF PARTITIONS
C      NPOIN=TOTAL NUMBER OF NODAL POINTS
C      NELEM=TOTAL NUMBER OF ELEMENTS
C      DT=TIME INCREMENT OF EACH TIME CYCLE
C      TL=TIME TO QUIT
C      BETA=THE COMPRESSIBILITY OF THE FLUID
C      RHO=DENSITY OF FLUID CONSIDERED
C      GY=GRAVITY ACCELERATION
C      POROS=POROSITY
C      SSTA=VERTICAL COMPRESSIBILITY OF THE SOLID  OR
C          =THE SPECIFIC STORAGE
C      XK    =THE HYDRAULIC CONDUCTIVITY OF HOMOGENEOUS, ISOTROPIC SAND
C      NFSF =FIRST NO. OF FREE SURFACE NODE
C      NFSL =FINAL NO. OF FREE SURFACE NODE
C      NBSF =FIRST NO. OF BOTTOM SIDE NODE
C      NBSL =FINAL NO. OF BOTTOM SIDE NODE
C      MFSF =FIRST ELEMENT ALONG FREE SURFACE
C      MFSL =FINAL ELEMENT ALONG FREE SURFACE
C      MBSF =FIRST ELEMENT ALONG BOTTOM SIDE
C      MBSL =FINAL ELEMENT ALONG BOTTOM SIDE
C      NLEFT=NODAL NO. OF FIRST NODE ON LEFT BOUNDARY
C      NRIGT=NODAL NO. OF FIRST NODE ON RIGHT BOUNDARY
C      NBOND=TOTAL NUMBER OF NODE ON EACH BOUNDARY
C      NSHFT=CORRENT COUNTER TO CHECK WHETHER OR NOT TO SHIFT NODAL COORDINATES
C            WHEN NSHFT=NST
C      NST   =TOTAL NO. OF TIME STEP ALLOWED UNTIL CHECKING THE SHIFT OF NODAL
C            COORDINATES
C      NITER=CORRENT NO. OF ITERATION TO CORRECT THE POSITION OF FREE SURFACE
C      LITER=TOTAL NO. OF ITERATION ALLOWED TO CORRECT POSITION OF FREE SURFACE
C      NCONV=TOTAL NO. OF NODES ON FREE SURFACE WHICH ARE SATISFIED CONVERGENT
C            CRITERIA AT EVERY ITERATION.
C      SYE   =THE SPECIFIC YIELD OF THE POROS MEDIUM
C      FIE   =THE NET AVERAGE RATE OF INFILTRATION
C      YLENS =IF ANY ABSOLUTE VALUE OF (Y(I)-YFOLD(I)) ALONG FREE SURFACE GREATER
C            THAN  YLENS , SHIFT COORDINATES
C      X(I) =X-COORDINATES OF NODES W. R. TO COMMON COORDINATES AT ANY TIME STEP
C      Y(I) =Y-COORDINATES OF NODES W. R. TO COMMON COORDINATES AT TIME STEP N
C      YOLD(I)=Y-COORD. OF  FREE SURFACE AT TIME STEP N-1
C      YFOLD(I)=Y-COORD. OF FREE SURFACE AT FIRST TIME STEP OF AFTER SHIFTING
C               NODAL COORDINATES
C      YDUMY(I)=DUMY Y-COORD. OF INNER NODES FOR CORRECTION OF Y(I) DUE TO
C               SHIFTING COORD.
C      YLC   =Y-COORD. OF FIRST NODE ON LEFT BOUNDARY AT FIRST TIME STEP AFTER
C            SHIFTING
C      YRC   =Y-COORD. OF FIRST NODE ON RIGHT BOUNDARY AT FIRST TIME STEP AFTER
C            SHIFTING
C      YLOLD=Y-COORD. OF FIRST NODE ON LEFT BOUNDARY AT TIME STEP N-1
```

```
C      YRCLD=Y-COORD. OF FIRST NODE ON RIGHT BOUNDARY AT TIME STEP N-1
C      YLEFT=Y-COORD. OF FIRST NODE ON LEFT BOUNDARY AT TIME STEP N
C      YRIGT=Y-COORD. OF FIRST NODE ON RIGHT BOUNDARY AT TIME STEP N
C      H(I)=PIEZOMETER HEAD OF NODES
C      HDUMY(I)=DUMY H(I) OF INNER NODES FOR CORRECTION DUE TO SHIFTING COORD.
C      NCARD=NUMBER OF CARDS READ IN FOR THE PREVIOUS SET, USED FOR CHECKING
C      NOD1(K)=FIRST NODE(THAT IS, NODE I) OF THE TRIANGLE ELEMENT K
C      NOD2(K)=SECOND NODE(THAT IS, NODE J) OF THE TRIANGLE ELEMENT K
C      NOD3(K)=THIRD NODE(THAT IS, NODE M) OF THE TRIANGLE ELEMENT K
C      BC1(IJ) = COLUME 1 OF ROW J ON FIRST PART OF ELEMENT MATRIX OF ELEMENT I
C      BC2(IJ) = COLUME 2 OF ROW J ON FIRST PART OF ELEMENT MATRIX OF ELEMENT I
C      BC3(IJ) = COLUME 3 OF ROW J ON FIRST PART OF ELEMENT MATRIX OF ELEMENT I
C      SKN1(IJ)= COLUME 1 OF ROW J ON SECOND PART OF ELEMENT MATRIX OF ELEMENT I
C      SKN2(IJ)= COLUME 2 OF ROW J ON SECOND PART OF ELEMENT MATRIX OF ELEMENT I
C      SKN3(IJ)= COLUME 3 OF ROW J ON SECOND PART OF ELEMENT MATRIX OF ELEMENT I
C      BCC1(IJ) =CORRECTING MATRICE OF  BC1(IJ) DUE TO CHANGE OF FREE SURFACE
C      BCC2(IJ) =CORRECTING MATRICE OF  BC2(IJ) DUE TO CHANGE OF FREE SURFACE
C      BCC3(IJ) =CORRECTING MATRICE OF  BC3(IJ) DUE TO CHANGE OF FREE SURFACE
C      SKNC1(IJ)=CORRECTING MATRICE OF SKN1(IJ) DUE TO CHANGE OF FREE SURFACE
C      SKNC2(IJ)=CORRECTING MATRICE OF SKN2(IJ) DUE TO CHANGE OF FREE SURFACE
C      SKNC3(IJ)=CORRECTING MATRICE OF SKN3(IJ) DUE TO CHANGE OF FREE SURFACE
C      P(IJ) =FIRST  PART OF  OVER-ALL MATRICE
C      Q(IJ) =SECOND PART OF  OVER-ALL MATRICE
C      R(I)  =CONSTANT MATRICE
C      D(IJ) =DUMMY MATRICE TO AVOID DESTROYING P(IJ) & Q(IJ) IN COMPUTATION
C      E(IJ) =DUMMY MATRICE TO AVOID DESTROYING R(I)          IN COMPUTATION
C      HT(I) =TIME DERIVATIVE OF H(I)
C      V(I) =DRAINAGE VELOCITY OF ELEMENTS ALONG BOTTOM BOUNDARY
C      RCLD(I)=CORRECTING MATRICE OF R(I) DUE TO CHANGE OF FREE SURFACE
C      MNUM(IJ)=NUMBERING INDEX OF SOME ELEMENTS AROUND A INNER NODE WHICH IS
C      NEEDED TO CONSIDER THE CORRECTION OF H(I) AFTER SHIFTING NODAL COORD.
C      INNER=TOTAL NO. OF INNER NODES
C      FD,AND XT=DUMMY VARIABLES
C      A(IJ)   =FOURIER COSINE COEFF. OF BOTTOM DRAINAGE VELOCITY OF WELL ELEM. I
C      B(IJ)   =FOURIER   SINE COEFF. OF BOTTOM DRAINAGE VELOCITY OF WELL ELEM. I
C      VDUMY(I)=DUMMY VELOCITY FOR CALLING SUBROUTINE DRANV
C      DXV=LENGTH OF BOTTOM ELEMENT FOR CALLING SUBROUTINE DRANV
C      NPOV=NO. OF BOTTOM NODES FOR CALLING SUBROUTINE DRANV
C      BFLX(IJ)=DUMMY VARIABLES FOR CONSIDERING THE EFFECTS OF HORIZONTAL FLUX ON
C               OVER-ALL MATRICES
C
C
      DIMENSION X(74),Y(74),NOD1(110),NOD2(110),NOD3(110),YOLD(19),
     *H(74),BC1(110,3),BC2(110,3),BC3(110,3),SKN1(110,3),YFOLD(19),
     $SKN2(110,3),SKN3(110,3),P(74,74),Q(74,74),D(74,74),R(74),
     *V(20),E(74),HT(74),BCC1(40,3),BCO2(40,3),BCO3(40,3),ROLD(19),
     *SKNC1(40,3),SKNC2(40,3),SKNC3(40,3)
      DIMENSION MNUM(38,4),YDUMY(74),HDUMY(74),BFLX(4,3)
      DIMENSION A(12,6),B(12,6),VDUMY(10),XW(13),YW(13)
      COMMON DXV,NPOV,A,B
    1 FORMAT(3I6,4E12.4)
    2 FORMAT(1H1,6X,6HNPART=,I5,2X,6HNPOIN=,I5,2X,6HNELEM=,I5,2X,3HDT=,
     *E12.4,2X,3HXK=,E12.4,2X,3HTL=,E12.4,2X,6HPOROS=,E12.4///)
    3 FORMAT(I10,3F10.4)
    4 FORMAT(10X,1HI,6X,4HX(I),6X,4HY(I),6X,4HH(I)//)
    5 FORMAT(I10)
    6 FORMAT(1HO,2X,59H INITIAL DATA OF COORDINATES AND TOTAL HEAD OF
     * ALL NODES//)
    7 FORMAT(4I10)
    8 FORMAT(6(E12.4,3X))
    9 FORMAT(1HO,2X,75H THE NUMBERS OF THREE NODES IN TRIANGULAR ELEMENT
```

```
     * IN COUNTERCLOCKWISE SENSE//)
   10 FORMAT(9X,1HI,3X,7HNOD1(I),3X,7HNOD2(I),3X,7HNOD3(I)//)
   11 FORMAT(2X,216,2X,2E12.4)
   12 FORMAT(10X,2HT=,E12.4)
   13 FORMAT (6E12.4)
   14 FORMAT(I6,3X,E12.4)
   15 FORMAT(5I10)
   18 FORMAT(A7,6E12.4)
   19 FORMAT(I6,2E12.4)
   20 FORMAT(5I5)
   22 FORMAT(14I5)
   23 FORMAT(4F10.4)
   24 FORMAT ( E12.4)
   25 FORMAT(I6,E12.4)
   26 FORMAT(1HO,2X,15H PRINT MNUM(IJ)//)
   27 FORMAT(9X,1HI,4CH MNUM(I,1) MNUM(I,2) MNUM(I,3) MNUM(I,4)//)
   28 FORMAT(1HO,2X,50H FOURIER COEFFICIENTS OF BOTTOM DRAINAGE VELOCITY
     * //)
   29 FORMAT(1HO,2X,24H COORDINATES OF 13 WELLS///)
   30 FORMAT(5X,1HI,7X,5HXW(I),7X,5HYW(I)//)
   31 FORMAT(1HO,2X,5HNFSF=,I5,5X,5HNFSL=,I5,5X,5HNBSF=,I5,5X,5HNBSL=,I5
     *,5X,5HMFSF=,I5,5X,5HMFSL=,I5,5X,5HMBSF=,I5,5X,5HMBSL=,I5//2X,
     *6HNLEFT=,I5,5X,6HNRIGT=,I5,5X,6HNBOND=,I5,4X,6HLITER=,I5,6X,
     *4HNST=,I5,5X,6HINNER=,I5,2X,4HSYE=,E12.4//2X,4HFIE=,E12.4,2X,
     *6HYLENS=,E12.4,2X,6HFLEPS=,E12.4,2X,6HFDCON=,E12.4,2X,5HSSTA=,
     *E12.4///)
   32 FORMAT(1HO,2X,40HTOTAL HEAD OF NODES AT TIME T  I=1 TO 66//)
   33 FORMAT(8X,4HH(I),9X,6HH(I+1),9X,6HH(I+2),9X,6HH(I+3),9X,6HH(I+4),
     *9X,6HH(I+5)//)
   34 FORMAT(1HO,2X,44HY-COORDINATE OF FREE SURFACE NODES I=1 TO 18//)
   35 FORMAT(1HO,7X,5HY(19),10X,5HY(67),10X,5HY(71)//)
   36 FORMAT(1HO,2X,4HH(I),2X,62HNEW TOTAL HEAD OF NODES AFTER SHIFTING
     $COORDINATES OF ALL NODES///)
   37 FORMAT(1HO,2X,4HY(I),2X,65HNEW Y-COORDINATE OF NODES AFTER SHIFTIN
     *G COORDINATES OF ALL NODES///)
   39 FORMAT(6(E12.4,3X)///)
   46 FORMAT(5HSTOPA)
   48 FORMAT(5HSTOPC)
   50 FORMAT(5HSTOPE)
C
C
      IR=5
      IW=6
C
C     READ AND PRINT DATA REQUIRED
C
      READ(IR,1)NPART,NPOIN,NELEM,DT,XK,TL,POROS
      WRITE(IW,2)NPART,NPOIN,NELEM,DT,XK,TL,POROS
      READ(IR,22) NFSF,NFSL,NBSF,NBSL,MFSF,MFSL,MBSF,MBSL,NLEFT,NRIGT,
     *NBOND,LITER,NST,INNER
      READ(IR,13) SYE,FIE,YLENS,FLEPS,FDCON,FD
C
C     READ COORDINATES OF NODAL W.R. TO COMMON COORDINATES
C     READ INITIAL NODAL VALUE OF H(I)
C
      WRITE(IW,6)
      WRITE(IW,4)
      DO 51 I=1,NPOIN
      READ(IR,3)I,X(I),Y(I),H(I)
```

```
   51 WRITE(IW,3)I,X(I),Y(I),H(I)
      READ(IR,5)NCARD
      IF (NCARD-NPCIN) 53,52,53
   53 WRITE(IW,46)
      STOP
   52 CONTINUE
C
C     READ THE NUMBERS OF THREE NODAL IN TRIANGLE ELEMENT IN COUNTERCLOCKWISE
C     SENSE AND PROPERTIES OF ELEMENT
C
      WRITE(IW,9)
      WRITE(IW,10)
      DO 57 I=1,NELEM
      READ(IR,7)I,NOD1(I),NOD2(I),NOD3(I)
   57 WRITE(IW,7)I,NOD1(I),NOD2(I),NOD3(I)
      READ(IR,5)NCARD
      IF(NCARD-NELEM)59,58,59
   59 WRITE(IW,48)
      STOP
   58 CONTINUE
C
C     READ MNUM(IJ)
C
      WRITE(IW,26)
      WRITE(IW,27)
      DO 56 I=1,INNER
      READ(IR,20) I,MNUM(I,1),MNUM(I,2),MNUM(I,3),MNUM(I,4)
      WRITE(IW,15)   I,MNUM(I,1),MNUM(I,2),MNUM(I,3),MNUM(I,4)
   56 CONTINUE
C
C     READ FOURIER COEFF. OF BOTTOM DRAINAGE VELOCITY
C
      DO 54 I=1,12
      READ(IR,18) CDUMY,A(I,1),A(I,2),A(I,3),A(I,4),A(I,5),A(I,6)
   54 READ(IR,18) SDUMY,B(I,1),B(I,2),B(I,3),B(I,4),B(I,5),B(I,6)
      WRITE(IW,28)
      DO 55 I=1,12
      WRITE(IW,18)CDUMY,A(I,1),A(I,2),A(I,3),A(I,4),A(I,5),A(I,6)
   55 WRITE(IW,18)SDUMY,B(I,1),B(I,2),B(I,3),B(I,4),B(I,5),B(I,6)
C
C     READ COORDINATES OF 13 WELLS
C
      READ(IR,19) (I,XW(I),YW(I),I=1,13)
      WRITE(IW,29)
      WRITE(IW,30)
      WRITE(IW,19) (I,XW(I),YW(I),I=1,13)
C
C     MOBS=NO. OF ELEMENTS ALONG BOTTOM BOUNDARY
C
      MOBS=MBSL-MBSF+1
      DDT=1.0/DT
C
C     FOR AN UNCONFINED AQUIFER, THE STORAGE COEFF. EQUAL TO THE SPECIFIC YIELD,
C     THEREFORE  SSTA  OBTAINED ABOVE HOLDS ONLY FOR CONFINED AQUIFER, MAKE
C     THE CORRECTION AS SSTA=0.00125, SEE HYDROLOGY HANDBOOK BY CHOW
C
      READ(IR,19) NPOV,DXV,SSTA
C
      SSKI=SSTA/XK
      WRITE(IW,31)   NFSF,NFSL,NBSF,NBSL,MFSF,MFSL,MBSF,MBSL,NLEFT,
     *NRIGT,NBCND,LITER,NST,INNER,SYE,FIE,YLENS,FLEPS,FDCON,SSTA
```

```
      T=0.0
      NPRINT=0
      NKV=0
C
C     INITIALIZE THE OVER-ALL MATRIX FOR THE INNER ELEMENTS
C
  150 NSHFT=0
      DO 60 I=1,NFSL
   60 YFOLD(I)=Y(I)
      YLC=Y(NLEFT)
      YRC=Y(NRIGT)
      DO 73 I=1,NPOIN
      DO 71 J=1,NPOIN
      P(I,J)=0.0
   71 Q(I,J)=0.0
      YDUMY(I)=0.0
      HDUMY(I)=0.0
      E(I)=0.0
   73 R(I)=0.0
C
C     INITIALIZE THE CORRECTING MATRICES OF OVER-ALL MATRICES FOR EACH ITERATION
C     DUE TO EFFECT OF CHANGING FREE SURFACE
C
      DO 63 I=1,NFSL
   63 ROLD(I)=0.0
      DO 64 I=1,NFSL
      DO 64 J=1,3
      BOD1(I,J)=0.0
      BOD2(I,J)=0.0
      BOD3(I,J)=0.0
      SKND1(I,J)=0.0
      SKND2(I,J)=0.0
   64 SKND3(I,J)=0.0
      DO 1022 I=1,4
      DO 1022 J=1,3
 1022 BFLX(I,J)=0.0
C
C     FORMATION OF ELEMENT STIFFNESS MATRICES
C     OF INNER ELEMENTS WHICH ARE NOT ADJACENT TO THE FREE SURFACE
C
C     NI=SINCE USE THE SAME  PROGRAM LOOP  TO CALCULATE ELEMENT MATRIX OF BOTH
C        INNER AND FREE SURFACE ELEMENT, THEREFORE, USE  NI  AS CONTROL INTEGER
C        TO SKIP  COMPUTER JOB  TO APPROPRIATE LOOP
C     NJ=SAME PURPOSE AS NI EXCEPT TO CONTROL WHETHER OR NOT TO FIND ALL
C     PROPERTIES AT TIME STEP N-1
C
      N=NFSL+1
      NN=NELEM
      NI=0
      NJ=0
  201 DO 61 I=N,NN
C
C     TRANSFORM COORDINATES OF THE THREE NODALS OF TRIANGLE ELEMENT TO
C     NEW CENTROID COORDINATES SYSTEM
C
      I1=NOD1(I)
      I2=NOD2(I)
      I3=NOD3(I)
      AA=0.33333*(X(I1)+X(I2)+X(I3))
```

```
      BB=0.33333*(Y(I1)+Y(I2)+Y(I3))
      XN1=X(I1)-AA
      XN2=X(I2)-AA
      XN3=X(I3)-AA
      YN1=Y(I1)-BB
      YN2=Y(I2)-BB
      YN3=Y(I3)-BB
C
C     FIND VALUES REQUIRED FOR ELEMENT STIFFNESS MATRICES
C
      A1=XN2*YN3-XN3*YN2
      A2=XN3*YN1-XN1*YN3
      A3=XN1*YN2-XN2*YN1
      B1=YN2-YN3
      B2=YN3-YN1
      B3=YN1-YN2
      C1=XN3-XN2
      C2=XN1-XN3
      C3=XN2-XN1
      XX2=XN1*XN1+XN2*XN2+XN3*XN3
      YY2=YN1*YN1+YN2*YN2+YN3*YN3
      XY=XN1*YN1+XN2*YN2+XN3*YN3
      DELTA=XN2*YN3+XN3*YN1+XN1*YN2-YN1*XN2-YN2*XN3-YN3*XN1
      DELTA=0.5*DELTA
      DDELT=1.0/DELTA
      DDEL=0.25*DDELT
      F11=DDEL*(A1*A1+0.083333*B1*B1*XX2+C.083333*C1*C1*YY2+
     *0.166667*B1*C1*XY)
      F22=DDEL*(A2*A2+0.083333*B2*B2*XX2+C.083333*C2*C2*YY2+
     *0.166667*B2*C2*XY)
      F33=DDEL*(A3*A3+0.083333*B3*B3*XX2+C.083333*C3*C3*YY2+
     *0.166667*B3*C3*XY)
      AA=B1*C2+C1*B2
      F12=DDEL*(A1*A2+0.083333*AA*XY+0.083333*B1*B2*XX2+
     *0.083333*C1*C2*YY2)
      AA=B1*C3+C1*B3
      F13=DDEL*(A1*A3+0.083333*AA*XY+C.083333*B1*B3*XX2+
     *0.083333*C1*C3*YY2)
      AA=B2*C3+C2*B3
      F23=DDEL*(A2*A3+0.083333*AA*XY+0.083333*B2*B3*XX2+
     *0.083333*C2*C3*YY2)
      BC1(I,1)=DDEL*(B1*B1+C1*C1)*XK
      BC2(I,1)=DDEL*(B1*B2+C1*C2)*XK
      BC3(I,1)=DDEL*(B1*B3+C1*C3)*XK
      BC1(I,2)=BC2(I,1)
      BC2(I,2)=DDEL*(B2*B2+C2*C2)*XK
      BC3(I,2)=DDEL*(B2*B3+C2*C3)*XK
      BC1(I,3)=BC3(I,1)
      BC2(I,3)=BC3(I,2)
      BC3(I,3)=DDEL*(B3*B3+C3*C3)*XK
      SKN1(I,1)=SSKI*F11*XK
      SKN2(I,1)=SSKI*F12*XK
      SKN3(I,1)=SSKI*F13*XK
      SKN1(I,2)=SKN2(I,1)
      SKN2(I,2)=SSKI*F22*XK
      SKN3(I,2)=SSKI*F23*XK
      SKN1(I,3)=SKN3(I,1)
      SKN2(I,3)=SKN3(I,2)
      SKN3(I,3)=SSKI*F33*XK
   61 CONTINUE
      IF(NI) 202,202,203
```

```
C
C     FIND THE OVER-ALL MATRIX FOR THE INNER ELEMENTS
C
  202 N=MFSL+1
      NN=NELEM
  206 DO 72 I=N,NN
      I1=NOD1(I)
      I2=NOD2(I)
      I3=NOD3(I)
      P(I1,I1)=P(I1,I1)+BC1(I,1)
      P(I1,I2)=P(I1,I2)+BC2(I,1)
      P(I1,I3)=P(I1,I3)+BC3(I,1)
      P(I2,I1)=P(I2,I1)+BC1(I,2)
      P(I2,I2)=P(I2,I2)+BC2(I,2)
      P(I2,I3)=P(I2,I3)+BC3(I,2)
      P(I3,I1)=P(I3,I1)+BC1(I,3)
      P(I3,I2)=P(I3,I2)+BC2(I,3)
      P(I3,I3)=P(I3,I3)+BC3(I,3)
      Q(I1,I1)=Q(I1,I1)+SKN1(I,1)
      Q(I1,I2)=Q(I1,I2)+SKN2(I,1)
      Q(I1,I3)=Q(I1,I3)+SKN3(I,1)
      Q(I2,I1)=Q(I2,I1)+SKN1(I,2)
      Q(I2,I2)=Q(I2,I2)+SKN2(I,2)
      Q(I2,I3)=Q(I2,I3)+SKN3(I,2)
      Q(I3,I1)=Q(I3,I1)+SKN1(I,3)
      Q(I3,I2)=Q(I3,I2)+SKN2(I,3)
      Q(I3,I3)=Q(I3,I3)+SKN3(I,3)
   72 CONTINUE
      IF(NKV) 1005,1005,133
 1005 CONTINUE
C
C     FIND CONSTANT MATRICES DUE TO EFFECTS OF BOTTOM DRAINAGE VELOCITY
C     AT INITIAL TIME
C
      CALL DRANV(T,XW,VDUMY)
C
C     CONVERT DRAINAGE VELOCITY FROM VDUMY (I) INTO V(I),THIS PART ONLY HOLDS ON
C     THE PARTICULAR NODE-ELEMENT CONFIGURATION CONSIDERED
C
      NN=MOBS-3
      NE=1
      V(1)=0.0
      DO 74 I=2,NN,4
      V(I)=-VDUMY(NE)
      V(I+1)=-VDUMY(NE+1)
      V(I+2)=0.0
      V(I+3)=0.0
      NE=NE+2
   74 CONTINUE
      V(I+4)=-VDUMY(NE)
      V(I+5)=-VDUMY(NE+1)
      V(I+6)=0.0
      NE=0
      DO 75 I=MBSF,MBSL
      NE=NE+1
      I1=NOD1(I)
      I2=NOD2(I)
      R(I1)=R(I1)-0.5*V(NE)*(X(I2)-X(I1))
   75 R(I2)=R(I2)-0.5*V(NE)*(X(I2)-X(I1))
```

```
C
C      EFFECTS OF HORIZONTAL FLUX ON LEFT HAND SIDE BOUNDARY WHERE HYDROSTATIC
C      CONDITION IS PRESUMELY EXISTED.  THEREFORE, COMBINE ALL EFFECTS BY
C      DYE=THE TOTAL LENGTH OF THE WHOLE LEFT BOUNDARY
C
       I=MFSF
       DYE=Y(NLEFT)
       NFLUX=1
 1012  I1=NOD1(I)
       I2=NOD2(I)
       I3=NOD3(I)
       AA=0.33333*(X(I1)+X(I2)+X(I3))
       BB=0.33333*(Y(I1)+Y(I2)+Y(I3))
       XN1=X(I1)-AA
       XN2=X(I2)-AA
       XN3=X(I3)-AA
       YN1=Y(I1)-BB
       YN2=Y(I2)-BB
       YN3=Y(I3)-BB
       B1=YN2-YN3
       B2=YN3-YN1
       B3=YN1-YN2
       DELTA=XN2*YN3+XN3*YN1+XN1*YN2-YN1*XN2-YN2*XN3-YN3*XN1
       DELTA=0.5*DELTA
       DDEL=0.25/DELTA
       AA=XK*DYE*DDEL
       P(I1,I1)=P(I1,I1)+AA*B1-BFLX(NFLUX,1)
       P(I1,I2)=P(I1,I2)+AA*B2-BFLX(NFLUX,2)
       P(I1,I3)=P(I1,I3)+AA*B3-BFLX(NFLUX,3)
       P(I2,I1)=P(I2,I1)+AA*B1-BFLX(NFLUX,1)
       P(I2,I2)=P(I2,I2)+AA*B2-BFLX(NFLUX,2)
       P(I2,I3)=P(I2,I3)+AA*B3-BFLX(NFLUX,3)
       BFLX(NFLUX,1)=AA*B1
       BFLX(NFLUX,2)=AA*B2
       BFLX(NFLUX,3)=AA*B3
       GO TO (1013,1014,1015,1016),NFLUX
C
C      EFFECTS OF HORIZONTAL FLUX ON RIGHT HAND SIDE BOUNDARY WHERE NO HYDRO-
C      STATICS IS EXISTED,THEREFORE, THE EFFECTS OF INDIVIDUAL ELEMENT MUST BE
C      CONSISERED SEPERATELY
C
 1013  I=40
       DYE=Y(69)-Y(70)
       NFLUX=NFLUX+1
       GO TO 1012
 1014  I=90
       DYE=Y(68)-Y(69)
       NFLUX=NFLUX+1
       GO TO 1012
 1015  I=110
       DYE=Y(67)-Y(68)
       NFLUX=NFLUX+1
       GO TO 1012
 1016  CONTINUE
C
C      THE FOLLOWING PROGRAM REQUIRED FOR EACH TIME CYCLE
C
  133  CONTINUE
       T=T+DT
       WRITE(IW,12)T
       NPRINT=NPRINT+1
```

```
C
C     SETUP OLD COORDINATES OF FREE SURFACE BEFORE ITERATION
C
      DO 76 I=1,NFSL
   76 YOLD(I)=Y(I)
      YLOLD=Y(NLEFT)
      YROLD=Y(NRIGT)
      NITER=0
  130 NITER=NITER+1
      NI=1
      N=NFSF
      NN=NFSL
C
C     SETUP ELEMENT MATRICES OF ELEMENTS ALONG FREE SURFACE
C
      GO TO 201
C
C     CORRECT ELEMENT MATRICES DUE TO EFFECT OF FREE SURFACE
C
  203 DO 80 I=N,NN
      I2=NOD2(I)
      I3=NOD3(I)
      IF(I.EQ.1) GO TO 84
      IF(I.EQ.NFSL) GO TO 84
      IF(I2-NFSL) 81,81,80
   81 IF(I3-NFSL) 84,84,80
   84 CC=X(I2)-X(I3)
      DD=(CC*SYE)/6.0
      SKN2(I,2)=SKN2(I,2)+2.0*DD
      SKN3(I,2)=SKN3(I,2)+DD
      SKN2(I,3)=SKN2(I,3)+DD
      SKN3(I,3)=SKN3(I,3)+2.0*DD
      R(I2)=R(I2)+0.5*FIE*CC
      R(I3)=R(I3)+0.5*FIE*CC
   80 CONTINUE
      DO 87 I=1,NFSL
      R(I)=R(I)-ROLD(I)
   87 ROLD(I)=R(I)
C
C     SETUP OVER-ALL MATRICES DUE TO ELEMENTS ALONG FREE SURFACE
C
      DO 88 I=1,NFSL
      I1=NOD1(I)
      I2=NOD2(I)
      I3=NOD3(I)
      P(I1,I1)=P(I1,I1)+BC1(I,1)-BCO1(I,1)
      P(I1,I2)=P(I1,I2)+BC2(I,1)-BCO2(I,1)
      P(I1,I3)=P(I1,I3)+BC3(I,1)-BCO3(I,1)
      P(I2,I1)=P(I2,I1)+BC1(I,2)-BCO1(I,2)
      P(I2,I2)=P(I2,I2)+BC2(I,2)-BCO2(I,2)
      P(I2,I3)=P(I2,I3)+BC3(I,2)-BCO3(I,2)
      P(I3,I1)=P(I3,I1)+BC1(I,3)-BCO1(I,3)
      P(I3,I2)=P(I3,I2)+BC2(I,3)-BCO2(I,3)
      P(I3,I3)=P(I3,I3)+BC3(I,3)-BCO3(I,3)
      Q(I1,I1)=Q(I1,I1)+SKN1(I,1)-SKNO1(I,1)
      Q(I1,I2)=Q(I1,I2)+SKN2(I,1)-SKNO2(I,1)
      Q(I1,I3)=Q(I1,I3)+SKN3(I,1)-SKNO3(I,1)
      Q(I2,I1)=Q(I2,I1)+SKN1(I,2)-SKNO1(I,2)
      Q(I2,I2)=Q(I2,I2)+SKN2(I,2)-SKNO2(I,2)
```

```
      Q(I2,I3)=Q(I2,I3)+SKN3(I,2)-SKNO3(I,2)
      Q(I3,I1)=Q(I3,I1)+SKN1(I,3)-SKNO1(I,3)
      Q(I3,I2)=Q(I3,I2)+SKN2(I,3)-SKNO2(I,3)
      Q(I3,I3)=Q(I3,I3)+SKN3(I,3)-SKNO3(I,3)
      BCC1(I,1)=BC1(I,1)
      BCC2(I,1)=BC2(I,1)
      BCC3(I,1)=BC3(I,1)
      BCC1(I,2)=BC1(I,2)
      BCC2(I,2)=BC2(I,2)
      BCC3(I,2)=BC3(I,2)
      BCC1(I,3)=BC1(I,3)
      BCC2(I,3)=BC2(I,3)
      BCC3(I,3)=BC3(I,3)
      SKNC1(I,1)=SKN1(I,1)
      SKNC2(I,1)=SKN2(I,1)
      SKNC3(I,1)=SKN3(I,1)
      SKNC1(I,2)=SKN1(I,2)
      SKNC2(I,2)=SKN2(I,2)
      SKNC3(I,2)=SKN3(I,2)
      SKNC1(I,3)=SKN1(I,3)
      SKNC2(I,3)=SKN2(I,3)
      SKNC3(I,3)=SKN3(I,3)
   88 CONTINUE
      IF(NJ) 204,204,205
C
C     FIND PARTIAL DERIVATIVE OF TIME AT TIME (T-DT)
C
  204 CONTINUE
      NN=NPCIN/5
      ND=NN*5-1
      NDV=NN*5+1
C
C     AND READ B. C. AT TIME T
C
      READ(IR,23) YLEFT,YRIGT,DUMY,DUMY
      DO 101 I=1,NPCIN
      AA=0.0
      DO 102 J=1,NPCIN
      AA=AA-P(I,J)*H(J)
  102 CONTINUE
      E(I)=+AA+R(I)
  101 CONTINUE
C
C     FIND PRESCRIBED TIME-DERIVATIVES OF BOUNDARY AT TIME (T-DT)
C
      AA=(YLEFT-YLOLD)/DT
      BB=(YRIGT-YROLD)/DT
      NN=NLEFT+NBCNC-1
      DO 146 I=NLEFT,NN
  146 HT(I)=AA
      HT(NRIGT)=BB
      NFI=NRIGT-1
      DO 1 3 I=1,NFI
      DO 149 J=NRIGT,NPCIN
  149 E(I)=E(I)-Q(I,J)*HT(J)
  148 CONTINUE
C
C     SETUP DUMMY MATRICES C(IJ) FOR ARRAY AND SIMQ TO AVOID DESTROYING OF
C     MATRICE Q(IJ)
C
      DO 145 I=1,NPCIN
```

```
      DO 145 J=1,NPOIN
  145 D(I,J)=G(I,J)
C
      CALL ARRAY(2,NFI,NFI,NPOIN,NPOIN,C,D)
      CALL SIMQM(D,E,NFI,0)
C
      DO 106 I=1,NFI
  106 HT(I)=E(I)
C
C     FIND CONSTANT MATRICES DUE TO EFFECTS OF BOTTOM DRAINAGE VELOCITY
C     READ DRAINAGE VELOCITY AT TIME T
C
      CALL DRANV(T,XW,VDUMY)
C
C     CONVERT DRAINAGE VELOCITY FROM VDUMY (I) INTO V(I),THIS PART ONLYHOLDS FOR
C     THE PARTICULAR NODE-ELEMENT COFIGURATION CONSIDERED
C
      NN=MOBS-3
      NE=1
      V(1)=0.0
      DO 107 I=2,NN,4
      V(I)=-VDUMY(NE)
      V(I+1)=-VDUMY(NE+1)
      V(I+2)=0.0
      V(I+3)=0.0
      NE=NE+2
  107 CONTINUE
      V(I+4)=-VDUMY(NE)
      V(I+5)=-VDUMY(NE+1)
      V(I+6)=0.0
      DO 104 I=NBSF,NBSL
  104 R(I)=0.0
      R(NLEFT+NBCNC-1)=0.0
      R(NRIGT-NBCNC+1)=0.0
      NE=0
      DO105 I=MBSF,MBSL
      NE=NE+1
      I1=NCC1(I)
      I2=NCC2(I)
      R(I1)=R(I1)-0.5*V(NE)*(X(I2)-X(I1))
  105 R(I2)=R(I2)-0.5*V(NE)*(X(I2)-X(I1))
C
C     EFFECTS OF HORIZONTAL FLUX ON LEFT HAND SIDE BOUNDARY WHERE HYDROSTATIC
C     CONDITION IS PRESUMELY EXISTED.  THEREFORE, COMBINE ALL EFFECTS BY
C     DYE=THE TOTAL LENGTH OF THE WHOLE LEFT BOUNDARY
C
      I=MFSF
      DYE=Y(NLEFT)
      NFLUX=1
 1017 I1=NCC1(I)
      I2=NCC2(I)
      I3=NCC3(I)
      AA=0.33333*(X(I1)+X(I2)+X(I3))
      BB=0.33333*(Y(I1)+Y(I2)+Y(I3))
      XN1=X(I1)-AA
      XN2=X(I2)-AA
      XN3=X(I3)-AA
      YN1=Y(I1)-BB
      YN2=Y(I2)-BB
```

```
      YN3=Y(I3)-BB
      B1=YN2-YN3
      B2=YN3-YN1
      B3=YN1-YN2
      DELTA=XN2*YN3+XN3*YN1+XN1*YN2-YN1*XN2-YN2*XN3-YN3*XN1
      DELTA=0.5*DELTA
      DDEL=0.25/DELTA
      AA=XK*DYE*DDEL
      P(I1,I1)=P(I1,I1)+AA*B1-BFLX(NFLUX,1)
      P(I1,I2)=P(I1,I2)+AA*B2-BFLX(NFLUX,2)
      P(I1,I3)=P(I1,I3)+AA*B3-BFLX(NFLUX,3)
      P(I2,I1)=P(I2,I1)+AA*B1-BFLX(NFLUX,1)
      P(I2,I2)=P(I2,I2)+AA*B2-BFLX(NFLUX,2)
      P(I2,I3)=P(I2,I3)+AA*B3-BFLX(NFLUX,3)
      BFLX(NFLUX,1)=AA*B1
      BFLX(NFLUX,2)=AA*B2
      BFLX(NFLUX,3)=AA*B3
      GO TO (1018,1019,1020,1021),NFLUX
C
C     EFFECTS OF HORIZONTAL FLUX ON RIGHT HAND SIDE BOUNDARY WHERE NO HYDRO-
C     STATICS IS EXISTED,THEREFORE, THE EFFECTS OF INDIVIDUAL ELEMENT MUST BE
C     CONSISERED SEPERATELY
C
 1018 I=40
      DYE=Y(69)-Y(70)
      NFLUX=NFLUX+1
      GO TO 1017
 1019 I=90
      DYE=Y(68)-Y(69)
      NFLUX=NFLUX+1
      GO TO 1017
 1020 I=110
      DYE=Y(67)-Y(68)
      NFLUX=NFLUX+1
      GO TO 1017
 1021 CONTINUE
C
      DO110 I=1,NPOIN
      BB=HT(I)+2.0*DDT*H(I)
  110 HT(I)=BB
C
C     SETUP PRESCRIBED PIEZOMETER HEAD OF BOUNDARY AT TIME T
C
      NN=NLEFT+NBOND-1
      DO 114 I=NLEFT,NN
  114 H(I)=YLEFT
      Y(NLEFT)=YLEFT
      H(NRIGT)=YRIGT
      Y(NRIGT)=YRIGT
C
C     TO FIND H(I) AT TIME T
C
  205 CONTINUE
      DO 111 I=1,NPOIN
      DO 111 J=1,NPOIN
  111 D(I,J)=P(I,J)+2.0*DDT*Q(I,J)
      DO 112 I=1,NPOIN
      AA=0.0
      DO 113 J=1,NPOIN
      AA=AA+Q(I,J)*HT(J)
  113 CONTINUE
```

```
      E(I)=AA+R(I)
  112 CONTINUE
C
C     SUBSTITUTING   PR-ESCRIBED VALUE FOR SOME H(I)
C
      NFI=NRIGT-1
      DO 116 I=1,NFI
      DO 117 J=NRIGT,NPOIN
  117 E(I)=E(I)-D(I,J)*H(J)
  116 CONTINUE
C
      CALL ARRAY(2,NFI,NFI,NPOIN,NPOIN,D,D)
      CALL SIMQM(D,E,NFI,KS)
C
      DO 118 I=1,NFI
  118 H(I)=E(I)
      IF(NPRINT-10) 1009,1008,1009
 1008 CONTINUE
      WRITE(IW,32)
      WRITE(IW,33)
      DO 92 I=1,66,6
   92 WRITE(IW,8) H(I),H(I+1),H(I+2),H(I+3),H(I+4),H(I+5)
C
C     CORRECT THE POSITION OF FREE SURFACE
C
C     EPS=CONVEGENT CRITERIA
C     FDCON=CORRECTING FACTOR TO GET CONVEGENT CRITERIA
C     FLEPS=LENGTH OF BOTTOM BOUNDARY
C
 1009 NCONV=0
      AA=YRIGT-YROLD
      BB=YLEFT-YLOLD
      AA=ABS(AA)
      BB=ABS(BB)
      IF(AA.GE.BB) GO TO 141
      EPS=BB*FDCON
      GO TO 142
  141 EPS=AA*FDCON
  142 CONTINUE
C
C     NEXT CARD CAN BE CHANGED, NOW ( EPS.GE.4.5 ) BE CHOSEN
C
      IF(EPS-4.5) 144,143,143
  144 EPS=4.5
  143 DO 120 I=NFSF,NFSL
      CC=(X(I)+50.0)/FLEPS+0.4
      CC=CC*EPS
      AA=ABS(H(I)-YOLD(I))
      IF(AA-EPS) 121,122,122
  122 AA=H(I)-YOLD(I)
      IF(AA) 123,124,124
  124 H(I)=YOLD(I)+0.05*CC
      GO TO 120
  123 H(I)=YOLD(I)-0.05*CC
      GO TO 120
  121 NCONV=NCONV+1
  120 CONTINUE
      DO 125 I=NFSF,NFSL
  125 Y(I)=H(I)
```

```
      IF(NPRINT-10) 1011,1010,1011
 1010 CONTINUE
      WRITE(IW,34)
      DO 93 I=1,18,6
   93 WRITE(IW,8) Y(I),Y(I+1),Y(I+2),Y(I+3),Y(I+4),Y(I+5)
      WRITE(IW,35)
      WRITE(IW,39)Y(19),Y(67),Y(71),FD,FD,FD
      NPRINT=0
 1011 CONTINUE
      IF(NITER-LITER) 126,127,127
  127 WRITE(IW,50)
      GO TO 128
  126 IF(NCONV-NFSL) 129,128,128
  129 NJ=1
      GO TO 130
  128 IF(T-TL) 132,131,131
  132 NJ=0
 1000 NSHFT=NSHFT+1
      IF(NSHFT.EQ.NST) GO TO 134
      GO TO 133
C
C     IF ANY NODE ON F.S. SHIFTING TOO MUCH
C
  134 DO 135 I=1,NFSL
      AA=ABS(Y(I)-YFOLD(I))
      IF(AA.GT.YLENS) GO TO 139
  135 CONTINUE
      NSHFT=0
      GO TO 133
C
C     THE FOLLOWING PROGRAM  ONLY CAN BE APPLIED TO SPECIAL NODE-ELEMENT
C     CONFIGURATION CONSIDERED IN THIS PROGRAM
C
C     SHIFTING THE NODES OF SECOND ROW
C
  139 N=NFSL+1
      NN=2*NFSL
      NE=1
      DO 136 I=N,NN
      DY=Y(NE)-YFOLD(NE)
      YDUMY(I)=Y(I)+DY
  136 NE=NE+1
C
C     SHIFTING THE NODES OF THIRD ROW
C
      N=NN+1
      NN=N+NFSL/2
      NE=1
      DO 137 I=N,NN
      DY=Y(NE)-YFOLD(NE)
      YDUMY(I)=Y(I)+DY
  137 NE=NE+2
C
C     SHIFTING THE NODES OF FOURTH ROW
C
      N=NN+1
      NN=N+NFSL/2-1
      NE=2
      DO 138 I=N,NN
      DY=Y(NE)-YFOLD(NE)
      YDUMY(I)=Y(I)+DY
```

```
  138 NE=NE+2
C
C     THE FOLLOWING PROGRAM IS USED TO CORRECT H(I) DUE TO SHIFTING THE COORD.
C     OF NODES
C
C     CORRECT H(I) OF NODES ON SECOND ROW
      N=NFSL+1
      NN=2*NFSL
      NJ=1
  312 DO 299 JJ=N,NN
      MI1=MNUM(JJ-NFSL,1)
      MI2=MNUM(JJ-NFSL,2)
      MI3=MNUM(JJ-NFSL,3)
      MI4=MNUM(JJ-NFSL,4)
      I1=NOD1(MI4)
      I2=NOD2(MI4)
      I3=NOD3(MI4)
      IF(YDUMY(JJ).LT.Y(I1)) GO TO 306
      NI=1
  310 AA=0.33333*(X(I1)+X(I2)+X(I3))
      BB=0.33333*(Y(I1)+Y(I2)+Y(I3))
      XN1=X(I1)-AA
      XN2=X(I2)-AA
      XN3=X(I3)-AA
      YN1=Y(I1)-BB
      YN2=Y(I2)-BB
      YN3=Y(I3)-BB
C
C     FIND VALUES REQUIRED FOR ELEMENT STIFFNESS MATRICES
C
      A1=XN2*YN3-XN3*YN2
      A2=XN3*YN1-XN1*YN3
      A3=XN1*YN2-XN2*YN1
      B1=YN2-YN3
      B2=YN3-YN1
      B3=YN1-YN2
      C1=XN3-XN2
      C2=XN1-XN3
      C3=XN2-XN1
      XX2=XN1*XN1+XN2*XN2+XN3*XN3
      YY2=YN1*YN1+YN2*YN2+YN3*YN3
      XY=XN1*YN1+XN2*YN2+XN3*YN3
      DELTA=XN2*YN3+XN3*YN1+XN1*YN2-YN1*XN2-YN2*XN3-YN3*XN1
      DELTA=0.5*DELTA
      DDELT=1.0/DELTA
      FN1=0.5*DDELT*(A1+B1*(X(JJ)-AA)+C1*(YDUMY(JJ)-BB))
      FN2=0.5*DDELT*(A2+B2*(X(JJ)-AA)+C2*(YDUMY(JJ)-BB))
      FN3=0.5*DDELT*(A3+B3*(X(JJ)-AA)+C3*(YDUMY(JJ)-BB))
      GO TO (302,303,302,303),NI
  302 H1=FN1*H(I1)+FN2*H(I2)+FN3*H(I3)
  304 GO TO(300,301,305,301),NI
  300 I1=NOD1(MI1)
      I2=NOD2(MI1)
      I3=NOD3(MI1)
      NI=2
      GO TO 310
  303 H2=FN1*H(I1)+FN2*H(I2)+FN3*H(I3)
      GO TO 304
  301 HDUMY(JJ)=0.5*(H1+H2)
```

```
      GO TO 299
  306 I1=NOD1(MI2)
      I2=NOD2(MI2)
      I3=NOD3(MI2)
      NI=3
      GO TO 310
  305 I1=NOD1(MI3)
      I2=NOD2(MI3)
      I3=NOD3(MI3)
      NI=4
      GO TO 310
  299 CONTINUE
      GO TO(311,313),NJ
C     CORRECT H(I) OF THE NODES ON FOURTH ROW
  311 N=NN+1
      NN=N+NFSL/2
      N=NN+1
      NJ=2
      NN=N+NFSL/2-1
      GO TO 312
C     CORRECT H(I) OF THE NODES ON THIRD ROW
  313 CONTINUE
      N=NFSL+1
      NN=2*NFSL
      N=NN+1
      NN=N+NFSL/2
      DO 314 JJ=N,NN
      MI1=MNUM(JJ-NFSL,1)
      MI2=MNUM(JJ-NFSL,2)
      MI3=MNUM(JJ-NFSL,3)
      I1=NOD1(MI3)
      I2=NOD2(MI3)
      I3=NOD3(MI3)
      IF(YDUMY(JJ).LT.Y(I1)) GO TO 315
      NI=1
  318 AA=0.33333*(X(I1)+X(I2)+X(I3))
      BB=0.33333*(Y(I1)+Y(I2)+Y(I3))
      XN1=X(I1)-AA
      XN2=X(I2)-AA
      XN3=X(I3)-AA
      YN1=Y(I1)-BB
      YN2=Y(I2)-BB
      YN3=Y(I3)-BB
C
C     FIND VALUES REQUIRED FOR ELEMENT STIFFNESS MATRICES
C
      A1=XN2*YN3-XN3*YN2
      A2=XN3*YN1-XN1*YN3
      A3=XN1*YN2-XN2*YN1
      B1=YN2-YN3
      B2=YN3-YN1
      B3=YN1-YN2
      C1=XN3-XN2
      C2=XN1-XN3
      C3=XN2-XN1
      XX2=XN1*XN1+XN2*XN2+XN3*XN3
      YY2=YN1*YN1+YN2*YN2+YN3*YN3
      XY=XN1*YN1+XN2*YN2+XN3*YN3
      DELTA=XN2*YN3+XN3*YN1+XN1*YN2-YN1*XN2-YN2*XN3-YN3*XN1
      DELTA=0.5*DELTA
      DDELT=1.0/DELTA
```

```
      FN1=0.5*DDELT*(A1+B1*(X(JJ)-AA)+C1*(YDUMY(JJ)-BB))
      FN2=0.5*DDELT*(A2+B2*(X(JJ)-AA)+C2*(YDUMY(JJ)-BB))
      FN3=0.5*DDELT*(A3+B3*(X(JJ)-AA)+C3*(YDUMY(JJ)-BB))
      GO TO (316,319,316),NI
  316 H1=FN1*H(I1)+FN2*H(I2)+FN3*H(I3)
  320 GO TO (317,321,322),NI
  317 I1=NOD1(MI1)
      I2=NOD2(MI1)
      I3=NOD3(MI1)
      NI=2
      GO TO 318
  319 H2=FN1*H(I1)+FN2*H(I2)+FN3*H(I3)
      GO TO 320
  321 HDUMY(JJ)=0.5*(H1+H2)
      GO TO 314
  315 I1=NOD1(MI2)
      I2=NOD2(MI2)
      I3=NOD3(MI2)
      NI=3
      GO TO 318
  322 HDUMY(JJ)=H1
  314 CONTINUE
      NDMF=NFSL+1
      N=NFSL+1
      NN=2*NFSL
      N=NN+1
      NN=N+NFSL/2
      N=NN+1
      NN=N+NFSL/2-1
      NDML=NN
      DO 326 I=NDMF,NDML
      Y(I)=YDUMY(I)
  326 H(I)=HDUMY(I)
C
C     CORRECT Y(I) OF THE BOUNDARY NODES
C
      NN=NLEFT+NBCND-2
      DY=YLEFT-YLO
      NNL=NLEFT+1
      DO 331 I=NNL,NN
  331 Y(I)=Y(I)+DY
      NN=NRIGT-NBCND+2
      DY=YRIGT-YRO
      NNR=NRIGT-1
      DO 332 I=NN,NNR
  332 Y(I)=Y(I)+DY
C
C     SINCE ALREADY SET-UP PRESCRIBED H(I) ON BOUNDARY, NO NEED TO CORRECT IT.
C     RE-INITIALIZE THE VALUE OF FIRST TIME CYCLE AFTER SHIFTING NODAL COORD.
C
      YLO=YLEFT
      YRO=YRIGT
      DO 336 I=NFSF,NFSL
  336 YFOLD(I)=Y(I)
C
      WRITE(IW,36)
      DO 337 I=1,72,6
  337 WRITE(IW,8) H(I),H(I+1),H(I+2),H(I+3),H(I+4),H(I+5)
      WRITE(IW,8) H(73),H(74),FD,FD,FD,FD
```

```
      WRITE(IW,37)
      DO 338 I=1,72,6
  338 WRITE(IW,8) Y(I),Y(I+1),Y(I+2),Y(I+3),Y(I+4),Y(I+5)
      WRITE(IW,8) Y(73),Y(74),FC,FC,FC,FD
      NKV=1
 1001 GO TO 150
  131 STOP
      END
```

```
      SUBROUTINE DRANV(T,XW,V)
C     SUBROUTINE DRANV FOR FINDING DRAINAGE VELOCITY OF WELLS AND EVEN ELEMENTS
C     WITH GIVEN FOURIER COEFF. OF WELL DRAINAGE VELOCITY
C     ALL UNIT SHOULD BE IN C.G.S. SYSTEM
C     PERIOD=100*15*60, WHERE  100  MEANS 100 CYCLES,  15  MEANS 15 MINUTES PER
C            CYCLE,  60  MEANS 1 MINUTE EQUAL TO 60 SECONDS
C     INPUT  A(IJ) =FOURIER COSINE COEFFICIENTS OF WELL DRAINAGE VELOCITY
C            B(IJ) =FOURIER SINE COEFFICIENTS OF WELL DRAINAGE VELOCITY
C            XW(I) =X-COORDINATES OF 13 WELLS
C            DX    =LENGTH OF EVEN ELEMENTS
C            T     =CORRENT TIME
C            NPOI1 =TOTAL NO. OF NODAL POINTS MINUS 1
C     OUTPUT
C            V(I)  =DRAINAGE VELOCITY OF EVEN ELEMENTS
C     A(I,J)=FOURIER COSINE COEFFICIENTS
C     B(I,J)=FOURIER SINE COEFFICIENTS
      DIMENSION VW(12),V(20),A(12,6),B(12,6),XW(13)
      COMMON DX,NPOI1,A,B
C     FIND DRAINAGE VELOCITY BETWEEN TWO WELLS BY FOURIER SERIES APPROXIMATION
      CC=2.0*3.1416/(15.0*60.0*100.0)
      DO 51 I=1,12
      SUM=A(I,1)
      DO 52 J=2,6
      AA=A(I,J)
      BB=B(I,J)
      FJ=J-1
      DD=FJ*CC*T
   52 SUM=SUM+AA*COS(DD)+BB*SIN(DD)
   51 VW(I)=SUM
C     FIND DRAINAGE VELOCITY FOR EACH ELEMENT WITH EVEN LENGTH
      X=0.5*DX
      DO 60 I=1,NPOI1
      DO 61 J=1,12
      IF(X-XW(J+1))63,65,66
   63 V(I)=VW(J)
      AA=XW(J+1)-X
      IF(AA-0.5*DX) 64,69,69
   64 BB=X+0.5*DX-XW(J+1)
      CC=(0.5*DX+AA)*VW(J)+BB*VW(J+1)
      V(I)=CC/DX
      GO TO 69
   65 V(I)=0.5*VW(J+1)+0.5*VW(J)
      GO TO 69
   66 AA=X-XW(J+1)-0.5*DX
      IF(AA) 67,61,61
   67 BB=X-XW(J+1)+0.5*DX
      CC=XW(J+1)-X+0.5*DX
      V(I)=(BB*VW(J+1)+CC*VW(J))/DX
      GO TO 69
   61 CONTINUE
   69 X=X+DX
   60 CONTINUE
      RETURN
      END
      SUBROUTINE SIMQM(A,B,N,KS)
      DIMENSION A(1),B(1)                                              SIMQ   2
C        FORWARD SOLUTION                                              SIMQ   3
      TOL=0.0                                                          SIMQ   4
      KS=0                                                             SIMQ   5
      JJ=-N                                                            SIMQ   6
```

```
      DO 65 J=1,N                                                    SIMQ   7
      JY=J+1                                                         SIMQ   8
      JJ=JJ+N+1                                                      SIMQ   9
      BIGA=0                                                         SIMQ  10
      IT=JJ-J                                                        SIMQ  11
      DO 30 I=J,N                                                    SIMQ  12
C        SEARCH FOR MAXIMUM COEFFICIENT IN COLUMN                    SIMQ  13
      IJ=IT+I                                                        SIMQ  14
      IF(ABS(BIGA)-ABS(A(IJ))) 20,30,30                              SIMQ  15
   20 BIGA=A(IJ)                                                     SIMQ  16
      IMAX=I                                                         SIMQ  17
   30 CONTINUE                                                       SIMQ  18
C        TEST FOR PIVOT LESS THAN TOLERANCE (SINGULAR MATRIX)        SIMQ  19
      IF(ABS(BIGA)-TOL) 35,35,40                                     SIMQ  20
   35 KS=1                                                           SIMQ  21
      RETURN                                                         SIMQ  22
C        INTERCHANGE ROWS IF NECESSARY                               SIMQ  23
   40 I1=J+N*(J-2)                                                   SIMQ  24
      IT=IMAX-J                                                      SIMQ  25
      DO 50 K=J,N                                                    SIMQ  26
      I1=I1+N                                                        SIMQ  27
      I2=I1+IT                                                       SIMQ  28
      SAVE=A(I1)                                                     SIMQ  29
      A(I1)=A(I2)                                                    SIMQ  30
      A(I2)=SAVE                                                     SIMQ  31
C        DIVIDE EQUATION BY LEADING COEFFICIENT                      SIMQ  32
   50 A(I1)=A(I1)/BIGA                                               SIMQ  33
      SAVE=B(IMAX)                                                   SIMQ  34
      B(IMAX)=B(J)                                                   SIMQ  35
      B(J)=SAVE/BIGA                                                 SIMQ  36
C        ELIMINATE NEXT VARIABLE                                     SIMQ  37
      IF(J-N) 55,70,55                                               SIMQ  38
   55 IQS=N*(J-1)                                                    SIMQ  39
      DO 65 IX=JY,N                                                  SIMQ  40
      IXJ=IQS+IX                                                     SIMQ  41
      IT=J-IX                                                        SIMQ  42
      DO 60 JX=JY,N                                                  SIMQ  43
      IXJX=N*(JX-1)+IX                                               SIMQ  44
      JJX=IXJX+IT                                                    SIMQ  45
      A(IXJX)=A(IXJX)-(A(IXJ)*A(JJX))                                SIMQ  46
C     FOLLOWING THREE CARDS ARE USED FOR ELIMINATING UNDERFLOW
      AA=ABS(A(IXJX))
      IF(AA-1.0E-30) 100,100,60
  100 A(IXJX)=0.0
   60 CONTINUE
      B(IX)=B(IX)-(B(J)*A(IXJ))
C     FOLLOWING THREE CARDS ARE USED FOR ELIMINATING UNDERFLOW
      BB=ABS(B(IX))
      IF(BB-1.0E-30) 101,101,65
  101 B(IX)=0.0
   65 CONTINUE
C        BACK SOLUTION                                               SIMQ  48
   70 NY=N-1                                                         SIMQ  49
      IT=N*N                                                         SIMQ  50
      DO 80 J=1,NY                                                   SIMQ  51
      IA=IT-J                                                        SIMQ  52
      IB=N-J                                                         SIMQ  53
      IC=N                                                           SIMQ  54
      DO 80 K=1,J                                                    SIMQ  55
      B(IB)=B(IB)-A(IA)*B(IC)                                        SIMQ  56
      IA=IA-N                                                        SIMQ  57
```

```
   80 IC=IC-1                                                        SIMC  58
      RETURN                                                         SIMC  59
      END                                                            SIMC  60
//GO.SYSIN    DD  *
```

C VALUES OF PARAMETERS REQUIRED

NFSF =	1	NFSL =	19	NBSF =	58	NBSL =	66	MFSF =	1
MFSL =	40	MBSF =	91	MBSL =	110	INNER=	38	NST =	5
NLEFT=	71	NRIGT=	70	NBOND=	4	LITER=	5	NPART=	2
NPOIN=	74	NELEM=	110	SYE =0.0		FIE =0.0		SSTA =0.003125	
YLENS=2.5		FDCON=5.0		XK =0.014		POROS=0.34		FLEPS=5000.0	
DT =900.0		TL =90000.0							

C INITIAL DATA OF COORDINATES AND TOTAL HEAD OF ALL NODES

I	X(I)	Y(I)	H(I)
1	250.0000	105.3559	105.3559
2	500.0000	104.8118	104.8118
3	750.0001	104.2677	104.2677
4	1000.0001	103.0536	103.0536
5	1250.0002	100.4414	100.4414
6	1500.0002	97.8293	97.8293
7	1750.0002	95.3784	95.3784
8	2000.0002	92.9900	92.9900
9	2250.0004	90.7200	90.7200
10	2500.0004	89.0416	89.0416
11	2750.0004	86.5262	86.5262
12	3000.0004	83.7504	83.7504
13	3250.0004	81.2805	81.2805
14	3500.0004	79.8035	79.8035
15	3750.0004	77.0463	77.0463
16	4000.0004	76.0687	76.0687
17	4250.0009	74.2668	74.2668
18	4500.0009	71.0677	71.0677
19	4750.0009	68.8162	68.8162
20	250.0000	83.1811	105.3559
21	500.0000	81.6423	104.8118
22	750.0001	80.1035	104.2677
23	1000.0001	78.5647	103.0536
24	1250.0002	77.0259	100.4414
25	1500.0002	75.4871	97.8293
26	1750.0002	73.9483	95.3784
27	2000.0002	72.4095	92.9900
28	2250.0004	70.8707	90.7200
29	2500.0004	69.3319	89.0416
30	2750.0004	67.7931	86.5262
31	3000.0004	66.2543	83.7504
32	3250.0004	64.7155	81.2805
33	3500.0004	63.1767	79.8035
34	3750.0004	61.6379	77.0463
35	4000.0004	60.0991	76.0687
36	4250.0009	58.5603	74.2668
37	4500.0009	57.0215	71.0677
38	4750.0009	55.4827	68.8162
39	250.0	67.8732	105.3
40	750.0001	65.3726	104.2677
41	1250.0002	62.8721	100.4414

42	1750.0002	60.3715	95.3784
43	2250.0004	57.8710	90.7200
44	2750.0004	55.3704	86.5262
45	3250.0004	52.8699	81.2805
46	3750.0004	50.3693	77.0463
47	4250.0009	47.8688	74.2668
48	4750.0009	45.3682	68.8162
49	500.0000	51.0264	104.8118
50	1000.0001	49.1029	103.0536
51	1500.0002	47.1794	97.8293
52	2000.0002	45.2559	92.9900
53	2500.0004	43.3324	89.0416
54	3000.0004	41.4089	83.7504
55	3500.0004	39.4854	79.8035
56	4000.0004	37.5619	76.0687
57	4500.0009	35.6384	71.0677
58	500.0000	0.0000	104.8118
59	1000.0001	0.0000	103.0536
60	1500.0002	0.0000	97.8293
61	2000.0002	0.0000	92.9900
62	2500.0004	0.0000	89.0416
63	3000.0004	0.0000	83.7504
64	3500.0004	0.0000	79.8035
65	4000.0004	0.0000	76.0687
66	4500.0009	0.0000	71.0677
67	5000.0009	0.0000	67.4299
68	5000.0009	33.7149	67.4299
69	5000.0009	53.9439	67.4299
70	5000.0009	67.4299	67.4299
71	0.0000	105.9000	105.9000
72	0.0000	84.7200	105.9000
73	0.0000	52.9500	105.9000
74	0.0000	0.0000	105.9000

C THE NUMBERS OF THREE NODES IN TRIANGULAR ELEMENT IN COUNTERCLOCKWISE SENSE

I	NOD1(I)	NOD2(I)	NOD3(I)
1	72	1	71
2	72	20	1
3	20	21	1
4	21	2	1
5	21	3	2
6	21	22	3
7	22	23	3
8	23	4	3
9	23	5	4
10	23	24	5
11	24	25	5
12	25	6	5
13	25	7	6
14	25	26	7
15	26	27	7
16	27	8	7
17	27	9	8
18	27	28	9
19	28	29	9
20	29	10	9
21	29	11	10
22	29	30	11

23	30	31	11
24	31	12	11
25	31	13	12
26	31	32	13
27	32	33	13
28	33	14	13
29	33	15	14
30	33	34	15
31	34	35	15
32	35	16	15
33	35	17	16
34	25	36	17
35	36	37	17
36	37	18	17
37	37	19	18
38	37	38	19
39	38	69	19
40	69	70	19
41	39	20	72
42	39	21	20
43	40	22	21
44	40	23	22
45	41	24	23
46	41	25	24
47	42	26	25
48	42	27	26
49	43	28	27
50	43	29	28
51	44	30	29
52	44	31	30
53	45	32	31
54	45	33	32
55	46	34	33
56	46	35	34
57	47	36	35
58	47	37	36
59	48	38	37
60	48	69	38
61	73	39	72
62	73	49	39
63	49	21	39
64	49	40	21
65	49	50	40
66	50	23	40
67	50	41	23
68	50	51	41
69	51	25	41
70	51	42	25
71	51	52	42
72	52	27	42
73	52	43	27
74	52	53	43
75	53	29	43
76	53	44	29
77	53	54	44
78	54	31	44
79	54	45	31
80	54	55	45
81	55	33	45

```
        82          55          46          33
        83          55          56          46
        84          56          35          46
        85          56          47          35
        86          56          57          47
        87          57          37          47
        88          57          48          37
        89          57          68          48
        90          68          69          48
        91          74          49          73
        92          74          58          49
        93          58          59          49
        94          59          50          49
        95          59          51          50
        96          59          60          51
        97          60          61          51
        98          61          52          51
        99          61          53          52
       100          61          62          53
       101          62          63          53
       102          63          54          53
       103          63          55          54
       104          63          64          55
       105          64          65          55
       106          65          56          55
       107          65          57          56
       108          65          66          57
       109          66          67          57
       110          67          68          57
```

```
C     MNUM(IJ), NUMBERING INDEX OF SOME ELEMENTS AROUND A INNER NODE WHICH IS
      NEEDED TO CONSIDER THE CORRECTION OF H(I) AFTER SHIFTING NODAL COORDINATES

     I    *    *    *    *
     * MNUM(I,1)    *    *
     *    * MNUM(I,2)    *
     *    *    * MNUM(I,3)
     *    *    *    * MNUM(I,4)
     *    *    *    *    *

     1    2   41   42    3
     2    4   63   64    5
     3    6   43   44    7
     4    8   66   67    9
     5   10   45   46   11
     6   12   69   70   13
     7   14   47   48   15
     8   16   72   73   17
     9   18   49   50   19
    10   20   75   76   21
    11   22   51   52   23
    12   24   78   79   25
    13   26   53   54   27
    14   28   81   82   29
    15   30   55   56   31
    16   32   84   85   33
    17   34   57   58   35
    18   36   87   88   37
    19   38   59   60   39
    20   41   62   42    0
```

21	43	65	44	0
22	45	68	46	0
23	47	71	48	0
24	49	74	50	0
25	51	77	52	0
26	53	80	54	0
27	50	83	56	0
28	57	86	58	0
29	59	89	60	0
30	63	92	93	64
31	66	94	95	67
32	69	96	97	70
33	72	98	99	73
34	75	100	101	76
35	78	102	103	79
36	81	104	105	82
37	84	106	107	85
38	87	108	109	88

C FOURIER COEFFICIENTS OF BOTTOM DRAINAGE VELOCITY

1COS	0.2060E-04	-0.2555E-04	0.3933E-04	-0.1161E-04	0.7523E-05	-0.2118E-05
1SIN	0.0000E 00	-0.4224E-05	-0.1677E-05	0.6999E-05	-0.1689E-04	-0.9095E-05
2COS	0.3689E-04	-0.1483E-04	0.7028E-04	-0.2182E-04	0.1646E-04	0.3183E-05
2SIN	0.0000E 00	-0.6800E-05	-0.2002E-04	0.6440E-05	-0.2374E-04	-0.1631E-04
3COS	0.3666E-04	-0.1003E-04	0.1005E-03	-0.4412E-04	0.2276E-04	0.3765E-05
3SIN	0.0000E 00	-0.8123E-05	-0.5320E-04	0.1999E-05	-0.3054E-04	-0.2445E-04
4COS	0.4971E-04	-0.9646E-05	0.1261E-03	-0.6833E-04	0.2999E-04	0.6248E-05
4SIN	0.0000E 00	-0.7289E-05	-0.8863E-04	-0.8633E-06	-0.3150E-04	-0.2679E-04
5COS	0.6418E-04	-0.8761E-05	0.1453E-03	-0.9076E-04	0.3359E-04	0.6758E-05
5SIN	0.0000E 00	-0.7440E-05	-0.1177E-03	-0.2665E-05	-0.3154E-04	-0.2828E-04
6COS	0.5345E-04	-0.7978E-05	0.1637E-03	-0.1162E-03	0.3628E-04	0.6731E-05
6SIN	0.0000E 00	-0.3818E-05	-0.1470E-03	-0.2576E-05	-0.2888E-04	-0.2791E-04
7COS	0.7328E-04	-0.4882E-05	0.1783E-03	-0.1286E-03	0.4556E-04	0.1265E-04
7SIN	0.0000E 00	-0.1082E-05	-0.1770E-03	-0.8028E-05	-0.2667E-04	-0.2772E-04
8COS	0.8153E-04	0.7425E-05	0.2038E-03	-0.1508E-03	0.5643E-04	0.1902E-04
8SIN	0.0000E 00	-0.1136E-05	-0.2246E-03	-0.1760E-04	-0.2682E-04	-0.3179E-04
9COS	0.1070E-03	0.1214E-04	0.2185E-03	-0.1908E-03	0.5860E-04	0.2009E-04
9SIN	0.0000E 00	-0.6813E-05	-0.2831E-03	-0.2555E-04	-0.1887E-04	-0.2813E-04
10COS	0.1245E-03	0.8425E-05	0.2222E-03	-0.2390E-03	0.5734E-04	0.2059E-04
10SIN	0.0000E 00	-0.1079E-04	-0.3439E-03	-0.2934E-04	-0.5645E-06	-0.1428E-04
11COS	0.1214E-03	0.2163E-04	0.2230E-03	-0.2915E-03	0.6012E-04	0.2998E-04
11SIN	0.0000E 00	-0.2396E-04	-0.4261E-03	-0.3836E-04	0.2684E-04	0.5779E-05
12COS	0.7925E-04	-0.7718E-04	0.1126E-03	-0.4094E-03	0.2125E-04	0.3222E-04
12SIN	0.0000E 00	-0.1256E-04	-0.4542E-03	0.3179E-04	0.1628E-03	0.1422E-03

C COORDINATES AND INITIAL WATER TABLES OF 13 WELLS

I	XW(I)	YW(I)
1	0.0000E+00	1.0590E+02
2	9.1900E+02	1.0390E+02
3	1.5698E+03	0.9710E+02
4	2.2083E+03	0.9100E+02
5	2.5360E+03	0.8880E+02
6	2.8560E+03	0.8540E+02
7	3.1790E+03	0.8170E+02
8	3.5006E+03	0.7980E+02
9	3.8176E+03	0.7630E+02
10	4.1331E+03	0.7590E+02
11	4.4409E+03	0.7160E+02
12	4.7518E+03	0.6880E+02
13	5.0779E+03	0.6700E+02

RESULTANT WATER TABLES OF ILLUSTRATED EXAMPLE

C TIME T= 0.9000E 04

HEIGHT OF NONES ALONG FREE SURFACE

I	YW(I)	YW(I+1)	YW(I+2)	YW(I+3)	YW(I+4)
1	0.1057E 03	0.1049E 03	0.1040E 03	0.1031E 03	0.1010E 03
6	0.9886E 02	0.9629E 02	0.9375E 02	0.9162E 02	0.8943E 02
11	0.8695E 02	0.8451E 02	0.8232E 02	0.8005E 02	0.7802E 02
16	0.7580E 02	0.7246E 02	0.6904E 02	0.6922E 02	

C TIME T= 0.1800E 05

HEIGHT OF NONES ALONG FREE SURFACE

I	YW(I)	YW(I+1)	YW(I+2)	YW(I+3)	YW(I+4)
1	0.1059E 03	0.1053E 03	0.1041E 03	0.1030E 03	0.1010E 03
6	0.9908E 02	0.9649E 02	0.9387E 02	0.9150E 02	0.8910E 02
11	0.8652E 02	0.8393E 02	0.8126E 02	0.7847E 02	0.7591E 02
16	0.7314E 02	0.6951E 02	0.6586E 02	0.6005E 02	

C TIME T= 0.2700E 05

HEIGHT OF NONES ALONG FREE SURFACE

I	YW(I)	YW(I+1)	YW(I+2)	YW(I+3)	YW(I+4)
1	0.1050E 03	0.1045E 03	0.1032E 03	0.1019E 03	0.9982E 02
6	0.9775E 02	0.9498E 02	0.9220E 02	0.8966E 02	0.8708E 02
11	0.8437E 02	0.8163E 02	0.7883E 02	0.7593E 02	0.7357E 02
16	0.7106E 02	0.6844E 02	0.6570E 02	0.5560E 02	

C TIME T= 0.3600E 05

HEIGHT OF NONES ALONG FREE SURFACE

I	YW(I)	YW(I+1)	YW(I+2)	YW(I+3)	YW(I+4)
1	0.1046E 03	0.1044E 03	0.1032E 03	0.1018E 03	0.9958E 02
6	0.9718E 02	0.9491E 02	0.9252E 02	0.9003E 02	0.8756E 02
11	0.8510E 02	0.8265E 02	0.8018E 02	0.7772E 02	0.7604E 02
16	0.7437E 02	0.7075E 02	0.6764E 02	0.6012E 02	

C TIME T= 0.4500E 05

HEIGHT OF NONES ALONG FREE SURFACE

I	YW(I)	YW(I+1)	YW(I+2)	YW(I+3)	YW(I+4)
1	0.1058E 03	0.1065E 03	0.1055E 03	0.1046E 03	0.1022E 03
6	0.9949E 02	0.9885E 02	0.9802E 02	0.9641E 02	0.9488E 02
11	0.9362E 02	0.9246E 02	0.9132E 02	0.9023E 02	0.8902E 02
16	0.8812E 02	0.8467E 02	0.8209E 02	0.8980E 02	

C TIME T= 0.5400E 05

HEIGHT OF NONES ALONG FREE SURFACE

I	YW(I)	YW(I+1)	YW(I+2)	YW(I+3)	YW(I+4)
1	0.1079E 03	0.1076E 03	0.1070E 03	0.1063E 03	0.1042E 03
6	0.1022E 03	0.1016E 03	0.1010E 03	0.1001E 03	0.9925E 02
11	0.9840E 02	0.9754E 02	0.9678E 02	0.9597E 02	0.9423E 02
16	0.9253E 02	0.9332E 02	0.9411E 02	0.9549E 02	

C TIME T= 0.6300E 05

HEIGHT OF NONES ALONG FREE SURFACE

I	YW(I)	YW(I+1)	YW(I+2)	YW(I+3)	YW(I+4)
1	0.1087E 03	0.1077E 03	0.1067E 03	0.1056E 03	0.1041E 03
6	0.1026E 03	0.1005E 03	0.9841E 02	0.9704E 02	0.9566E 02
11	0.9375E 02	0.9179E 02	0.8931E 02	0.8674E 02	0.8493E 02
16	0.8313E 02	0.8139E 02	0.7905E 02	0.7277E 02	

C TIME T= 0.7200E 05

HEIGHT OF NONES ALONG FREE SURFACE

I	YW(I)	YW(I+1)	YW(I+2)	YW(I+3)	YW(I+4)
1	0.1089E 03	0.1079E 03	0.1068E 03	0.1057E 03	0.1040E 03
6	0.1022E 02	0.1003E 03	0.9832E 02	0.9654E 02	0.9478E 02
11	0.9261E 02	0.9045E 02	0.8791E 02	0.8541E 02	0.8318E 02
16	0.8108E 02	0.7943E 02	0.7826E 02	0.6709E 02	

C TIME T= 0.8100E 05

HEIGHT OF NONES ALONG FREE SURFACE

I	YW(I)	YW(I+1)	YW(I+2)	YW(I+3)	YW(I+4)
1	0.1078E 03	0.1077E 03	0.1067E 03	0.1056E 03	0.1036E 03
6	0.1014E 03	0.1008E 03	0.1000E 03	0.9877E 02	0.9755E 02
11	0.9640E 02	0.9529E 02	0.9392E 02	0.9265E 02	0.9225E 02
16	0.9207E 02	0.9314E 02	0.9481E 02	0.7718E 02	

C TIME T= 0.9000E 05

HEIGHT OF NONES ALONG FREE SURFACE

I	YW(I)	YW(I+1)	YW(I+2)	YW(I+3)	YW(I+4)
1	0.1082E 03	0.1084E 03	0.1078E 03	0.1071E 03	0.1059E 03
6	0.1046E 03	0.1043E 03	0.1040E 03	0.1035E 03	0.1030E 03
11	0.1024E 03	0.1018E 03	0.1016E 03	0.1015E 03	0.1024E 03
16	0.1034E 03	0.9738E 02	0.9169E 02	0.1017E 03	

Security Classification

DOCUMENT CONTROL DATA - R & D

(Security classification of title, body of abstract and indexing annotation must be entered when the overall report is classified)

1. ORIGINATING ACTIVITY (Corporate author)	2a. REPORT SECURITY CLASSIFICATION
Virginia Institute of Marine Science	UNCLASSIFIED
	2b. GROUP

3. REPORT TITLE

Investigation of the Water Table in a Tidal Beach

4. DESCRIPTIVE NOTES (Type of report and inclusive dates)

Technical Report (1 July 1969—30 September 1971)

5. AUTHOR(S) (First name, middle initial, last name)

W. Harrison; J. D. Boon, III; C. S. Fang; L. E. Fausak; and S. N. Wang

6. REPORT DATE	7a. TOTAL NO. OF PAGES	7b. NO. OF REFS
October 1971	165	

8a. CONTRACT OR GRANT NO.	9a. ORIGINATOR'S REPORT NUMBER(S)
Nonr-N00014-70-C-0004	
b. PROJECT NO. NR-388-097	Special Scientific Report No. 60
c.	9b. OTHER REPORT NO(S) (Any other numbers that may be assigned this report)
d.	

10. DISTRIBUTION STATEMENT

This document has been approved for public release and sale; its distribution is unlimited.

11. SUPPLEMENTARY NOTES	12. SPONSORING MILITARY ACTIVITY
Support for one field man provided by NSF	Geography Branch Office of Naval Research Arlington, Virginia 22217

13. ABSTRACT

Fluctuations in the beach water table at Virginia Beach, Virginia, were studied to better understand the causes and consequences of the oscillations. Special instrumentation for monitoring the water-table surface was designed and is described in the report. The major environmental variables responsible for the fluctuations were evaluated by multiregression analysis in which the dependent variable was the rise of the water table in a well (over a half-tidal cycle) and the independent variables were atmospheric pressure, the rise in ocean still-water-level (SWL), the distance of the well from the foreshore, and a measure of the contribution of the uprush to the water table.

One and two-dimensional finite-element models were constructed to model the groundwater flow. Results show general accuracy of the methods used. Descriptions of and listings for the FORTRAN computer programs are given.

Changes in foreshore sand volume, as a result of fluctuations in the water table, changes in head gradient, and oscillations in the oceanic SWL were also studied. Predictor equations for changes in quantity of foreshore sand over intervals of one-half and entire tidal cycles are developed. Tests of the equations on independent data indicate that they are more reliable than any developed heretofore.

DD FORM 1 NOV 65 1473 (PAGE 1)

S/N 0101-807-6811

Security Classification

A-31408

14. KEY WORDS	LINK A		LINK B		LINK C	
	ROLE	WT	ROLE	WT	ROLE	WT
Groundwater flow						
Beach dynamics						
Mathematical modeling						
Water-table instrumentation						
Finite-element analysis						
Tidal effects						
Tidal beaches						
Sand transport						
Fluid-sediment interactions						